WIND LOADS ON SOLAR PANEL SYSTEMS ATTACHED TO BUILDING ROOFS

Eleni Xypnitou

A Thesis

In

The Department

of

Building, Civil and Environmental Engineering

Presented in Partial Fulfillment of the Requirements

for the Degree of Master of Applied Science (Building Engineering) at

Concordia University

Montreal, Quebec, Canada

August 2012

CONCORDIA UNIVERSITY

School of Graduate Studies

This is to certify that the thesis prepared

By: Eleni Xypnitou

Entitled: WIND LOADS ON SOLAR PANEL SYSTEMS ATTACHED TO BUILDING ROOFS

and submitted in partial fulfillment of the requirements for the degree of

Master of Applied Science (Building, Civil and Environmental Engineering)

complies with the regulations of the University and meets the accepted standards with respect to originality and quality.

Signed by the final examining committee:

Dr. R. Zmeureanu Chair

Dr. K. Galal Examiner

Dr. G. Vatistas External Examiner

Dr. T. Stathopoulos Supervisor

Approved by _____
Chair of Department or Graduate Program Director

_____
Dean of Faculty

Date _____

ABSTRACT

WIND LOADS ON SOLAR PANEL SYSTEMS

ATTACHED TO BUILDING ROOFS

ELENI XYPNITOU

Solar panel systems placed either on building roofs or in the fields have become popular worldwide during the last decades since their contribution to environmental friendly energy production is remarkable. Their exposure to wind loads results to wind-induced loading which cannot be predicted efficiently because design standards and codes provide very little information. The main objective of this study is to determine and assess how different combination of parameters can affect the wind flow and thus the pressure distribution on the surface of the panels. For this purpose, wind tunnel tests were performed in the Building Aerodynamics laboratory of Concordia University.

Literature review was conducted demonstrating experimental results from previous studies for stand-alone panels and those attached to building roofs. A 1:200 scale model was fabricated consisting of a building and panels attached to the roof. The model was tested in the wind tunnel for different configurations, such as two different building heights and the case without the building, two panel locations and 4 panel inclinations for 13 angles of wind attack.

The acquired data was transformed into mean and peak force, local and area-averaged pressure coefficients. Different configurations result in different pressure distribution indicating those parameters contributing to the most critical cases. The results of the study will be made available to the wind code and standards committees for possible utilization.

ACKNOWLEDGMENTS

I would like to express my appreciation to all the individuals who contributed to the completion of this thesis.

I would like to thank my supervisor Dr. Theodore Stathopoulos for his helpful guidance and advice for this research work. I am also grateful for the assistance given by lab members and especially Ioannis Zisis for reviewing this work. Special thanks to Josef Hrib, laboratory technician, who provided me with a state of the art testing model.

I would also like to thank my parents Angeliki Lamprou and Michail Xypnitos for their continuous love, support and encouragement, as well as, all my friends.

Finally, I would like to thank Andrianos Argyropoulos for his unconditional help, support and encouragement.

TABLE OF CONTENTS

LIST OF FIGURES

LIST OF TABLES

LIST OF SYMBOLS

A	area	(m^2)
α_i	area	(m^2)
C_F	force coefficient	
$C_{F,max}$	maximum force coefficient	
$C_{F,mean}$	mean force coefficient	
$C_{F,min}$	minimum force coefficient	
C_p	pressure coefficient	
$C_{p'}$	peak fluctuating pressure coefficient	
$C_{p,area\text{-}averaged}$	area-averaged pressure coefficient	
$C_{p,\,ls}$	lower surface pressure coefficient	
$C_{p,max}$	maximum pressure coefficient	
$C_{p,mean}$	mean pressure coefficient	
$C_{p,min}$	minimum pressure coefficient	
$C_{p,net}$	net pressure coefficient	
$C_{p,\,us}$	upper surface pressure coefficient	
$C_{p,\,peak}$	peak pressure coefficient	
F	force	(N)

k	Von Karman constant	
H	building height	(m)
I_r	turbulence intensity	
P	pressure	(Pa)
P’	peak fluctuating pressure	(Pa)
P_{mean}	mean pressure	(Pa)
p_s	stagnation pressure	(Pa)
p_a	ambient pressure	(Pa)
q	dynamic pressure	(Pa)
$\vec{V}$	wind velocity	(m/s)
V_g	gradient wind speed	(m/s)
$\overline{U}$, $\overline{U}$(z)	mean wind speed	(m/s)
Uz_{ref}	wind speed at reference height	(m/s)
u_*	friction velocity	(m/s)
u(x,y,z,t)	fluctuating longitudinal velocity component	(m/s)
v(x,y,z,t)	fluctuating lateral velocity component	(m/s)
w(x,y,z,t)	fluctuating vertical velocity component	(m/s)

z	height from ground level	(m)
z_{ref}	reference height from ground level	(m)
z_o	roughness length	(m)
α	power law exponent	
δ	boundary layer thickness	(m)
τ_o	shear stress	(Pa)
ρ	ambient air density	(kg/m^3)

CHAPTER 1: INTRODUCTION

1.1 OVERVIEW

The evaluation of wind-induced loads applied on solar panels plays a very important role for design purposes. During the last decades, a strong interest has been developed towards renewable energy resources and to this end the utilisation of solar panels has been expanded. However, the effect of a number of factors such as the upstream exposure, the landscape, the panel inclination and location, the building height for panels attached to building roofs and the like have to be carefully considered in all experimental and computational procedures. Experiments can be performed nowadays with more sophisticated and cutting edge technology resulting in more accurate results.

Scientists and engineers have already made many efforts to define wind loading with results not always compatible. The main objective of such studies is to produce data that will be used for the improvement of building code provisions which in turn can lead to a more sufficient, economical and overall safer design. Many cases of damaged panels (Figure 1.1.1) have been observed when exposed to strong winds because of poor or non-available provisions related to this kind of structures in wind design standards or building codes of practice. Analysis based on simplifications or assumptions often lead to incorrect results and uneconomic design, which may result in poor safety and/or unreasonable construction cost. Although, there are a number of studies which have dealt with this issue, many of them are controversial and many aspects of the problem still

remain uncovered requiring more research in this field. Thus, a more detailed study based on experimental results is necessary to address this problem.

Figure 1.1.1 Damaged solar collectors (after Chung et al, 2008)

1.2 THESIS OBJECTIVES

The main scope of this thesis is the systematic study of wind-induced pressures applied on the surface of solar panels, placed on the ground or on the roof of buildings. For this purpose, a detailed literature review was completed as the first step to compare the experimental results generated by previous studies and indicate the areas for which further study may be necessary. Previous studies include full-scale, wind tunnel and simulation tests for stand-alone panels and panels attached to building roofs with different configurations.

As far as the current study is concerned, the most significant aspect of it was to examine the influence of a number of factors during the wind tunnel tests performed in the atmospheric boundary layer wind tunnel of Concordia University. The evaluation of

parameters such as building height, panel inclination, and location, as well as, the wind direction has a direct impact on design decisions for these structures. The collection of the experimental data, in addition to its analysis and transformation to pressure, force, and area-averaged pressure coefficients was of major significance in this work.

1.3 THESIS STRUCTURE

The introduction of this thesis is followed by six chapters:

- Chapter 2: Basic Wind Engineering concepts regarding structures are discussed in this chapter.
- Chapter 3: Detailed literature review based on previous wind tunnel, full-scale and computational studies is presented and comparison of previous experimental results is made.
- Chapter 4: The wind tunnel facilities and experimental equipment are presented along with the details concerning the building and panel model construction. In addition, the wind tunnel testing procedure is described, as well as, the process of the data interpretation.
- Chapter 5: The wind tunnel experimental results are presented. The results are given in terms of pressure, area-averaged pressure and force coefficients and the effect of a number of parameters are also discussed, namely: panels at the ground level, mounted on 7 m and 16 m high buildings, located at the front and back position of the building roof and finally inclined by 20, 30, 40 and 45 degrees.
- Chapter 6: Based on the results of the present study, conclusions and recommendations for further research are made.

CHAPTER 2: WIND ENGINEERING BASICS

2.1 GENERAL

This chapter is a summary of Wind Engineering basic concepts. The atmospheric boundary layer and the turbulent wind are introduced in the first part where their characteristics are also described. The mathematical description of the wind profile follows, as well as the mechanisms generating it. Moreover, in order to investigate the wind effects on structures, the Bernoulli equation applied for a wind tunnel and the dimensionless pressure and force coefficients are presented. Finally, the characteristics of the atmospheric boundary layer wind tunnels are described.

2.2 WIND ENGINEERING CONCEPTS

2.2.1 The atmospheric boundary layer

The lowest part of the troposphere, which is in contact with the earth's surface and in which there is wind motion, is called boundary layer. When the air is moving upon the earth's surface, a horizontal drag force exerted on it retards its flow. This force decreases as the height above the ground increases and thus its effect becomes negligible at a height δ, which is called height of the atmospheric boundary layer. Above this height, flow is assumed frictionless and the wind flows with the gradient wind velocity along the isobars. As a result, the atmosphere at a level greater than the boundary layer is called free atmosphere.

It is obvious, therefore, that the atmosphere can be divided into different layers, which have different characteristics according to their distance from the ground level. Nevertheless, it is the boundary layer of the atmosphere that is of main interest to the building and civil engineers since most of the structures are found on the ground surface and extend only to some meters above the ground level. The boundary layer's thickness is not fixed and it can vary from a few hundred meters to several kilometers. It is directly affected by the air temperature and the terrain characteristics such as the topography and the ground roughness.

Concluding, boundary layer is the area adjacent to the earth's surface where:

- The speed of the flow increases from zero at the surface where the no-slip condition is valid to the geostrophic wind speed where there is no friction and equilibrium of forces is applied.
- Small impulses take place on the surface per unit time, which is translated to a steady force acting on the body along the flow direction and is called "surface-friction drag".

2.2.2 Boundary layer thickness

The thickness of the boundary layer is considered to be extended to a distance δ from the surface where the velocity u at this point is 99% of the local free-stream velocity because of friction absence. Figure 2.2.1 (a) and (b) show the thickness of the boundary layer by plotting the height y as a function of the velocity x-component in both dimensional and

dimensionless form. The dimensionless form of the boundary layer is helpful when boundary layer profiles of different thickness are to be compared.

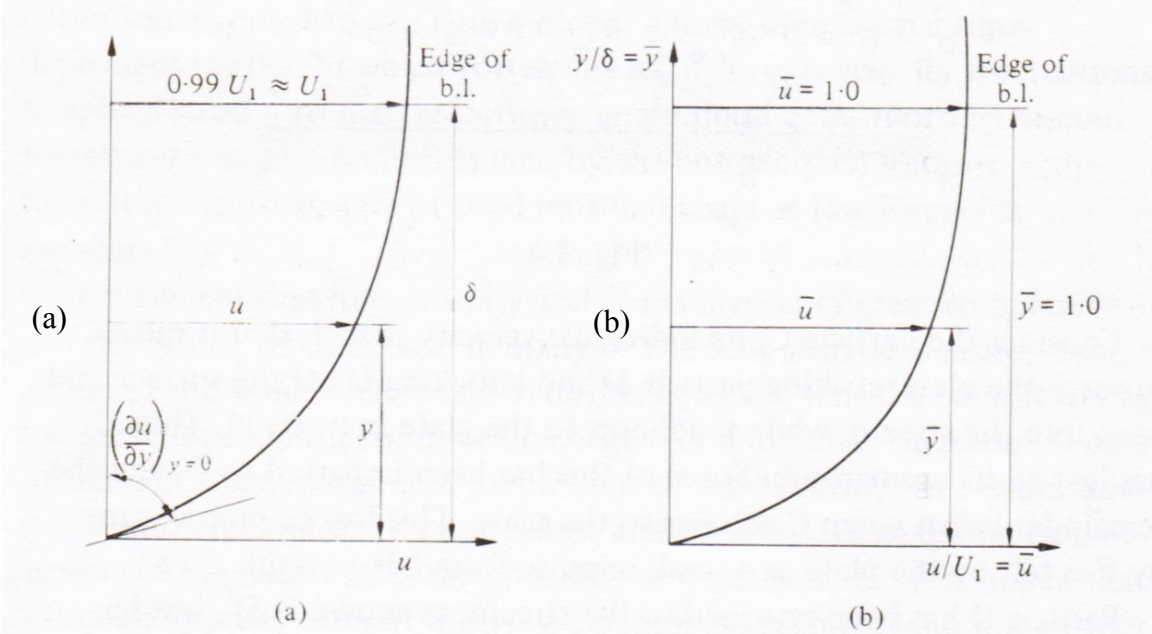

Figure 2.2.1 Dimensional (a) and dimensionless (b) wind velocity profiles (after Houghton and Carruthers, 1976)

2.2.3 Types of boundary layer

Study of the boundary layer leads to the conclusion that there may be two different regimes as far as the flow is concerned: (1) laminar flow, (2) turbulent flow

- Laminar flow appears when the fluid layers flow over one another with little mass fluid interchange of adjacent layers. Momentum exchanges happen only on molecular scale.
- Turbulent flow is characterized by chaotic and stochastic property changes. This means that fluid particles experience diffusion and convection between adjacent

layers, which results in rapid variation of pressure and velocity in space and time and important mixing of fluid properties. Velocity fluctuations are present because of this random motion of particles and mass transportation takes place between adjacent layers. If there is a flow with a mean velocity gradient then streamwise momentum interchanges between adjacent layers leads to the appearance of shearing stresses.

Figure 2.2.2 depicts the normalized laminar and turbulent profile where it is clear that the laminar velocity drops almost linearly at the lower part of the boundary layer until it reaches the zero value at the surface. However, it can be seen that for both boundary layer types, the shearing stress at the surface depends only on the slope of the velocity profile.

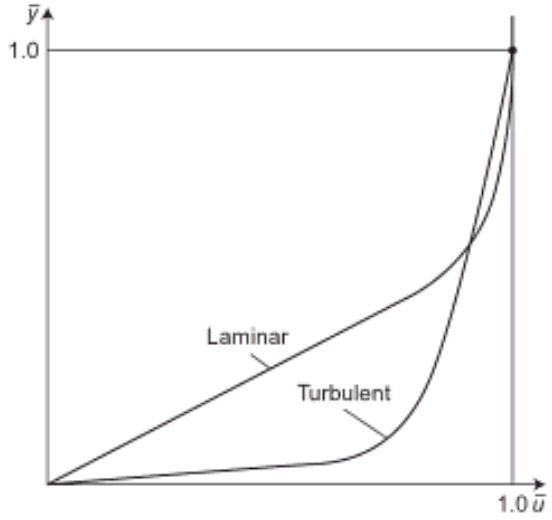

Figure 2.2.2 Normalized laminar and turbulent profile (after Houghton and Carruthers, 1976)

2.2.4 Turbulent wind

When it comes to studying the wind characteristics, it is more convenient to consider the following assumptions:

- At least a 10-minute period is applied when the mean wind velocity is to be calculated considering that the wind is stationary for this period of time
- It is assumed that the wind direction does not change with height (although the geostrophic equilibrium of forces cannot be maintained) and low buildings are not affected by directional change.

In order to describe mathematically the natural wind, a Cartesian coordinate system will be adopted with the x-direction being the mean wind velocity direction, which is of great importance since flow usually happens over a flat area. The y-axis is horizontal and the z-axis is vertical and perpendicular to the surface formed by the other two axes with positive direction considered when pointing out.

The velocities at a given time are given as:

Longitudinal component: $U(z) + u(x, y, z, t)$

Lateral component: $v(x, y, z, t)$

Vertical component: $w(x, y, z, t)$

Where $U(z)$ represents the mean wind velocity at a height z above the ground and is only dependent on the height z. The components u, v, w are the fluctuating components of the wind which are considered stationary with a zero mean value.

2.2.5 Mechanisms generating turbulent wind

Turbulence can be generated in the atmospheric boundary layer as a result of mechanical process, thermal process, or combination of both. The wind conditions appeared in the boundary layer can be generated mechanically because of the earth's surface roughness and are described mathematically by the mean wind velocity and the turbulent components. Moreover, the thermal effects of the atmosphere cannot be neglected especially when the wind velocities are less than 10 m/s. The presence of the sun results in heating the atmospheric layer and thus different air temperature leads to different density of the air molecules. This density difference gives rise to air mixing which takes place between adjacent atmospheric layers so as a stable state to be established. No heat exchange between the layers means that the atmosphere is under a neutral state, which is assumed to be the case for wind engineering applications.

2.2.6 Wind profile

The wind profile in the boundary layer can be defined by using mainly two characteristic length scales. For the lower part of the boundary layer, surface roughness is the most important length scale, while for its upper part, the height of the boundary layer is of great importance. Therefore, the wind profile close to the ground (50 m-100 m above the ground) where only the surface roughness is considered will be approximated by the logarithmic profile while, for greater heights power law is more appropriate since it takes into consideration the height above the ground.

- The logarithmic profile

The friction velocity u_* is given by the formula:

$$u_* = \sqrt{\frac{\tau_0}{\rho}} \quad (1)$$

where ρ is the air density and τ_0 is the shear stress at the ground level.

Dimensional analysis can give another expression for the logarithmic profile of the mean wind velocity:

$$U(z) = u_* \frac{1}{\kappa} \ln \frac{z}{z_0} \quad (2)$$

where κ is the Von Karman constant (κ = 0.4) and z_0 is the roughness length.

Friction between the ground surface and the air results in the formation of a vortex, the size of which can be described by the roughness length z_0. Formula (2) indicated that z_0 is the height where the mean wind velocity is zero. Table 2.2.1 gives typical values of the above properties for different terrains.

- Power law

As has already been mentioned, the logarithmic profile is more appropriate for heights closer to the surface. Nonetheless, when it comes to using it for higher levels, the logarithmic equation is corrected taking into account the height as well. The power law profile is empirical and is given as:

$$U(z) = U_{z_{ref}} \left(\frac{z}{z_{ref}} \right)^a \quad (3)$$

where z_{ref} is a reference height (10 m usually), α is power-law exponent which depends on roughness and other conditions. The power law is valid for any value of z in the boundary layer of δ thickness and so by setting $U_{Zref} = V_g$ and $z_{ref} = \delta$, it yields:

$$V(z) = V_g \left(\frac{z}{\delta}\right)^{\alpha} \quad (4)$$

Exposure category	Terrain roughness z_0 (cm)	Power-law exponent α	Atmospheric boundary layer thickness δ (m)
A= large cities	80	1/3	457
B= urban and suburban	20	2/9	366
C= open terrain	3.5	1/7	274
D= open coast	0.7	1/10	213

Table 2.2.1 Terrain roughness, power-law exponent and boundary layer thickness values corresponding to different exposure categories (after Liu 1991)

2.3 TURBULENT WIND CHARACTERISTICS

Wind is a turbulent flow and as such, random fluctuations characterize its velocity and pressure. To this term, it is necessary to introduce some statistical properties such as the mean, peak and RMS wind speed to fully describe this phenomenon.

Mean wind speed can be defined as the wind speed recorded at a given location and averaged over a certain period of time. However, in structural design the peak values are of main interest, which result from high winds of short duration. The definition of peak

wind speed varies according to the average time record. However, it can be observed that when the averaging time decreases, the peak wind speed increases for a given return period.

2.3.1 Turbulence intensity

The fluctuating velocity component of wind flow is called turbulence and results mainly from the terrain roughness. The wind velocity vector V can be decomposed into three components on x, y, z directions and as it has already been mentioned these constitute from the mean average value and the fluctuating components. Nonetheless, in most cases the flow is horizontal and since the turbulence in the x-direction is stronger, only the horizontal components will survive (U = V, v = 0, w = 0).

The relative intensity of turbulence is defined as the turbulence intensity divided by the mean velocity $\overline{U}$.

$$I_r = \frac{\sqrt{\overline{U^2}}}{\overline{U}} \tag{5}$$

Where $\sqrt{\overline{U^2}}$ is the root-mean-square (RMS) of the wind velocity at elevation z.

2.4 WIND EFFECTS ON STRUCTURES

2.4.1 Wind pressure on structures

One of the main scopes of wind engineering is to study the surface pressure applied on buildings which result from their exposure to natural wind. In order for this pressure to be

defined, it is necessary to introduce a reference pressure with which wind pressure can be compared. For prototype buildings, the reference pressure is the ambient pressure which is defined as the air pressure at the location where the structure is, as if the structure was not there and the flow was not obstructed. For a model building tested in a wind tunnel the ambient pressure is the air pressure in the test section which differs from the atmospheric. Theoretically, the external pressure (stagnation pressure) applied on a building can be accurately measured at the stagnation point, which is located above the center of the windward surface. Pressure on building surfaces can be either positive (pressure) or negative (suction) when compared to the ambient pressure. If a steady wind flow is assumed with uniform velocity, then application of Bernoulli's equation between the stagnation point and one upstream point can yield:

$$p_s = p_a + \frac{1}{2}\rho U^2 \tag{6}$$

Where:

p_s is the stagnation pressure, p_α is the atmospheric pressure, ρ is the air density and U is the upstream wind speed.

Measurement of wind pressure can become a very complicated task because of the large number of different parameters that have to be taken into consideration. Dimensional analysis, however, is really helpful to overcome these difficulties by introducing the local mean pressure coefficient which gives the pressure at an arbitrary point on a structure in dimensionless form as follows:

$$C_{P,mean} = \frac{P_{mean} - P_a}{\frac{1}{2}\rho U^2} \tag{7}$$

Where C_p is the pressure coefficient, P_{mean} is the mean pressure and U is the velocity at a reference height

Dimensional numbers have been also introduced for the case of peak pressure coefficients which are of great importance for designing purposes. So, for the case of peak fluctuating pressure p′

$$C_P' = \frac{P' - P_\alpha}{\frac{1}{2}\rho U^2} \quad (8)$$

It should be noted though, that the velocity U takes the mean time averaged free-stream value. Moreover, the dimensional coefficients offer the possibility to compare results coming from different studies even if different parameters have been considered.

The force applied on the structures can also be defined through the dimensionless force coefficient by the formula:

$$C_F = \frac{F}{\frac{1}{2}\rho U^2 A} \quad (9)$$

Where C_F is the force coefficient, F is the force applied on the surface considered and A is the area of the surface considered.

It is also important to define the net pressure coefficient:

$$C_{Pnet} = C_{P,us} - C_{P,ls} \quad (10)$$

Where, $C_{P,us}$ is the upper surface pressure coefficient and $C_{P,ls}$ is the lower surface pressure coefficient. When the net pressure coefficient takes negative values then suction occurs and the pressure direction is upwards.

The area-averaged pressure coefficients are given by the formula:

$$C_{P,area-averaged} = \frac{\sum_{i=1}^{n} C_{p,net}\, a_i}{\sum_{i=1}^{n} a_i} \quad (11)$$

The area-averaged pressure coefficients are defined as the integration of the net pressure coefficients over the corresponding area of the pressure taps and then divided by the whole area covered by the pressure taps considered.

2.4.2 Atmospheric boundary layer wind tunnels

In order to better investigate the wind effects on structures, engineers use atmospheric boundary layer wind tunnels where wind velocity properties are better simulated and the models' response is more accurately examined. For this purpose, the length, height and width of wind tunnel's test section have to be sufficient so as the wind velocity profile to be generated in the wind tunnel. Moreover, during wind tunnel testing sophisticated equipment is used in order to capture the wind-induced pressures on very small models. During studies conducted in a boundary layer wind tunnel it is crucial to satisfy certain similarity parameters. These are the geometrical, kinematic and dynamic similarity parameters which are not independent from each other. Wind tunnel models can be fabricated by different materials and under different scales according to the undertaken study.

CHAPTER 3: LITERATURE REVIEW

3.1 INTRODUCTION

Solar collector or photovoltaic (PV) systems placed either on building roofs or standing alone in the fields have been used extensively in recent years. These systems are sensitive to wind loading but design standards and codes of practice offer little assistance to the designers regarding provisions for wind-induced loading. This chapter reports a detailed literature survey, which has reviewed and compared the findings of some of the most recent and older experimental and numerical studies carried out for different solar collector system configurations.

Results show significant differences among different studies, some of which correspond to similar configurations. Comparisons are made in terms of mean and, if available, peak pressure and force coefficients for different wind directions. The data are organized separately for solar collectors on flat or pitched roofs and stand-alone panels. Also, the inclination of the collector, as well as its location on the roof, has been taken into account.

The review explains clearly the lack of design provisions in wind loading standards and codes of practice. It would indeed be very difficult to yield to an acceptable set of design provisions for solar collector and PV systems. The literature review concludes that a new comprehensive study would be necessary in order to put together a set of provisions for different configurations including both point and area-averaged loads.

3.2 WIND EFFECTS ON SOLAR PANELS

The increased interest on energy efficient residential construction enhanced the use of photovoltaic (PV) systems on such structures. From the structural engineering point of view, these integrated building attachments are exposed to the same environmental loads as other structural components. In particular, lightweight components like PV panels are predominantly sensitive to wind-induced loads. Moreover, their increased cost requires for special considerations during the design and installation stages.

This chapter focuses on presenting and comparing results from previous studies, which deal with wind loads applied on solar panels. More specifically, the cases considered refer to solar panels located on flat or pitched building roofs and stand-alone panels. For these cases, researchers investigated the wind-induced loads by using full-scale, wind tunnel and numerical simulation approaches.

The results coming out of these approaches, experimental or numerical, are usually expressed in terms of dimensionless pressure or force coefficients, which allows to directly compare results from different studies. However, some studies have been carried out under different conditions, such as different geometric scale, panel shape etc. In order to overcome this obstacle, an effort has been made to classify previous studies into different categories, according to the roof slope as well as the panel's location on it. Therefore, the limited studies on wind loads on solar collectors can be organized into the following categories:

- Solar panels attached to flat roofs
- Solar panels mounted on pitched roofs

- Solar panels and rooftop equipment near roof edges and corners
- Sloped solar panels on the ground

3.2.1 Solar panels attached to flat roofs

Description of Studies

There are a number of studies dealing with solar panels, which are attached to the surface of flat roofs as shown in Figure 3.2.1. The panels are either parallel or inclined with respect to the flat roof and the uplift force coefficients have been estimated using both experimental and numerical approaches.

One of the first wind tunnel studies on inclined solar panels attached on a five-storey flat roof building was conducted by Radu et al. (1986). The collector and building models were fabricated using a geometric scale of 1:50. The dimensions of the collector model were 0.04 m x 0.02 m and the building dimensions were 0.3 m x 0.43 m x 0.3 m (height x length x width). The solar collectors were located at the center of the roof at a 30-degree inclination with respect to the flat roof while the wind direction covered the whole spectrum from 0 to 360 degrees. The findings from the specific study were mainly presented in terms of mean net uplift coefficient values.

In a second study from Radu and Axinte (1989), wind tunnel experiments were carried out using a plate collector model located vertically on the building roof. The model dimensions were 0.08 m x 0.04 m (length x width) using a 1:50 geometric scale for its construction. For the particular study a small wind tunnel (0.3 m x 0.3 m x 2.5 m) was used and local dynamic pressures were measured for four different wind incidence angles

(0, 30, 90 and 180 degrees). The experimental findings were presented in terms of mean pressure coefficients on the upper surface of solar panel arrays.

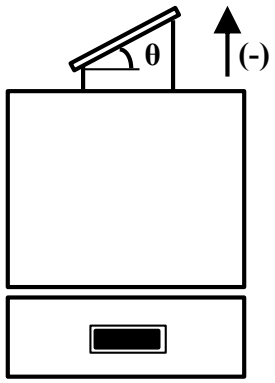

Figure 3.2.1 Cross-section and plan view of building model with attached panel on the roof

Wood et al. (2001) conducted wind tunnel experiments on a 1:100 industrial building model. The solar collector models were mounted parallel to the flat roof of the building which had dimensions 0.41 m x 0.27 m x 0.12 m (length x width x height) and covered the whole roof area. In this study, experiments with collectors located at three different heights above the roof cladding as well as three different lateral spacing values were carried out. The location considered is the mid-distance from the leading edge.

Ruscheweyh and Windhovel (2011) used 1:50-scale PV models mounted on top of a flat roof building. The instrumented PV panels were placed at different locations on top of the flat-roof building model and the net wind-induced pressures were measured.

Experimental Results

The main findings of the previously discussed studies are summarized in Figure 3.2.2. The results are presented in terms of mean and peak net uplift pressure coefficients as a function of the wind direction. More specifically, for the case of Wood et al. (2001) the maximum and minimum values observed at the mid normalized distance from the edges are presented for 0 and 90 degrees wind direction and for 0 degrees panel inclination.

The comparative results clearly show the differences among the considered studies that can be attributed mainly to the different configurations and in some cases different experimental approaches. As far as mean net pressure coefficients are concerned, no conclusion can be drawn as only a single value from the Ruscheweyh and Windhovel (2011) study is available. Nevertheless, the findings for 180 degrees wind angle are not too far from each other.

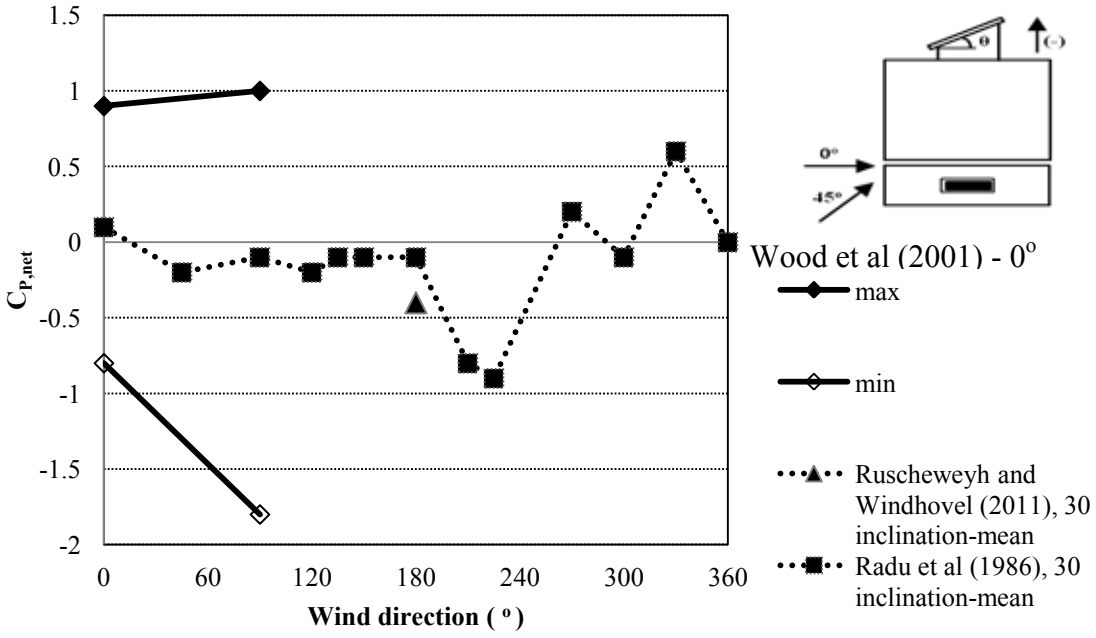

Figure 3.2.2 Net uplift pressure coefficients for solar panels attached to flat roofs

3.2.2 Solar panels mounted on pitched roofs

Description of Studies

There is a small number of studies that deal with wind-induced loads on solar panels attached on pitched roofs. Such studies have been carried out in both wind tunnel and full-scale facilities (e.g. Sparks et al. 1981, Blackmore and Geurts 2008, Geurts and Steenbergen 2009, Stenabaugh et al. 2010). A representative configuration of a building and PV models is shown in Figure 3.2.3.

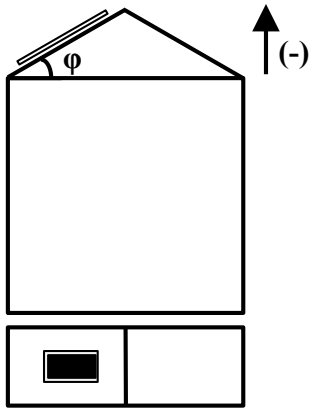

Figure 3.2.3 Cross-section and plan view of building model

In more detail, Sparks et al. (1981) carried out full-scale and wind tunnel experiments in order to determine the wind-induced forces on solar collectors. The wind tunnel experiments were performed on models of 1:24 geometric scale. The solar collectors were mounted on the roof of a single-storey building and they had eight pressure taps, which were placed on the upper and lower surface of each solar collector. In addition to the wind tunnel tests, this study made use of a full-scale building with external

dimensions of 4.09 m x 4.9 m x 4.09 m (width x length x height) and a 30 degrees pitched roof. The spacing between the collector and the roof was 150 mm.

Another full-scale study was carried out by Geurts and Steenbergen (2009). In this study, two dummy PV panels with 12 pressure taps on the upper and lower surface were used. The size of each panel was 1.6 m in length, 0.8 m in width and 0.018 m in thickness and its distance from the roof was 0.15 m. The panels were located on the building roof having a pitch of 42 degrees. The two panels were attached at two different locations; Panel 1 was attached to the Southern slope (orientation 150 degrees) and Panel 2 at the Western side (orientation 240 degrees). In addition to the full-scale experiments, Blackmore and Geurts (2008**)** performed wind tunnel experiments using a 1:100 scaled model of the actual building and PV panel. The spacing between the module and the roof could range from 0.00025 m to 0.003 m. The results presented in their study provided the values of pressure coefficients at some selected pressure taps, either on the upper or on the lower surface of the panels. Nevertheless, it was reported that the net pressure coefficients range from 0.24 to -0.31 for module to roof spacing of 3 mm and 0.25 mm respectively.

Finally, Stenabaugh et al. (2010) carried out a wind tunnel study using two different building models with 30 and 45 degrees roof angles. A scale of 1:20 was selected to attain an adequate resolution for the gap between the module and the roof. The solar array's dimensions were 0.025 m x 0.07275 m and each array was formed by 28 panels. Their experiments were repeated for different gaps between the panels and the roof and considered six different configurations by changing the position of the panel on the roof.

The results focused on design loads and therefore, the peak loads for different configurations were presented.

Experimental Results

The findings from the previously discussed studies have been considered in the comparisons shown in Figures 3.2.4 to 3.2.6 The results are presented in terms of mean and peak net pressure coefficients and are grouped in two sets, based on the roof shape (i.e. hipped and gable roofs). More specifically, Figure 3.2.4 presents the mean and maximum net uplift coefficients for solar panels attached parallel to a 30-degrees hipped roof that cover the whole roof surface (Sparks et al. 1981). The results include findings from both wind tunnel and full-scale experiments. The comparison of the two experimental methods shows that the mean values are in good agreement whereas the maximum net pressure coefficients are somewhat higher in the full-scale study.

Figure 3.2.5 summarizes the experimental findings for the Geurts and Steenbergen (2009) full-scale study. The results refer to two solar panel configurations that have different orientation and are attached to a 42-degree hipped roof. The comparisons of the two different configurations show that the mean and maximum net pressure coefficients are in good agreement for most of the examined wind angles. Some discrepancies occur for the mean values for the 60 to 180-degree range of wind directions. Such differences are even more pronounced for the minimum net pressure coefficients.

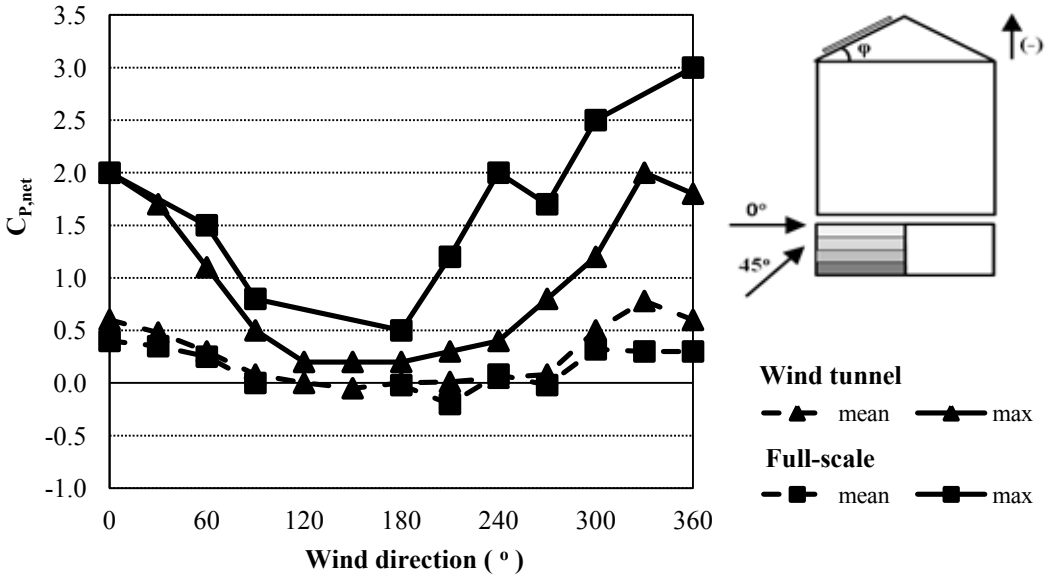

Figure 3.2.4 Net Uplift Pressure Coefficients for solar panels on buildings with 30-degree hipped roof (after Sparks et al. 1981)

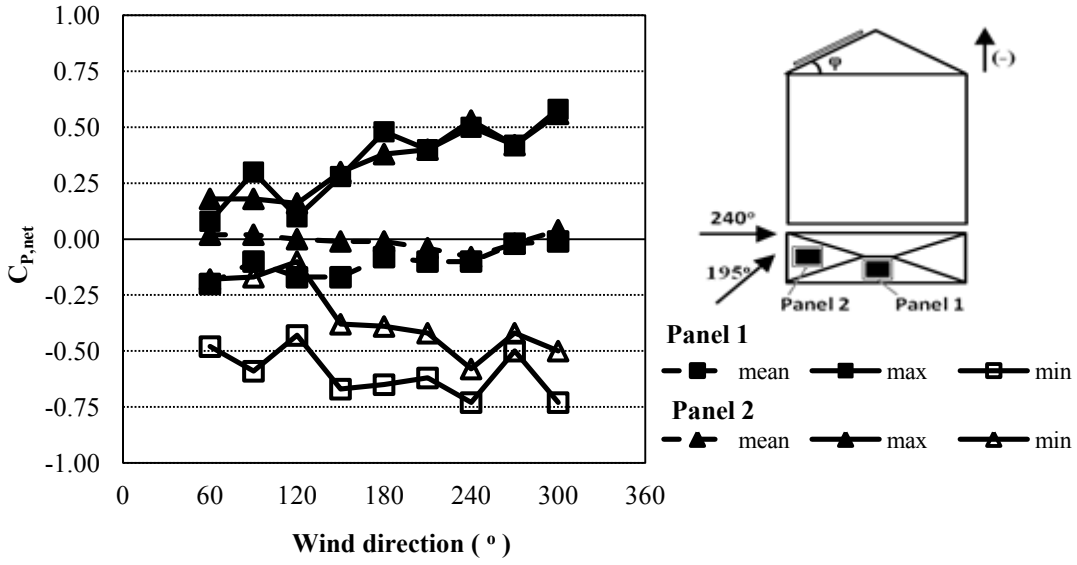

Figure 3.2.5 Net uplift pressure coefficients for solar panels on buildings with 42-degree hipped roof for T=0.1 sec (after Geurts and Steenbergen 2009)

Finally, Figure 3.2.6 presents findings from the Stenabaugh et al. (2010) wind tunnel study. The graph includes results from two building models with roof angles of 30 and 45 degrees respectively. It should be noted that only values obtained from the experiments with the solar panel located at the center of gable roof building are presented. The comparison of the peak uplift pressure coefficients for 90, 180 and 270-degree wind angles show significant differences while for the rest of the examined wind angles, the results are in better agreement.

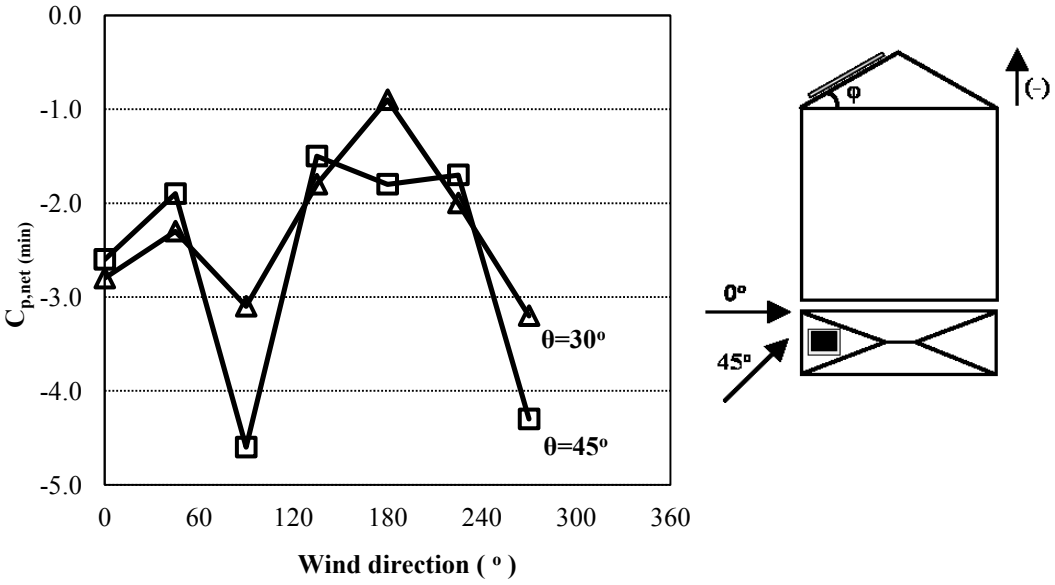

Figure 3.2.6 Minimum uplift pressure coefficients for solar panels located at the center of 30- and 45-degree pitched roofs (after Stenabaugh et al. 2010)

3.2.3 Solar panels and rooftop equipment near roof edges and corners

Description of Studies

There are a very limited number of studies dealing with wind loads applied on rooftop equipment and solar panels located at the edges of the roof. Because of the building geometry, the wind flow pattern will be different near the building edges and will change closer to the center.

Hosoya et al. (2001) conducted wind tunnel experiments in order to investigate the wind-induced loads, such as lateral, uplift forces and overturning moment, applied on a cubic model representing an air conditioner unit placed on top of a building. The geometric scale selected for this study was 1:50 and the dimensions of their cubic model were 0.0244 m x 0.0244 m x 0.0244 m. A total of 25 pressure taps were installed on the sidewall and top surfaces of the cubic model. The cubic model was placed at three different locations in order to examine the wind effect at different distances from the roof edges.

Another interesting study was conducted by Bronkhorst et al. (2010) which examined the wind-induced effect on an array of solar panels located at the roof edge of a flat-roof building. This study included both wind tunnel experiments and numerical simulation. The solar panels had a depth of 0.024 m (wind tunnel model) and an inclination of 35 degrees while 120 pressure taps were used, located along the solar panels. The building model was constructed using a 1:50 geometric scale and its dimensions were equal to 0.2 m x 0.6 m x 0.8 m (height x width x length).

Similar to the previous study, Bienkiewicz and Endo (2009) performed both wind tunnel tests and numerical simulations on loose-laid roofing systems. Pressure measurements were taken at points located at the roof corner region with and without the roofing system in place. The effect of permeability on the total wind-induced force was also examined. The results showed that the system permeability -which is also related to the gaps between the panels- and the flow resistance control the wind uplift reduction under the system, which corresponds to the spacing under the panel. Finally, as previously discussed, Erwin et al. (2011) and Saha et al. (2011) performed wind tunnel and full scale experiments for model configurations in which solar panels are located near roof edges.

A large-scale experimental study was carried out by Erwin et al. (2011) using the 6-fan Wall of Wind (WoW) facility at Florida International University creating turbulent flow conditions. A PV module with dimensions 1.57 m x 0.95 m x 0.041 m (length x width x thickness) was mounted on a flat roof building with dimensions 4.3 m x 4.3 m x 3.2 m. The PV modules were tested in two different positions; namely “Position 1” at the center and close to the roof edge and “Position 2” at the corner of the building. However, the results from this study cannot be compared to this section’s experimental findings since they apply only for the case in which the panels are located at the roof edge and no other study discussed data for such configuration.

Last but not least, Saha et al. (2011) tested an array of 18 solar collector models, two of which were equipped with pressure taps on both the upper and lower surface. The wind tunnel model was of 1:50 geometric scale and the size of each collector was 0.02 m x 0.04 m. The model was tested in suburban exposure with 0.2 power exponent. The solar collectors covered the whole roof of the flat roof building model which had dimensions

equal to 0.4 m x 0.45 m x 0.45 m (height x width x depth). Several different collector location configurations were examined such as edge and center areas by changing the position of the two-instrumented panels.

Experimental Results

Although, Hosoya et al. (2001) and Bronkhorst et al. (2010) examined the wind loads when the units were placed at the roof edge, the comparison between the results of the two studies is not possible due to the different model geometry; i.e. inclined panels vs. cubic attachment. Moreover, the area of the solar panel models is much bigger compared to that of the cubic model. However, comparisons were made for the studies of Erwin et al. (2011) and Saha et al. (2011) and are presented in Figure 3.2.7. Several cases for different inclinations have been included in this comparison and results are presented in terms of both mean and peak net pressure coefficients.

As far as the Erwin et al. (2011) study is concerned, both mean and peak values follow the same pattern for 15 and 45 degrees panel inclination. The inclination of the panels has a minimal effect on the mean values. The absolute minimum and maximum net pressure coefficients reach their peak for the wind directions of 45 and 135 degrees respectively. It should be noted that for wind directions greater than 45 degrees, the minimum and maximum values are really close for the configurations of 15 and 45-degree panel inclination. On the other hand, Saha et al. (2011) maximum values show a different trend and are in relative agreement to those of Erwin et al. (2011) only for the case of 0-degree wind direction. This phenomenon can be attributed to the fact that different geometries were considered for the building and solar panel models. Moreover, it should be noted

that Erwin et al. (2011) performed full-scale experiments while Saha et al. (2011) only wind tunnel tests.

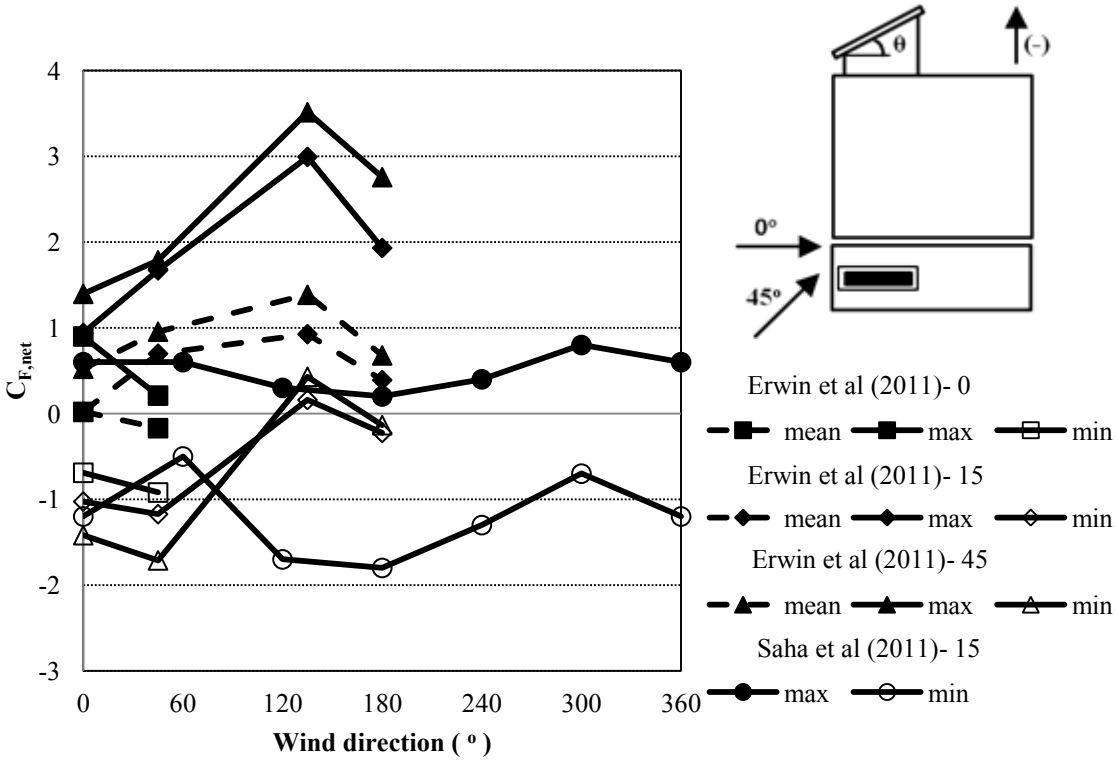

Figure 3.2.7 Force Coefficients for solar panels located near roof edges (corner position)

3.2.4 Sloped solar panels at the ground level

There are a few studies that have been carried out regarding the wind loads either applied on single solar collector panels or arrayed panels which are located in the fields. The data concerning those studies have been collected and presented in this section for inclined solar collectors at an angle greater than 10 degrees with respect to the flat surface.

Description of Studies

One very interesting study was conducted by Kopp et al (2002), who performed wind tunnel experiments on a solar collector system consisting of six parallel slender modules incorporated in a frame with curved top module surface using a 1:6 scale. The distance between the modules was 76 mm and the length of the module was 750 mm. The six wind tunnel scaled modules were equipped with 504 pressure taps in total. The Reynolds number was $7.6x10^4$. The results were presented in terms of wind uplift pressure coefficient and the worst cases occurred for 270^o and 330^o wind angles. Peak and mean pressure coefficients were estimated for turbulent flow for 45-degree inclination and 75-degree module angle.

Wind tunnel experiments were performed by Chung et al (2008) using a 60% scaled, commercial solar water heater (see Figure 3.2.8), which included a flat panel of 1.2 m x 0.6 m dimensions and a cylinder on top of it with 0.27 m diameter and 0.7 m length. The flat plate faced the flow direction and was inclined at an angle of 25 degrees, which is considered the worst case as far as the wind uplift pressure coefficient is concerned and the one commonly used for solar panels installation in Taiwan. The pressure was measured on the upper and lower surface of the flat panel by drilling the surface and placing 26 pressure taps along the centerline of the panel. A closed loop low speed wind tunnel was employed with constant area test section of 1.2 m high, 1.8 m wide and 2.7 m long while the turbulence intensity was 0.3% with the wind speed adjusted from 20 m/s to 50 m/s. Nevertheless, the main goal of the study was to focus on the effect of a steady wind and as a result, the flow was uniform instead of simulated boundary layer.

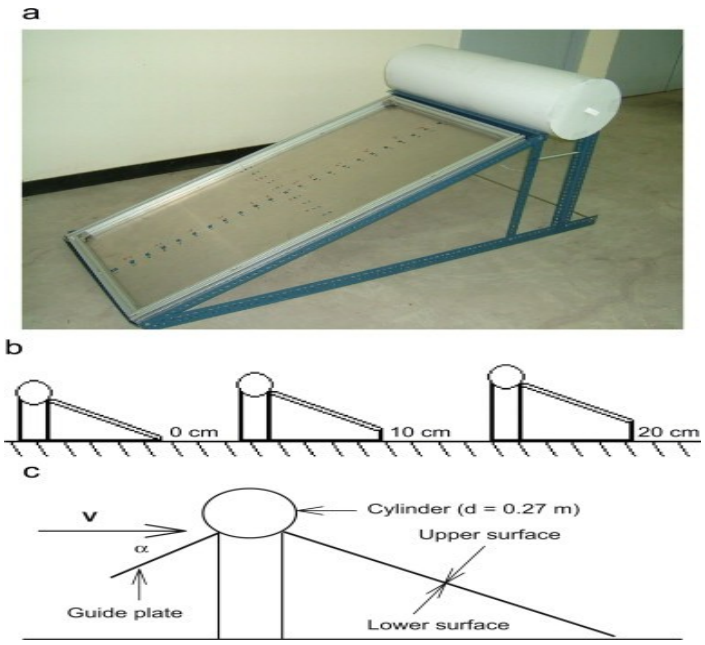

Figure 3.2.8 Solar water heater (after Chung et al, 2008)

In another study released one year later, again by Chung et al (2009) wind tunnel experiments were carried out using the same laboratory equipment and therefore the initial conditions remained the same. They changed, however, their models using a 60% scaled plate model with a cylinder, a 60% plate model that was only a flat panel and a 40% model with a flat plate panel. Their models were tested for inclinations of 15, 20, 25, and 30 degrees facing the flow direction.

CFD simulations were carried out by Shademan and Hangan (2009) on stand-alone and arrayed panels for a set of 3x4 solar panels. Each panel had dimensions 1 m in length, 0.5 m in width and 3 mm thickness with gaps of 0.01 m between two panels. The model formed, was 22 m in length, 15 m in width and 10 m in height, and was raised 0.6 m above the ground. The dimensions of the computational domain were 22 m in length,

15 m in width and 5 m in height. Two different inclinations (30 and 35 degrees) of the panel and three wind directions (30, 60, 90 degrees) were simulated in order for the wind loads to be investigated under different configurations.

More wind tunnel experiments followed by Chung et al (2011) who fabricated a 60% scaled commercial solar panel (1.2 m x 0.6 m) with horizontal cylinder (0.27 m in diameter and 0.7 m in length). They tested their model under the same conditions as in the previous studies, where the maximum blockage ratio was 8.75%. The residential flat panel under consideration was inclined, with a tilt angle of 15, 20 and 25 degrees respectively with respect to the flat ground level. The pattern followed for measuring the pressure on the upper and lower surface of the panel was the same as described in their previous experiments.

Shademan et al (2010) repeated their CFD simulation for 12 stand-alone panels arrayed using the same configuration. Four different inclinations (30^o, 35^o, 40^o, 50^o) and 7 wind directions (0^o, 30^o, 60^o, 90^o, 120^o, 150^o, 180^o) were simulated. The dimensions of the computational domain are 30 m in length, 21 m in width and 10 m in height while the Reynolds number under which the simulation was conducted is $Re = 2x10^6$. By testing all the different configurations described, it was found that the worst wind loads occurred for 0 and 180 degrees.

Two different methods used by Bitsuamlak et al (2010) tried to investigate the aerodynamic characteristics of panels located on the ground under boundary layer effect. The study included both computational simulations and full-scale experiments. For the numerical simulation, a typical panel of 1.3 m height was considered with inclination of

40 degrees. The angle of attack was 0, 30 and 180 degrees. The full-scale experiments took place at Florida International University and the wind uplift pressure coefficients on the panels were determined. The 11 pressure taps used, were located along a vertical line on the upper and lower surface of the panels. The dimensions of the panels were 1.3 m x1.1 m x0.019 m (length x width x depth) and they were attached to a frame inclined by 40 degrees angle while the incidence wind angle could take the values 0 and 180 degrees.

Meroney and Neff (2010) carried out some numerical calculations and wind tunnel experiments to estimate the uplift coefficient on solar collectors for 2-D and 3-D flow patterns using ½ scale models, which were inclined by 10 degrees with respect to the flat roof. They used eight additional dummy tiles so as an array 3x3 in size could be installed in the 1.8 meters wide wind tunnel.

Experimental Results

A summary of the experimental and simulation results for stand-alone solar panels inclined by an angle ranging from 10 to 25 degrees is shown in Table 3.2.1.

According to Meroney and Neff (2010) results, it can be said that for 10^{o} inclination, the net uplift pressure coefficient is greater for 180^{o} wind angle compared to the 0^{o} wind direction.

Chung et al (2008, 2009) experiments seem to be in agreement since only small differences can be observed concerning their examined model which is fabricated in a 60% scale. In addition, as the inclination gets greater values, the suction increases since its absolute value becomes greater.

Wind Direction	0^o	180^o
Meroney and Neff (2010) 10^o inclination		
CFD- 2D	-0.04	-0.183
Measured- 2D	0.07	-0.073
CFD- 3D	-0.02	-0.1
Measured- 3D	0.07	-0.07
Chung et al (2008), 25^o inclination		-1.1
Chung et al (2009)		
Case B, 15^o inclination		-0.6
Case C, 15^o inclination		-0.4
Case B, 20^o inclination		-0.8
Case C, 20^o inclination		-0.6
Case B, 25^o inclination		-1
Case C, 25^o inclination		-0.8
Chung et al (2011)		
15^o inclination		-0.8
20^o inclination		-1.0
25^o inclination		-1.1

Case B: 60% scaled model with a flat panel only

Case C: 40% scaled model with a flat panel only

Table 3.2.1 Stand-alone solar panels inclined by a 10 to 25 degrees angle

Figure 3.2.9 depicts the results for solar panels inclined by a 30 and 35 degrees slope. From this Figure, it can be observed that the uplift pressure coefficient takes only positive values when CFD methods apply. Therefore, the results coming out of Shademan and Hangan (2009, 2010) and Chung et al (2009) take values with opposite signs for 180 degrees wind angle. It can be seen that Shademan's CFD results are not in good agreement either and the only differences between the two studies is the computational domain considered.

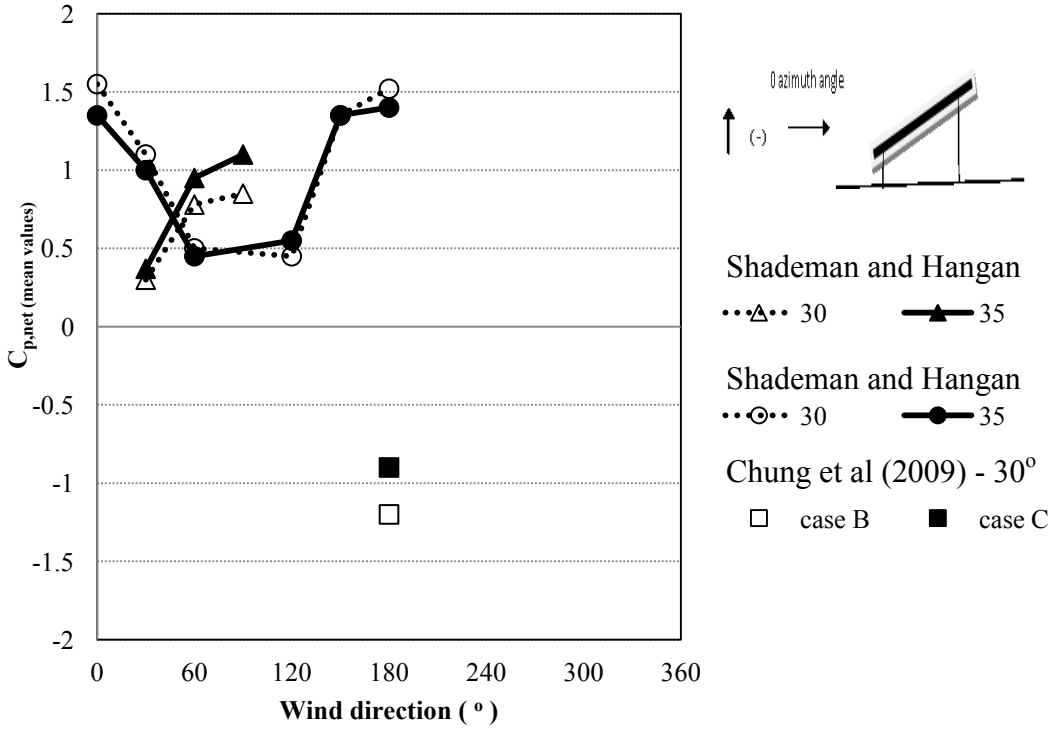

Figure 3.2.9 Net uplift pressure coefficient for solar panels inclined by 30 and 35 degrees angle on the ground level

However, it is necessary to mention that the results shown in Figure 3.2.9 are the values of the wind uplift pressure coefficients corresponding to those values recorded at the

middle of the flat solar panels. The particular location was selected because in some cases, the pressure coefficient is provided only along the centerline and therefore comparison can be feasible among different studies.

Figure 3.2.10 presents the results for solar panels inclined by a 40 to 50 degrees angle. Bitsuamlak et al (2010) study shows that their experimental results, although two different methods were used (full scale experiments and CFD simulations), are in good agreement. For wind angles in the range of 0 to 60 degrees wind angle Shademan and Hangan's results agree with those of Bitsuamlak. However, for a wind angle 180^{o}, the uplift pressure coefficient takes positive values for Shademan and Hangan study while for Bitsuamlak are negative.

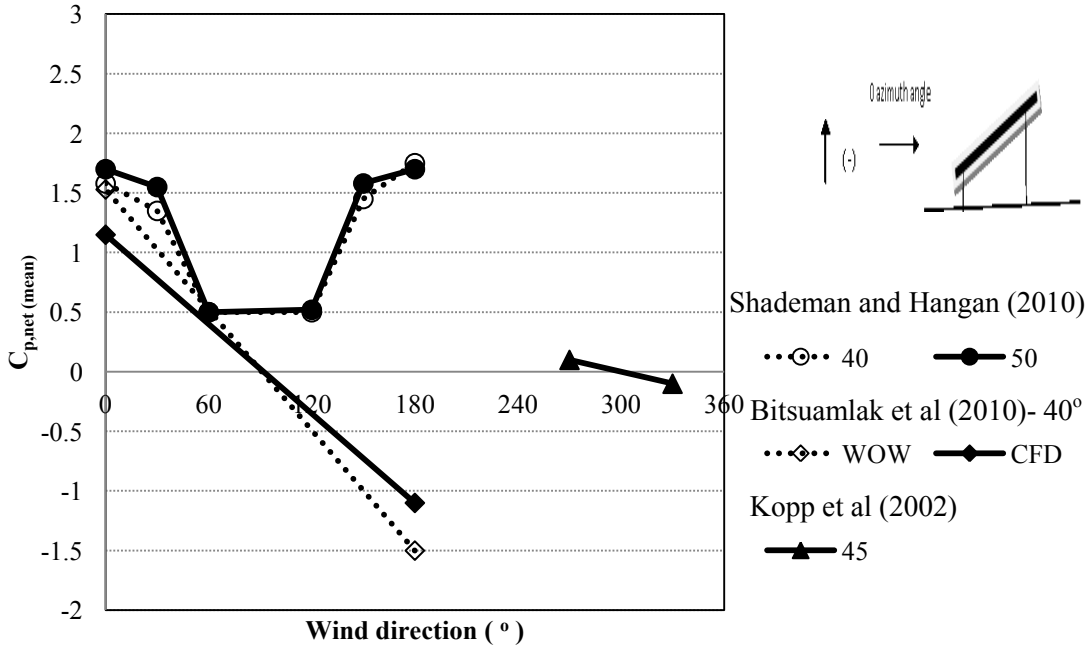

Figure 3.2.10 Net Uplift Pressure Coefficient for solar panels inclined by a 40-50 angle at the ground level

CHAPTER 4: WIND TUNNEL STUDY

4.1 GENERAL

Wind tunnel experiments play a very important role in determining the wind loads applied on structures. This chapter summarizes and describes all the necessary information related to wind tunnel testing such as the wind tunnel facilities, the boundary layer simulation, as well as, the models constructed and tested. Moreover, the equipment used, the wind tunnel experimental method, the data analysis procedure and finally the repeatability tests are also presented in this chapter.

4.2 WIND TUNNEL FACILITIES

The experiments described in this chapter took place at the Building Aerodynamic Laboratory located at the Engineering Building of Concordia University. The type of the wind tunnel falls in the category of an open circuit, blowdown tunnel having a working area 12 m long and cross-section 1.8 m wide and height ranging from 1.4 m to 1.8 m - see Figures 4.2.1 and 4.2.2. Models are usually located into the downstream section on a turntable of 1.21 m diameter which can operate manually or electrically and allows models to be tested for different wind attack angles. The wind speed can range from 3 m/s to 14 m/s inside the wind tunnel section.

The floor of the working section in the wind tunnel is covered with a certain type of carpet which is used to simulate the open country terrain. For different terrain types to be simulated, roughness elements are added on panels which can be inserted in the wind

tunnel test section. Additional details for the wind tunnel construction and characteristics are given by Stathopoulos (1984).

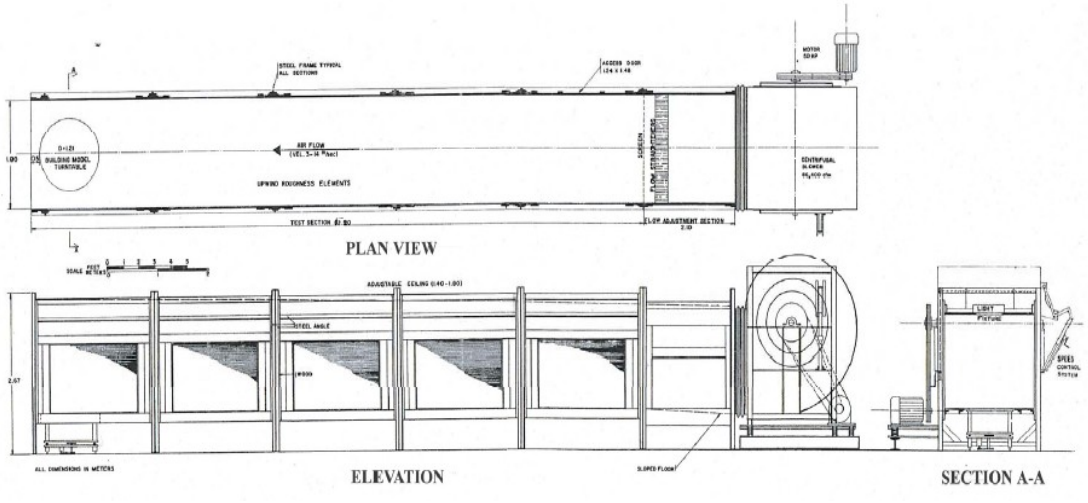

Figure 4.2.1 The Boundary Layer Wind Tunnel of Concordia University after Stathopoulos (1984)

Figure 4.2.2 Front View of the Boundary Layer Wind Tunnel with the building model in position

4.3 ATMOSPHERIC BOUNDARY LAYER

It is really crucial when performing wind tunnel experiments for building testing to accurately simulate the atmospheric boundary layer wind velocity profile. As has already been mentioned in a previous chapter, wind fluctuates randomly and this is the reason why it is characterized as turbulent. The floor of the atmospheric boundary layer wind tunnel of Concordia University is covered by carpet and thus is classified by default in the open terrain category.

Before starting with the experiments, the velocity wind profile had to be checked without the test model in its position. More specifically, the wind speed was measured at the center of the wind tunnel section at different heights. Figure 4.3.1 gives the curve of the wind speed measured at different heights as a function of the height in comparison with the theoretical curve resulting from the power law when $\alpha = 0.16$. Figure 4.3.2 presents the turbulence intensity profile which is 17.65% at the top of the 7 m high building and 13.9% at the top of the 16 m high building.

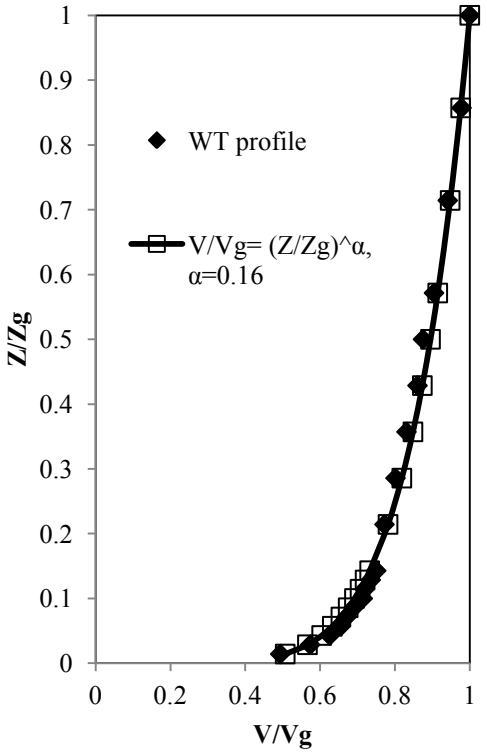

Figure 4.3.1 Wind velocity profile

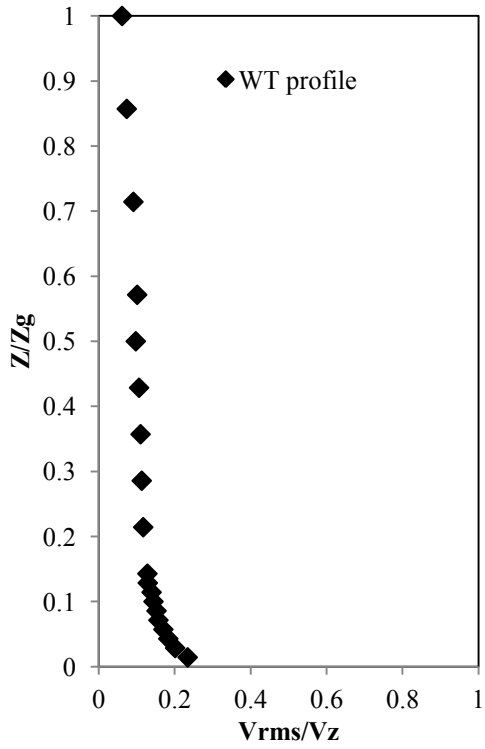

Figure 4.3.2 Turbulence intensity profile

4.4 BUILDING AND SOLAR PANEL MODEL

A geometrical scale 1:200 was selected, considering the similarity parameters that must be satisfied when performing wind tunnel tests. A sophisticated model was constructed so as to simulate a prototype building as realistically as possible. The model consists of a rectangular building model on top of which three identical panels were attached. Both panels and building model were constructed under 1:200 scale. Transparent plastic was used for the fabrication of the walls having a thickness of 10 mm at the front and back walls and 3 mm at the side walls, while the roof and the panels were metallic. The external dimensions of the building model were 15.3 cm (length) x 9.8 cm (width), while

the height corresponding to two different cases was 3.5 cm and 8 cm respectively (Figure 4.4.1).

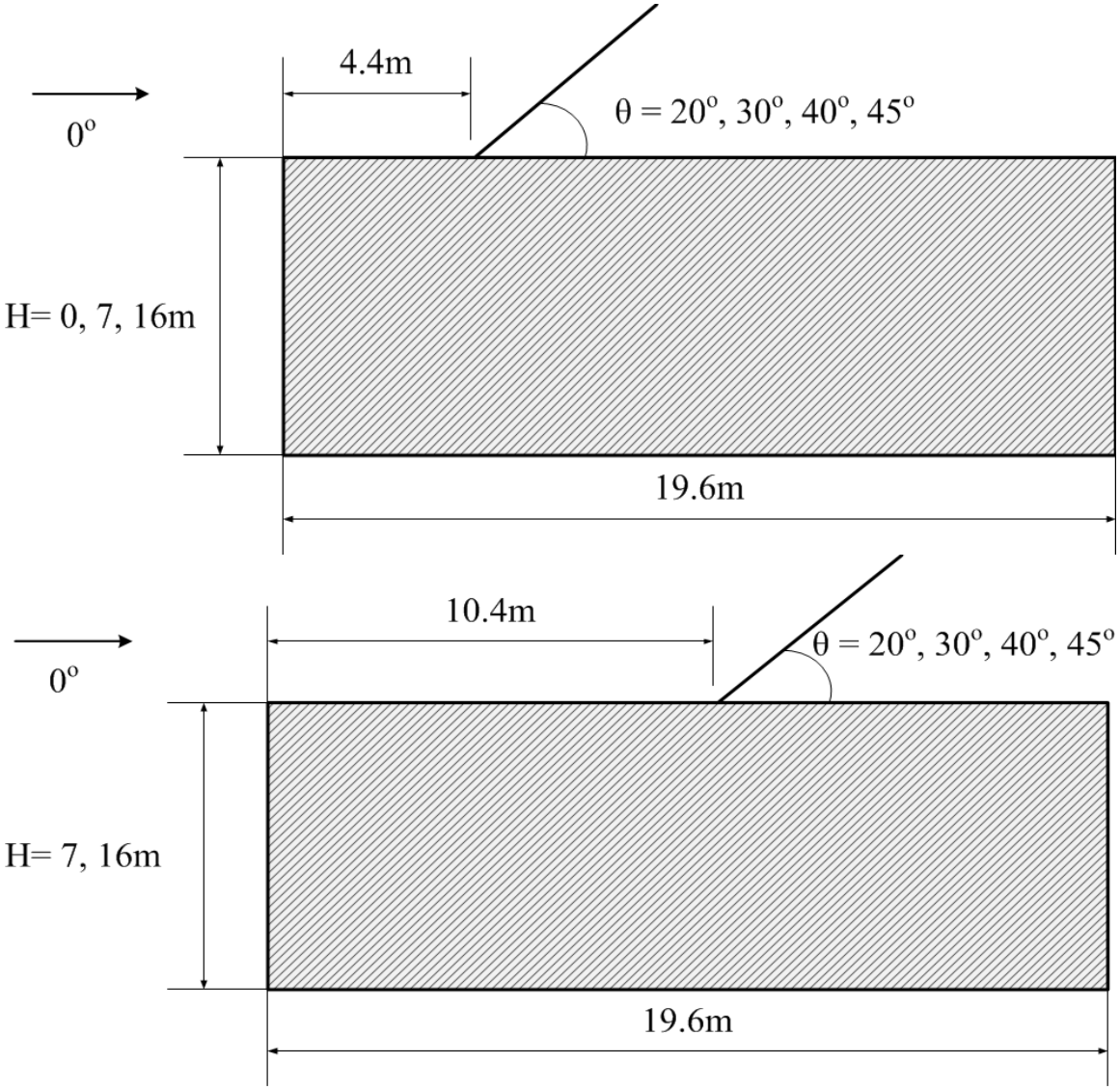

Figure 4.4.1 Elevation of building models with inclined solar panels attached

Three similar panels were mounted on the building roof. Their dimensions were 4.3 cm (length), 2.8 cm (width) and 1 mm (thickness). The panels were located in two different positions on the roof, the one closer to the side facing the 0° wind direction and the other

closer to the opposite side. For the front location, the distance between the panel base and the front edge is 2.2 cm and 1.2 cm from the side edge. For the back location, the base of the panel is found at a distance 5.2 cm from the front edge of the building and 1.2 cm from the side edge. The model allows the inclination of the panels to change with the smallest slope being 20 degrees.

In order to measure the wind loads applied on the solar panels, 36 pressure taps in total were attached on the panels measuring the pressure on the upper and lower surface of the panel. Each panel was equipped with 12 pressure taps, 6 on each side connected with tubing that passed inside the building through the roof. The brass taps were connected to transducers through flexible urethane tubes. A brass restrictor was placed at the 10/24 of the total length of the tubing (10:14 length ratio) so as the effects of the frequency response to be eliminated. Considering the three panels as one, the pressure taps were located at equal distances among them. Figures 4.4.2 and 4.4.3 show the pressure tap distribution on the panels' surface.

However, the main difficulty for such a structure is to connect the pressure taps located on the panel surface with the ZOC scanner. In most studies the tubing passes through the ceiling to end up inside the building and in this way the flow underneath the panel is obstructed. For this reason, for the current study three small metallic "legs" were constructed for each panel (Figure 4.4.4) through which the strings of the pressure taps passed. These legs have been adapted into small holes on the ceiling in which they can rotate and from where the metallic cables end up inside the building. The tubing was then attached to the metallic endings and finally connected to the ZOC (Figure 4.4.5).

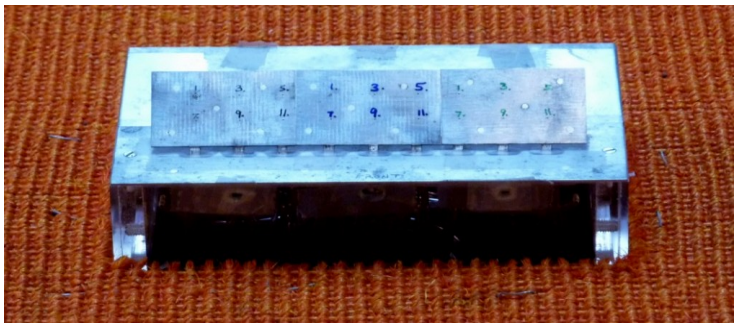

Figure 4.4.2 Pressure tap distribution on the solar panel surface

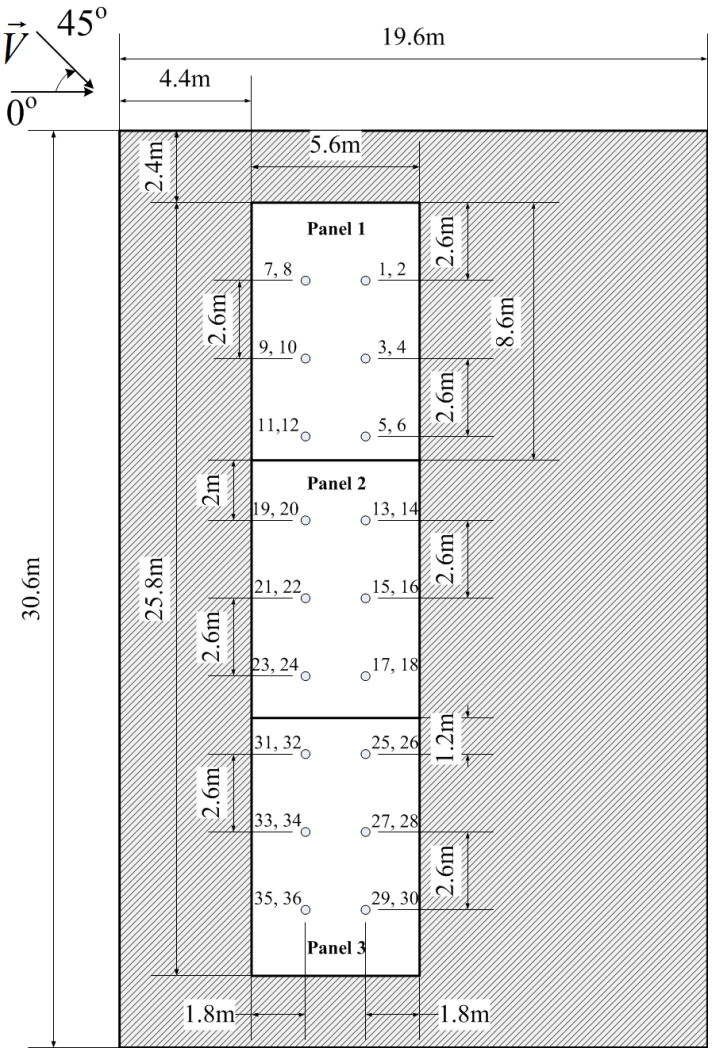

Figure 4.4.3 Top view of the building roof with solar panels attached and pressure tap notation

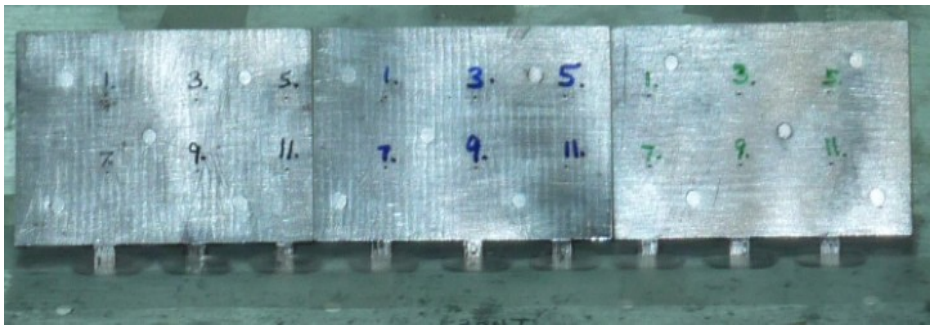

Figure 4.4.4 Detailed view of the solar panel “legs”

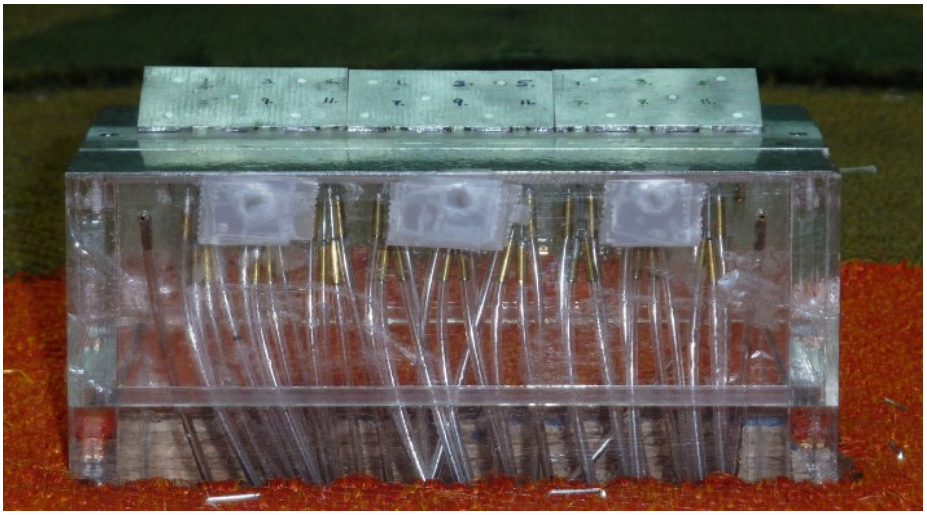

Figure 4.4.5 View of the pressure tap tubing

The building model was located on the turntable as illustrated in Figure 4.4.6 which can rotate 360 degrees and allows different wind attack angles to be tested. The building base that was set in the turntable allowed the building movement upwards and downwards so that the wind loads applied on the panels could be examined for different building heights.

Since the environment plays an important role for the flow, it needs to be clarified that the experiments were conducted for the case of an open terrain simulation. Additionally, sharp edges and corners on the building and panel models are really important for the flow separation to occur. In this way, kinematic and dynamic similarities can be assured even if the Reynolds number of the model is not the same as that for the prototype.

Figure 4.4.6 View of building model with panels placed on the turntable at 135^{o} wind direction

4.5 EQUIPMENT

This section presents the sophisticated instrumentation with which the wind tunnel is equipped. Figure 4.5.1 shows how the instruments are connected. The measurements of wind speed and turbulence intensity profile were conducted using the 4-hole Cobra probe. A 1000 Hz sampling rate was used for the velocity measurements and 30 seconds was the duration of each run. For the open terrain, the gradient mean wind velocity was approximately 13.6 m/s.

A sensitive pressure scanning system was used for pressure measurements. This system consists of a Digital Service Module (DSM 3400) and one pressure scanner ZOC33/64Px from Scanivalve. The DSM can be connected with up to 8 ZOC pressure scanners and through Ethernet all the output data can be transferred to a computer. A ZOC module can host up to 64 pressure sensors. Its temperature has to be maintained constant and this is why it is kept inside an insulated thermal unit. For the current experiment 36 pressure taps were connected through urethane tubing to the ZOC which in turn was connected to the DSM unit. The DSM system was scanning every 50 μs and as a result the sampling frequency was 312.5 Hz. In total, 8200 frames were scanned which means that the duration for each run was 26.25 sec. The output data acquired during the scanning process was in binary format and Ethernet connection was used for the transfer.

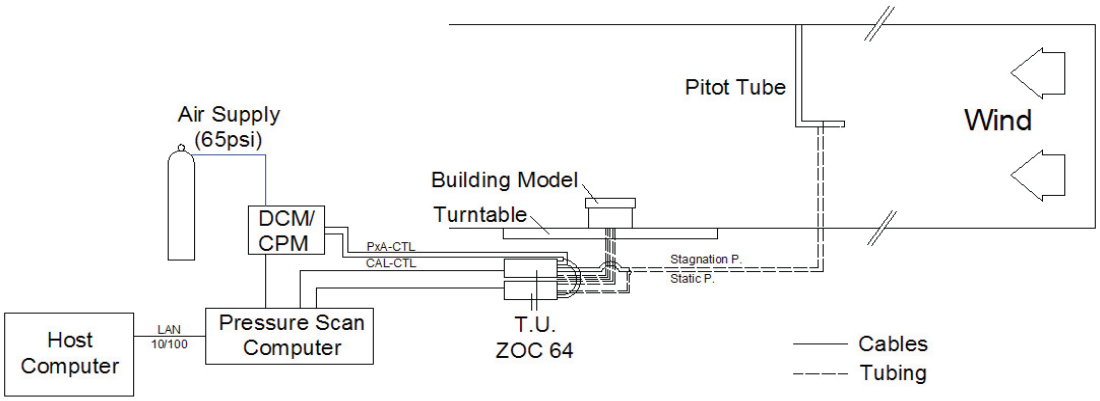

Figure 4.5.1 Sketch of the experimental wind tunnel equipment (after Zisis 2006)

4.6 WIND TUNNEL TESTS

For the experiments performed, the 36 pressure taps of the panels were connected to a ZOC module. A cable connected the ZOC module with the DSM unit and then the signals were transferred to a host computer. This computer is equipped with two software: DSM-Link which measures scans of low and moderate frequencies and Btel for higher frequencies.

The building model with the panels attached is symmetrical and for this reason the wind direction ranged from 0 to 180 degrees while a total number of 13 wind attack angles were tested with 15 degree intervals. The model can also be tested for different panel inclinations and for the present study the panel angles tested were 20, 30, 40 and 45 degrees.

The experimental procedure followed is described below:

- Choose and set the panel inclination examined
- Set all the panels at the same inclination

- Set the building at 0^o wind direction (facing the wind tunnel fan)
- Provide compressed air in the tubing
- Run DSM-Link and perform a zero calibration for all the channels
- Turn on the wind tunnel fan
- Open B-Tel file, scan, close and save the file
- Change the direction of the turntable and continue the same procedure for 15^o increments for wind direction ranging from 0-180 degrees
- Turn off the wind tunnel fan
- Repeat zero calibration

The zero calibration was performed so as the drift of the sensors measuring the pressure to be estimated and corrected. The files were all saved with two characteristic numbers, one indicating the panel slope and the other the wind attack angle.

In total four rounds of measurements took place, each one for different panel slope and for 13 different wind directions with 15 degree intervals.

4.7 DATA ANALYSIS

The mean and peak pressure coefficients have been derived by applying dimensional analysis. The following formulas have been used:

$$C_{p,mean} = \frac{P_{mean} - P_a}{1/2\rho U^2} \quad (4.1)$$

$$C_{p,peak} = \frac{P_{peak} - P_a}{1/2\rho U^2} \quad (4.2)$$

The units that have been used for the above equations are kPa for the pressure, m/s for the wind speed and kg/m^3 for the air density. The measurements of the pressure are given in binary format from the software. The procedure followed was the same for all the cases and is described below:

- Import the record of the pressure scanned for all wind attack angles for each slope
- Import the record of the error-drift for each case
- Subtract the corresponding drift values for each channel

In order to estimate the C_p values, it is necessary to know the dynamic pressure at the building height. Using the power law for $\alpha = 0.16$ at the gradient height h = 70 cm and knowing the building height for each case, the dynamic pressure at building height is acquired. A division of the corrected pressure value with the dynamic pressure at building height gives the pressure coefficient. More specifically, for the mean pressure coefficients, the average value of the estimated pressure coefficient for each channel is calculated, whereas, for the peak pressure coefficients the average value of the ten maximum and ten minimum values are computed for each channel.

The force coefficients for each panel, considering that the area corresponding to each pressure tap was approximately equal, were calculated by adding the net local pressure coefficients and then dividing by the number of the pressure taps.

Basically, the output data has a signal form as depicted in Figure 4.7.1. It is this signal that is corrected accordingly and transformed so as the pressure and force coefficients to be acquired. The signal of Figure 4.7.1 corresponds to the pressure tap number 1, when

wind direction is 0^o, the panel inclination is 20^o, the building height is 7 m and the panel is located at front position.

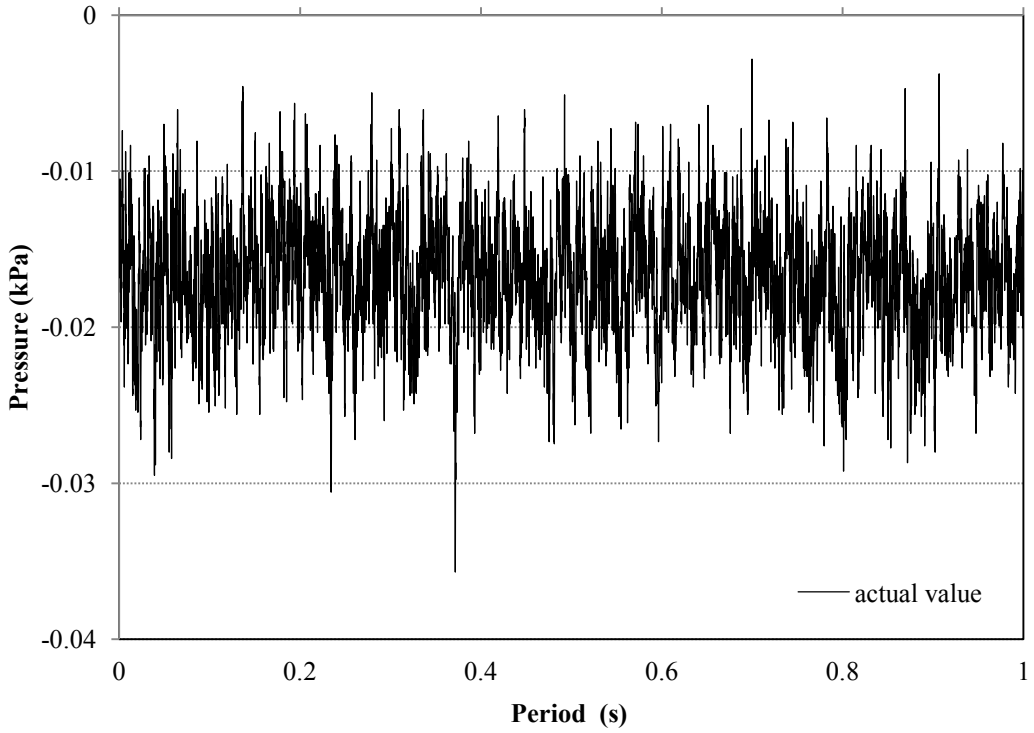

Figure 4.7.1 Pressure signal over a period for pressure tap # 1, for 20^o panel inclination, 7 m building height, front location

4.8 REPEATABILITY OF DATA

During the experimental process, it is really important to confirm the validity of the experimental results. Therefore, two identical experiments took place with eleven days difference. The model was tested for the case of 16 m building height, 20^o panel inclination, with panels located at front position for all wind directions. As depicted in Figure 4.8.1 both experiments show almost identical experimental results as far as the mean and peak pressure coefficients are concerned. The fact that the data shows good repeatability can be further used so as to reassure that the experimental instruments and equipment function properly and provide valid data.

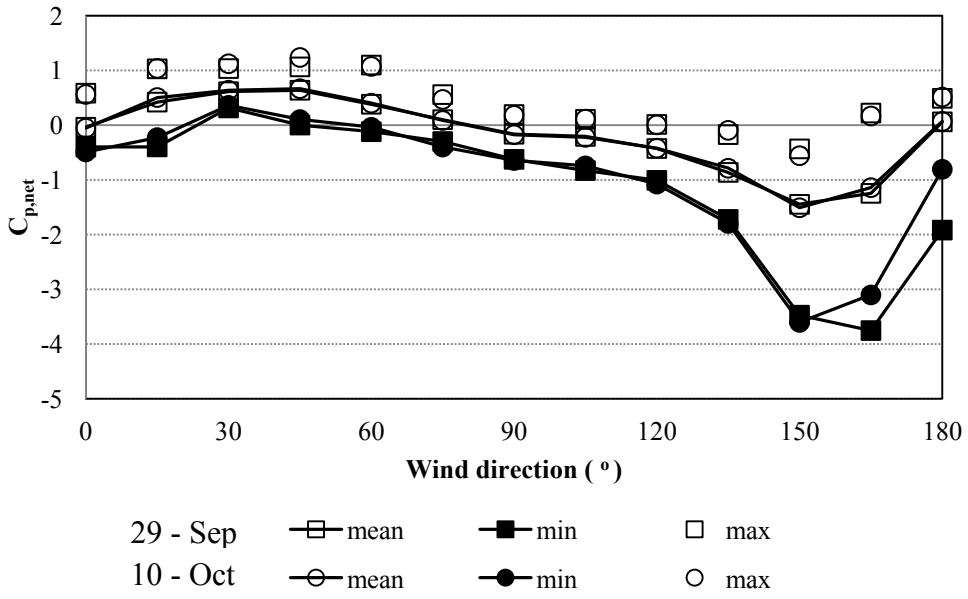

Figure 4.8.1 Repeatability of data for mean and peak net pressure coefficients for panel (pressure tap #1) attached to 16 m building height, 20^o panel inclination, front location and 0^o wind direction

CHAPTER 5: RESULTS AND DISCUSSION

5.1 GENERAL

The output data after the completion of the wind tunnel experiments were all organized in different sections in this chapter so as the effect of different parameters to be shown and discussed. The experiments were performed for two different building heights and two different panel locations; namely front (closer to the building edge facing the 0^o wind direction – see Figure 5.1.1) and back (closer to the opposite edge – see Figure 5.1.2). In addition, a third configuration was examined, for panels located at ground level – see Figure 5.1.1). Moreover, thirteen different wind directions were examined starting from 0^o to 180^o with 15^o intervals and four different panel inclinations namely 20-, 30-, 40-, 45- degrees. A selection of the most critical cases are presented in this chapter, additional data are shown in Appendices A and B.

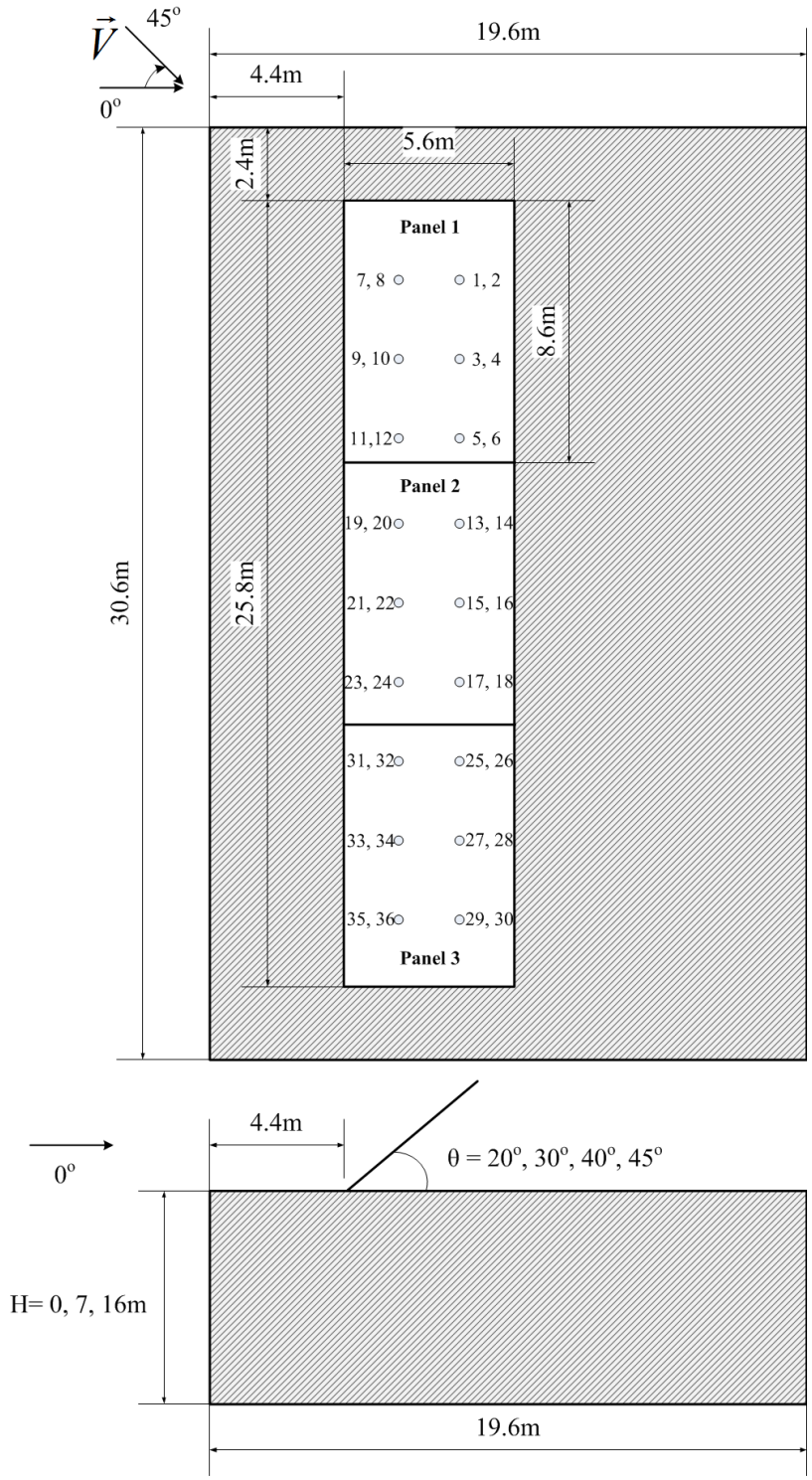

Figure 5.1.1 Top and side building views with front panel configuration

Note: Odd numbers correspond to the upper panel surface while even numbers to the lower panel surface.

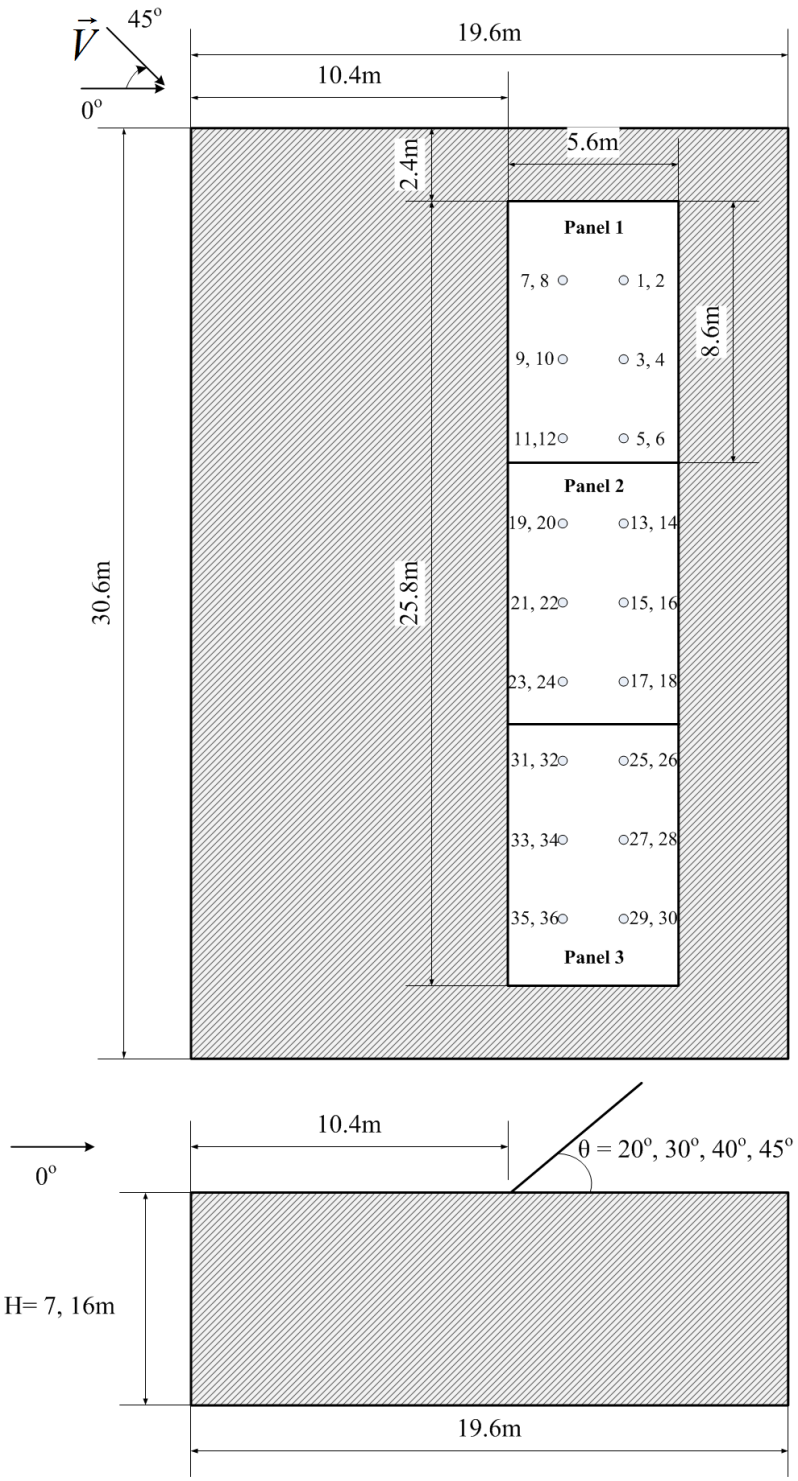

Figure 5.1.2 Top and side building views with back panel configuration

Wind tunnel experiments produced a wide range of data which were further analyzed so as to better understand the wind-induced response of these structures. The values of mean and peak pressure coefficients were all evaluated for individual set of taps on solar panels corresponding either on the upper or the lower panel surface. Moreover, the net pressure coefficients were calculated by considering simultaneously the upper and lower surface pressure traces. Calculation of net pressure coefficients for individual set of taps on solar panels shows that minimum values are more critical since in terms of absolute values are greater compared to those of the maxima. Further investigation of the acquired data can provide information for the exact location at which extremes occur as well as for their magnitude.

This kind of information concerning the exact location is provided in Table 5.1.1 which summarizes the pressure tap numbers for which the most extreme values of the net minima are observed. It should be noted that all tested wind directions were considered as well as all model configurations. The grey-coloured boxes indicate for which wind direction the most extreme values occur, while the number in the grey boxes corresponds to the pressure tap. Clearly, the most critical minima do occur for wind directions ranging from 120^{o} to 165^{o} and especially for 135^{o} wind direction for which most configurations get their peak value. Along with 135^{o} wind direction, pressure tap number 1 is experiencing the greatest pressure.

The most critical case, in terms of net pressure coefficients, is for approaching wind direction 135 degrees. For this reason, detailed contour plots have been drawn for wind direction 135^{o} so as the most typical and at the same time critical results to be presented.

Contour lines are really helpful in illustrating the pressure field created on the surface of panels during their exposure to wind. The results were grouped in different categories showing the mean and peak values of pressure coefficients for upper and lower panel surface separately, as well as the net values by considering the upper and lower surface simultaneously.

	azimuth / inclination	0	15	30	45	60	75	90	105	120	135	150	165	180
	Pressure tap #													
At ground level	**20°**	15	15	15	15	15	15	7	7	5	5	3	1	1
	30°	15	15	15	15	15	15	15	13	13	3	3	1	9
	40°	15	15	15	15	15	15	7	13	1	1	1	9	9
	45°	15	15	15	15	15	15	7	1	1	1	7	9	19
On 7 m roof	**20° front**	23	19	21	23	23	7	7	15	13	5	1	1	29
	20° back	5	35	35	5	5	7	7	7	7	3	1	1	7
	30° front	3	35	35	35	35	7	7	13	1	1	1	1	9
	30° back	13	13	13	13	13	13	7	7	5	1	1	9	33
	40° front	29	29	35	35	35	7	1	1	1	1	1	1	9
	40° back	13	13	13	13	13	13	7	7	1	1	1	9	9
	45° front	3	29	35	29	29	7	7	1	1	1	1	9	19
	45° back	13	13	35	13	13	13	7	1	1	1	7	9	9
On 16 m roof	**20° front**	7	7	21	23	7	7	7	17	15	5	1	1	1
	20° back	13	13	33	13	13	13	9	9	7	3	1	1	9
	30° front	7	7	19	23	7	7	7	13	13	5	1	1	35
	30° back	13	23	33	13	13	13	9	15	7	1	1	7	7
	40° front	7	23	7	31	23	7	7	15	19	9	9	9	9
	40° back	13	23	33	13	13	13	9	15	1	1	7	7	33
	45° front	23	19	33	31	33	7	7	13	13	9	1	9	9
	45° back	13	23	33	13	13	13	7	15	1	1	7	7	33
Total number of pressure taps										**2**	**10**	**5**	**3**	

Table 5.1.1 Pressure taps experiencing extreme net pressure coefficients

5.2 EFFECT OF PANEL INCLINATION ON MEASURED PRESSURE COEFFICIENTS

One of the most interesting aspects of the present study is the illustration of the pressure field using contour plots. These plots are representative of the field created because of panels' exposure to wind. The wind angle 135^o is the most critical and for that reason, the pressure fields have all been plotted for this wind direction. The numbers along the contour lines denote the magnitude of mean and peak pressure coefficients. The mean values of pressure coefficients, which correspond to upper, lower surface and the net values are first depicted for panels attached to 7 m-high building and front located; the minima and maxima of pressure coefficients follow.

Figures 5.2.1, 5.2.2 and 5.2.3 present the mean upper, lower surface and net pressure coefficients respectively, for 20-, 30-, 40- and 45- degree inclination and for panels at the front location of the 7 m-high building.

As demonstrated in Figure 5.2.1, suction occurs for all panel inclinations on the upper surface of the solar panels. Contour lines, however, become less dense with increasing inclination and as a result, suction is smaller. The greatest suction is observed for 20^o and 30^o panel inclination at the upper part of panel 1 for both cases.

Positive mean pressure coefficients are measured for lower panel surface, which vary slightly with panel inclination as depicted by contour lines in Figure 5.2.2. However, slight suction occurs at the edges of panel 1 and panel 3, which diminishes with increasing panel inclination. This phenomenon might be caused because of flow separation that happens near panel edges.

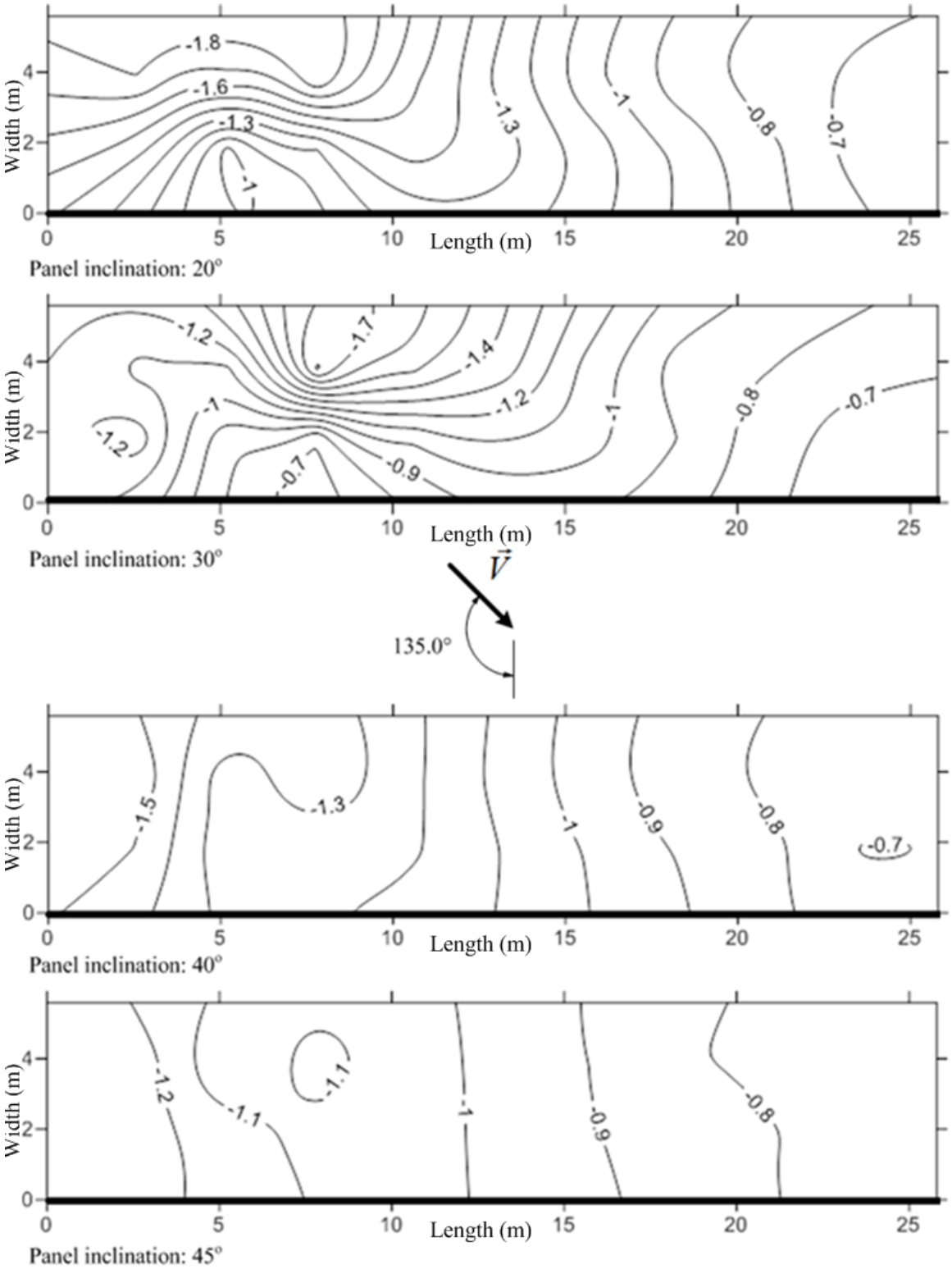

Figure 5.2.1Mean C_p values on upper surface for 7 m building height, front location and 135^o wind direction

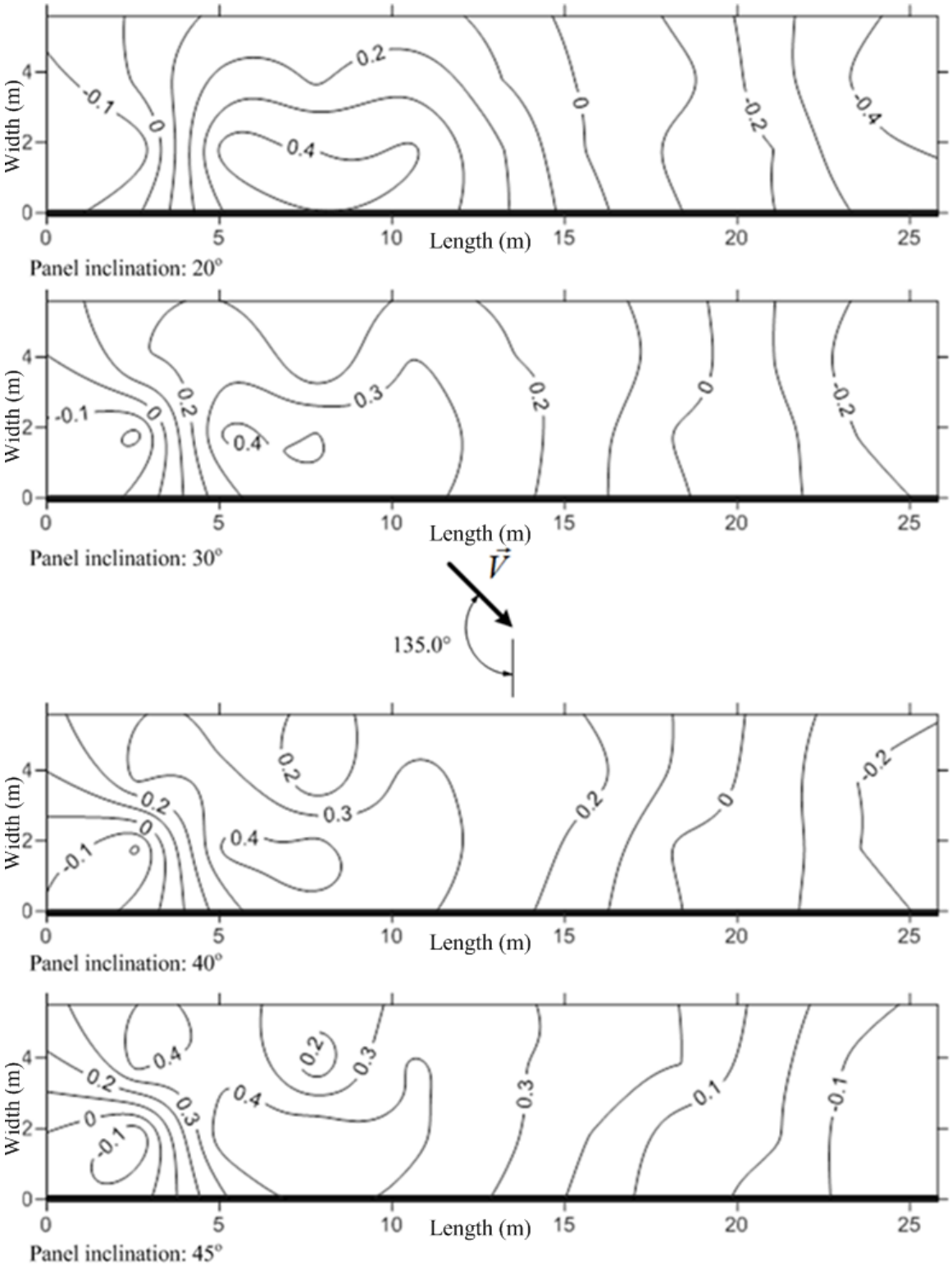

Figure 5.2.2 Mean C_p values on lower surface for 7 m building height, front location and 135^o wind direction

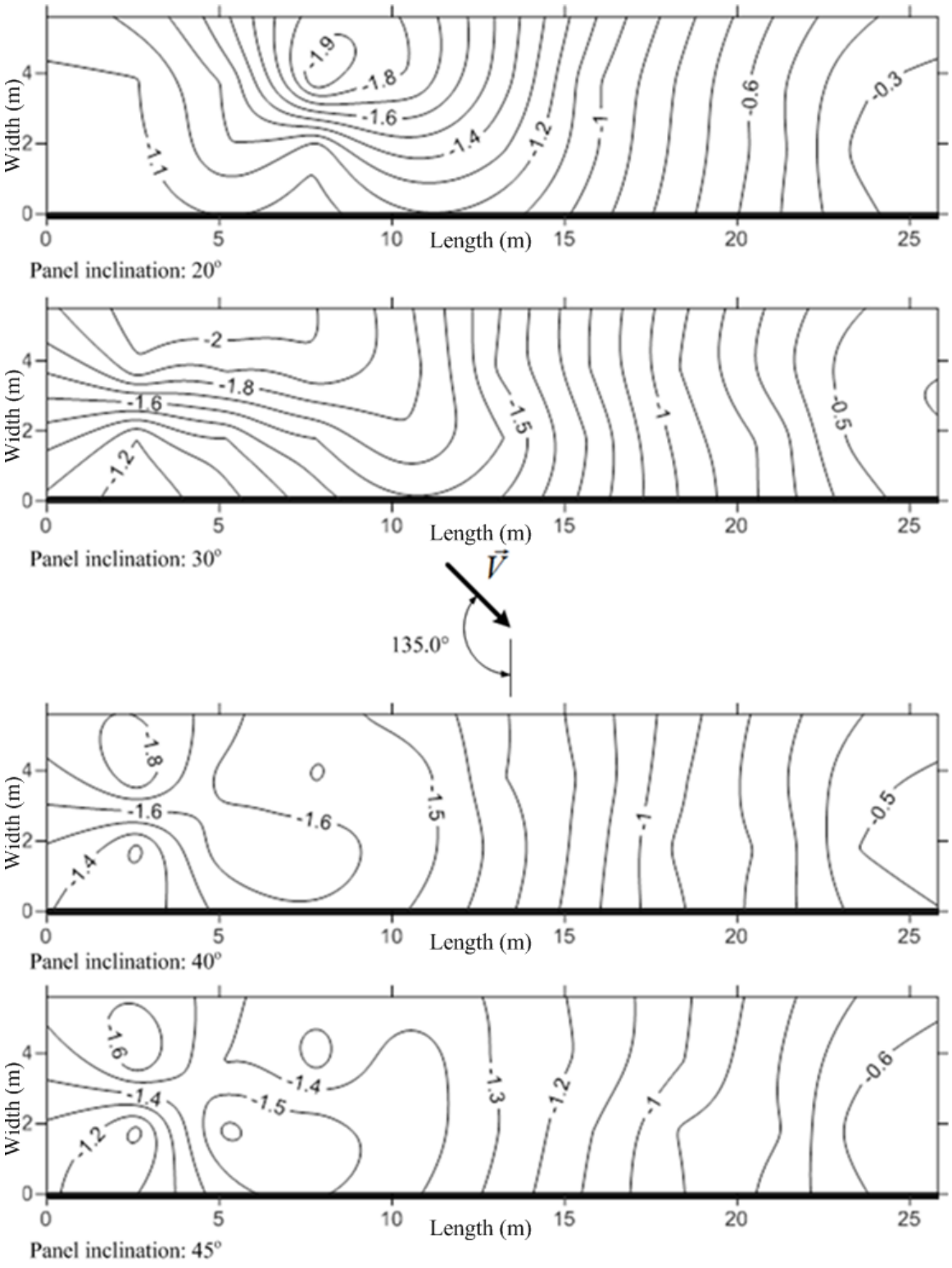

Figure 5.2.3 Net mean C_p values for 7 m building height, front location and 135° wind direction

Combination of the two previous contour maps results in Figure 5.2.3 in which net values of the pressure coefficients offer the overall suction (negative sign) applied on the solar panel. Contour lines indicate that panel 1 is mostly affected by the wind since the field becomes more complex over its surface, while the field over panels 2 and 3 consists of almost parallel contour lines of, generally, smaller values. It is also evident that increasing panel inclination results in decreasing net pressure coefficients due to lower pressure exerted on them. The greatest suction detected, occurs at the upper edge of panel 1 for panel inclination 30^{o}, which slightly differs from the values recorded for 20^{o} panel inclination.

As far as the peak values are concerned, Figures 5.2.4 to 5.2.9 demonstrate the resulting net pressure coefficient derived by combining simultaneously the pressure coefficients applied on upper and lower surfaces.

Minimum C_p values observed on the upper surface of the panel are illustrated in Figure 5.2.4 which shows that suction occurs for all inclinations. According to this figure, greatest suction appears for 30^{o} panel inclination at the upper corner of panel 1 near to the edge, which is greater compared to the peaks occurring for other panel inclinations. Contour lines also indicate that suction does not change significantly for panels 2 and 3 when they are inclined by 20, 40 and 45 degrees.

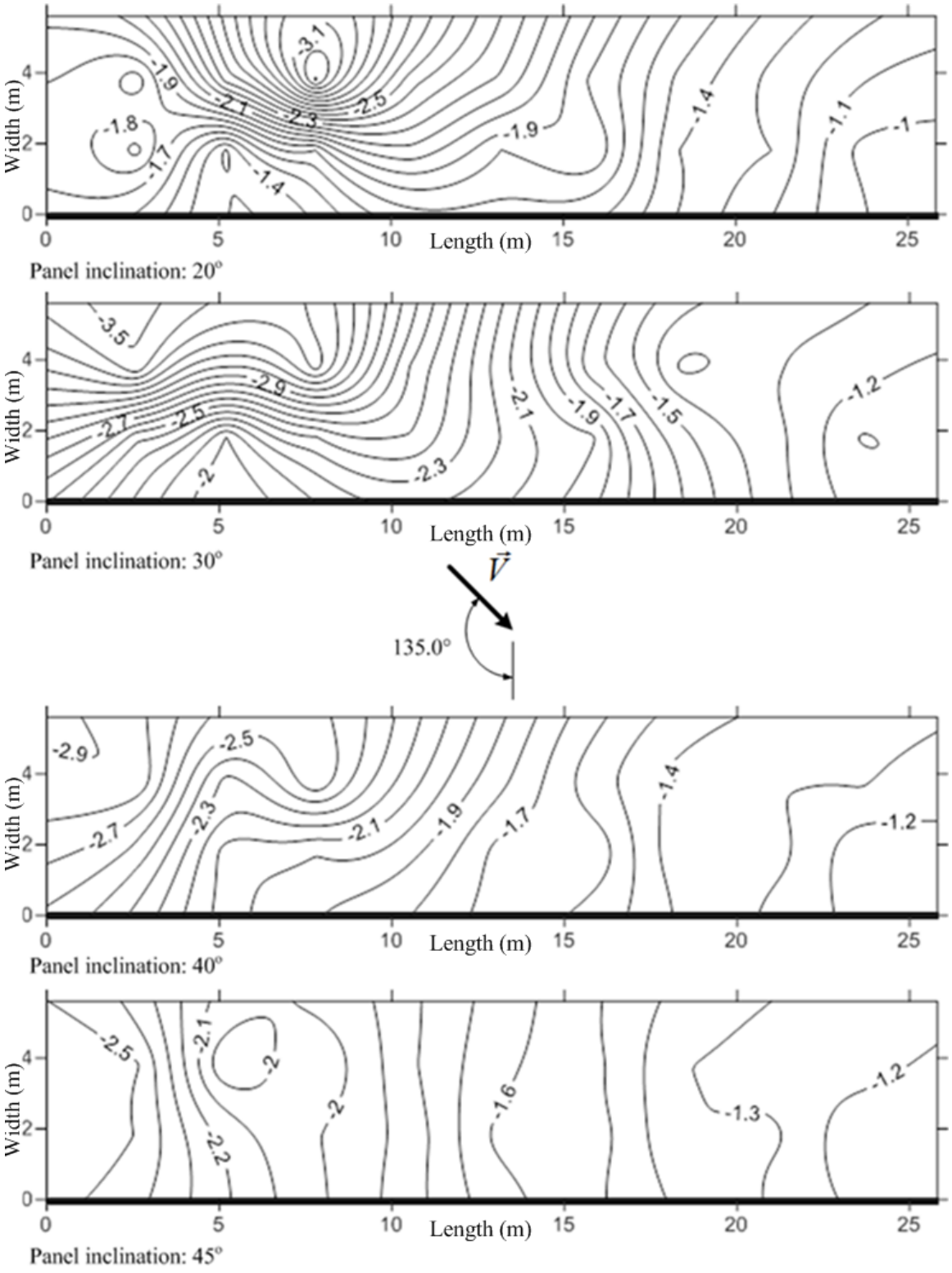

Figure 5.2.4 Minimum C_p values on upper surface for 7 m building height, front location

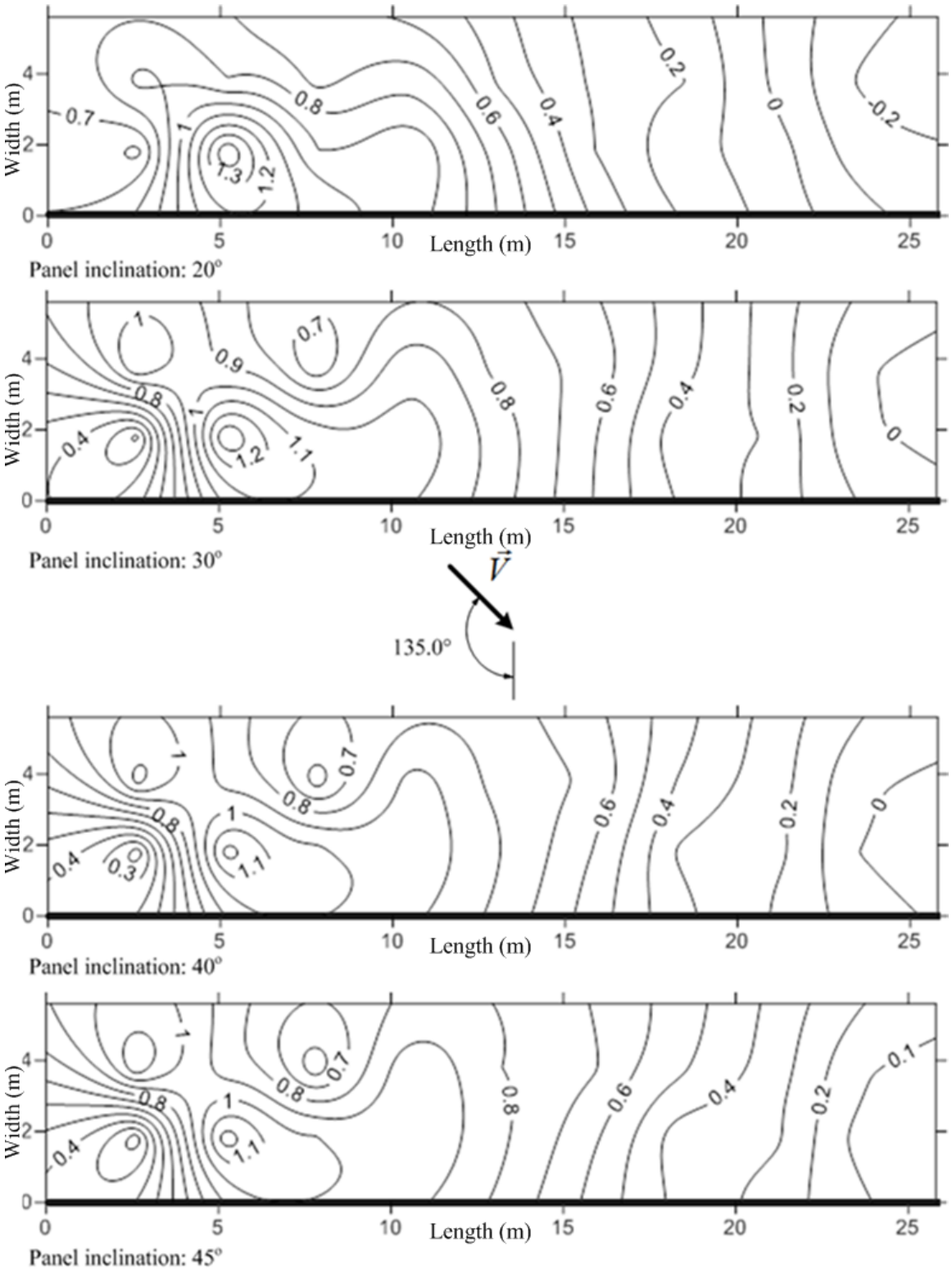

Figure 5.2.5 Maximum C_p values on lower surface for 7 m building height, front location

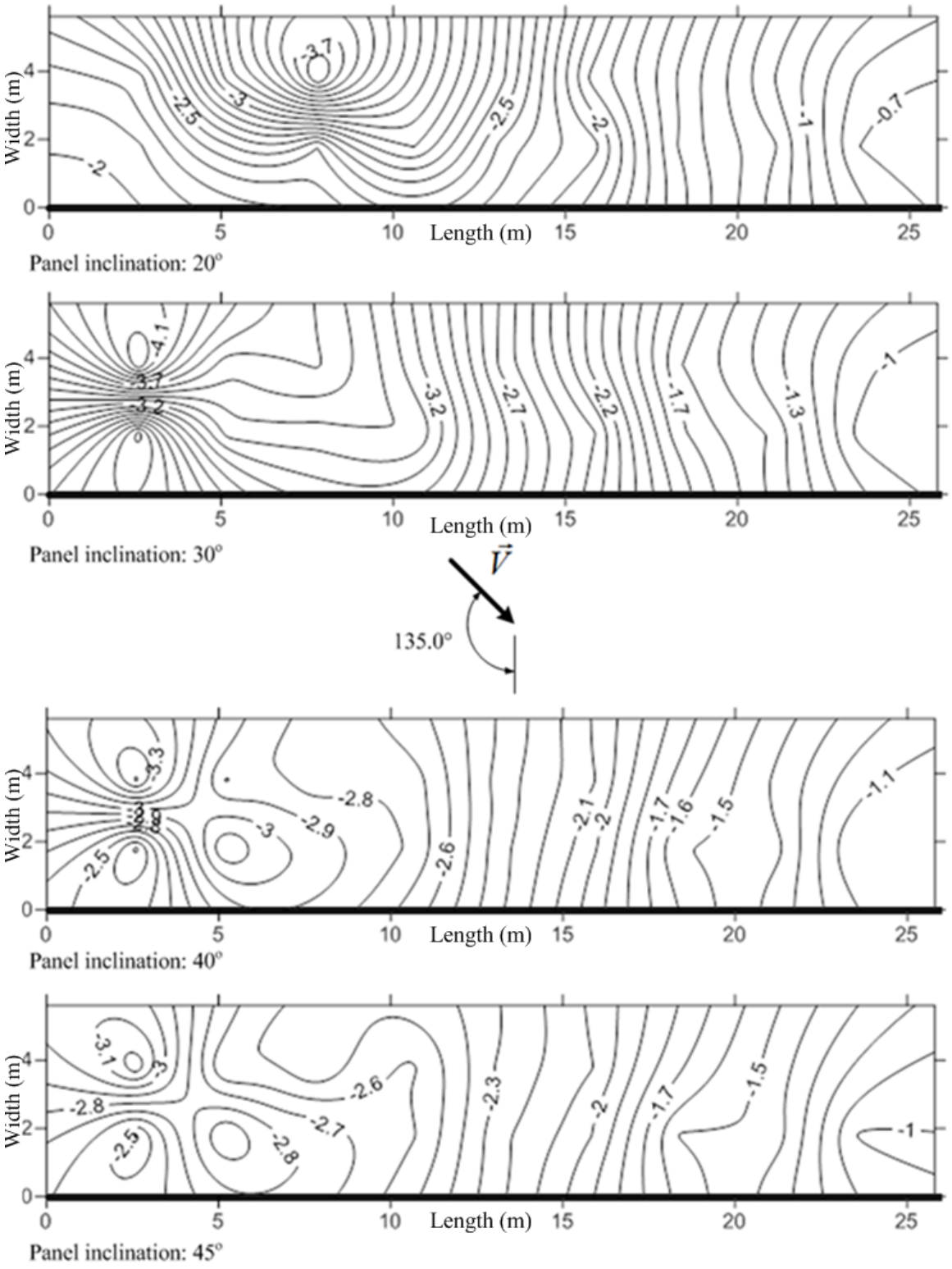

Figure 5.2.6 Minimum net C_p values for 7 m building height, front location

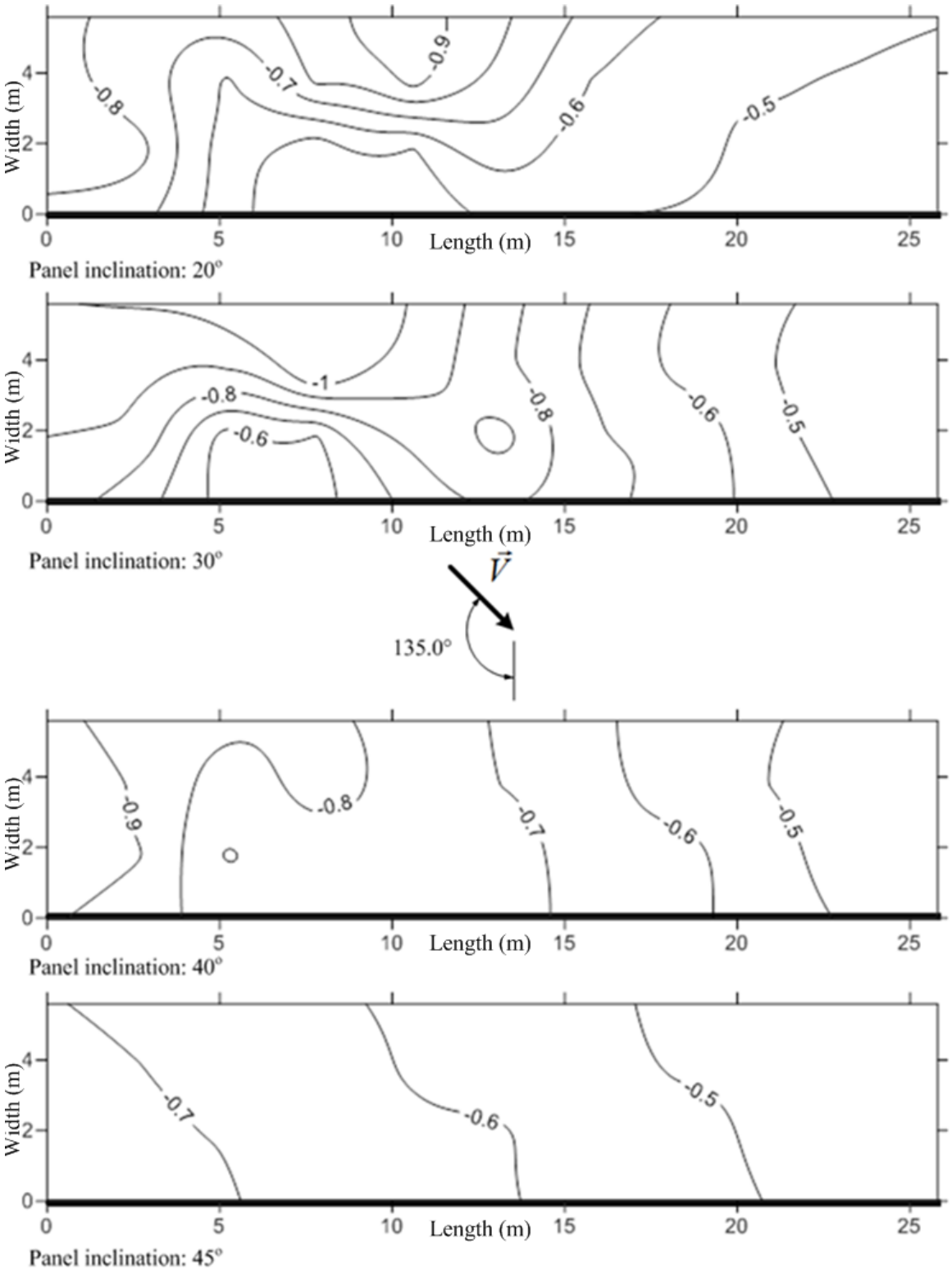

Figure 5.2.7 Maximum C_p values on upper surface for 7 m building height, front location

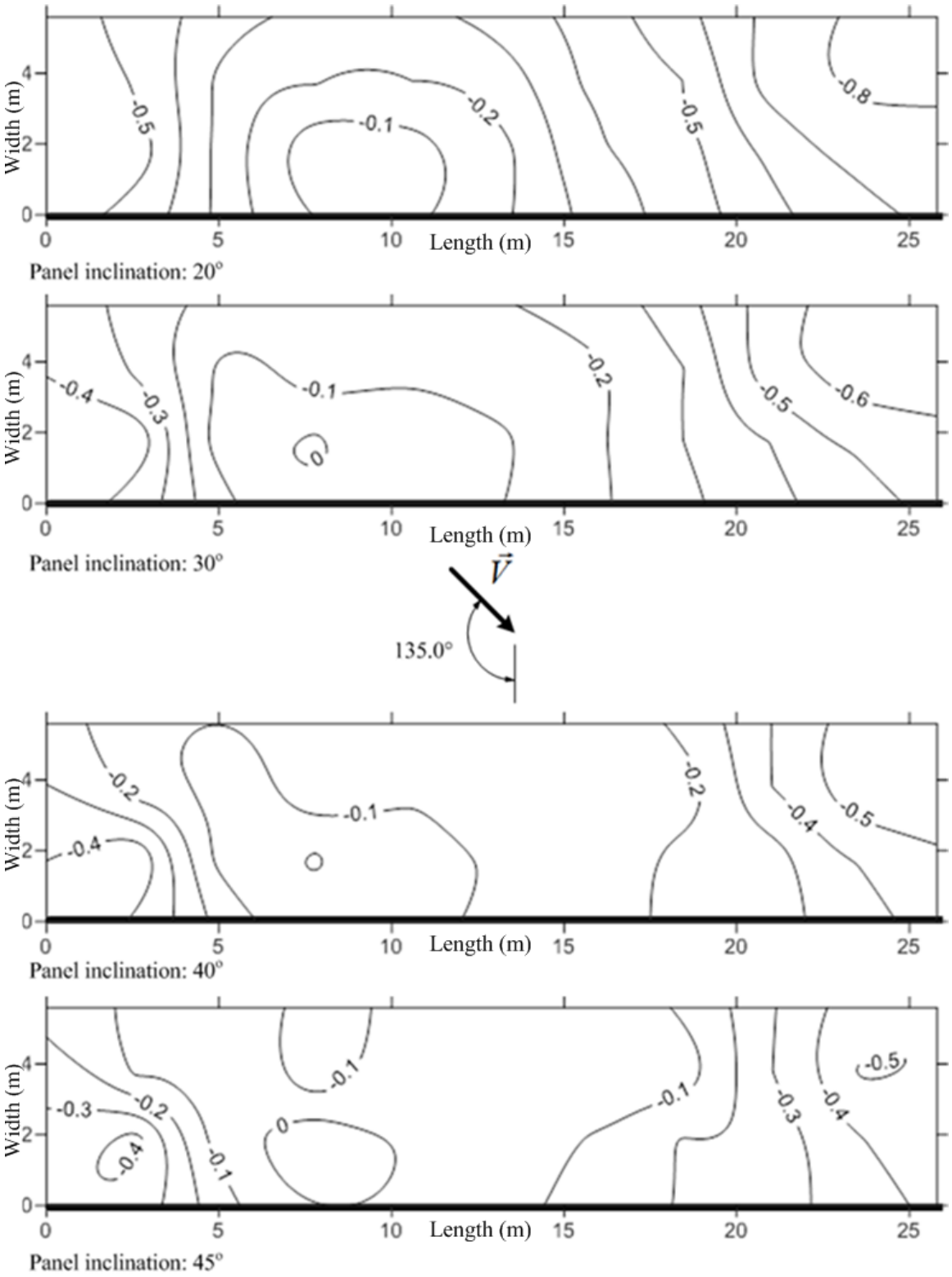

Figure 5.2.8 Minimum C_p values on lower surface for 7 m building height, front location

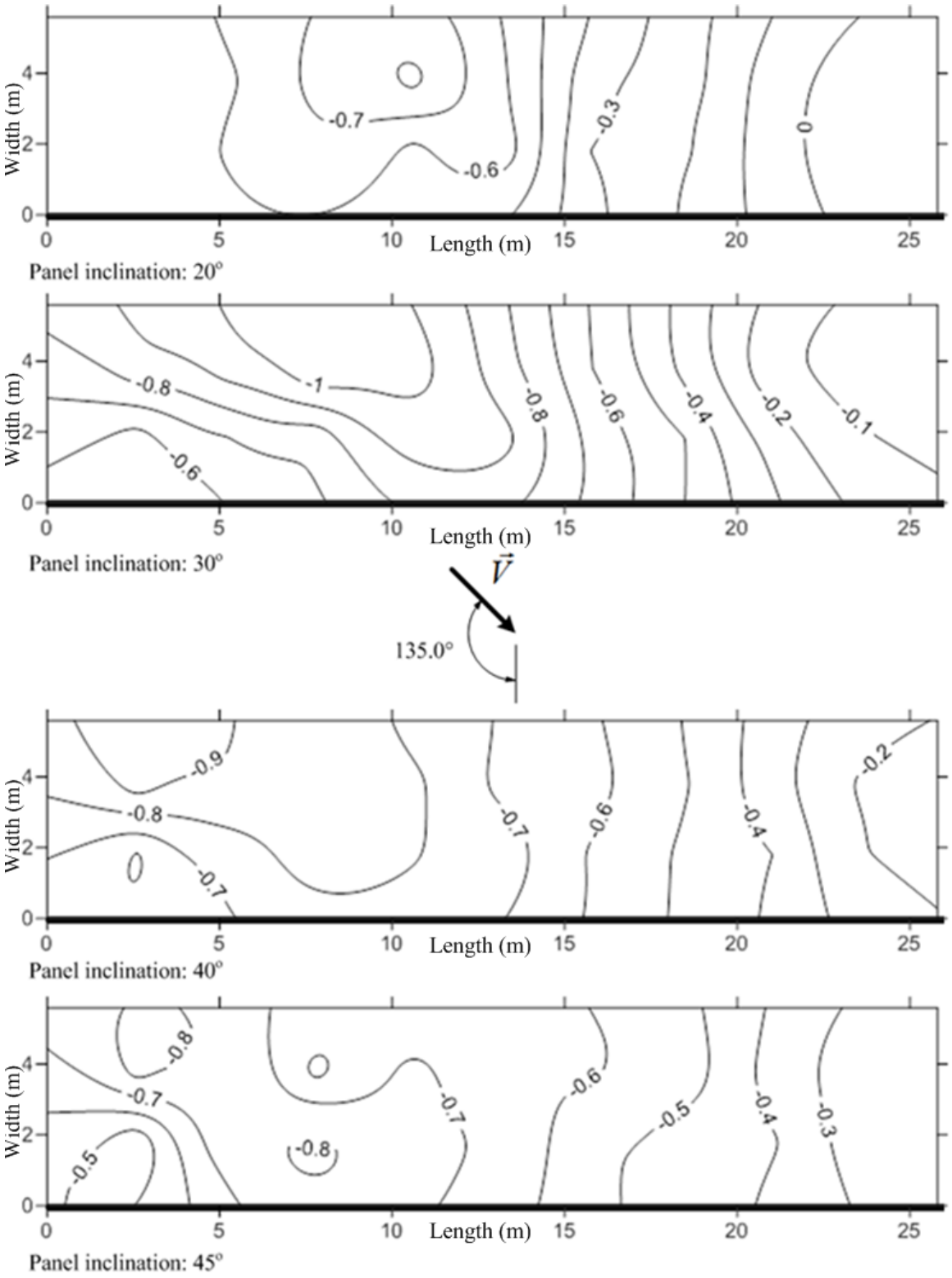

Figure 5.2.9 Maximum net C_p values for 7 m building height, front location

Figure 5.2.5 depicts the maximum values of the pressure coefficients corresponding to the lower surface of the panel. Contour lines clearly show that overpressure appears all over the surface of the panels for all the panel inclinations. The extreme value of the positive pressure coefficients is recorded for 20^o panel inclination at the lower edge of panel 1. As far as panels 2 and 3 are concerned, the pressure field corresponding to them remains almost constant and unaffected by the panel inclination.

The upper and lower surface panel pressure fields are combined and the resulting field appears in Figure 5.2.6 which demonstrates that suction is applied on the entire surface of the panels. Since contour lines at the lower surface don't change radically with panel inclination, the contour lines in Figure 5.2.6 follow the same pattern with that of the upper surface. Therefore, it can be concluded that the pressure field above panel 1 is mostly affected by the wind flow while panels 2 and 3 appear almost under the same field for all the panel inclinations. As has already been shown, greater panel inclination results in lower suction with only exception being the 30^o panel inclination for which the extreme value appears around pressure tap number 1 near the edge of panel 1, where the extreme values for the other panel inclinations can also be detected.

Figure 5.2.7 shows the maximum values of the pressure coefficients occurring at the upper surface while Figure 5.2.8 shows the minima at the lower surface from where it is clear that suction appears for both of them. Contour lines become less dense when panel inclination increases showing that suction becomes lower. Additionally, maximum values of C_p corresponding to the upper surface are slightly greater in terms of absolute value compared to the minimum values of lower surface, indicating that greater suction occurs at the upper surface.

Figure 5.2.9 presents the net pressure coefficients which were calculated by simultaneously adding the two traces as measured at the upper and lower panel surface. The resulting pressure fields as depicted in Figure 5.2.9 show that only suction occurs which varies slightly with panel inclination, particularly for 20-degress panel inclination.

Additional contours corresponding to different configurations have been plotted for the most critical cases and are available in Appendix A.

As mentioned in Chapter 4, in order to investigate the effect of panel inclination, a careful study of measured pressure coefficients for several configurations is necessary and this is presented in this section.

The data are given as a function of the panel inclination for the critical 135^{o} wind direction. It should be noted that only the extreme values have been considered for the cases of stand-alone panels and panels attached to buildings. For the cases of the attached panels on buildings, both building heights (i.e. 7 m and 16 m) and both panel locations (i.e. front and back) are presented.

For the upper surface, the data are depicted in Figure 5.2.10 (a) in which the maximum C_p values follow the same pattern for all the panel inclinations while minimum values vary with different inclination. The pressure coefficients corresponding to the trends for 7 m and 16 m front location decrease with increasing inclination while those corresponding to the back location increase with increasing inclination. For the stand-alone-panels, increase of the panel inclination leads to greater suction and consequently the peak appears for 45^{o} panel inclination which is overall the greatest suction.

Figure 5.2.10 (b) shows what happens at the lower panel surface for 135^o wind angle and all the configurations. The minimum and the maximum values of pressure coefficients differ slightly for different building heights and panel locations. However, the greatest suction occurs for panels on the 16 m high building, back located and inclined by 20 degrees, while the positive greatest value of the pressure coefficient for the 7 m high building, at the back location and 20^o panel inclination.

The net values of the pressure coefficients referring to the whole solar panel appear in Figure 5.2.11. The maximum C_p values decrease somewhat with increasing panel inclination (from -0.5 to < -1.0). On the contrary, the minimum values show smaller suction with increasing panel inclination for both 7 m and 16 m building height and front location. The trends for back location show that increasing inclination results in higher suction for every building height and the stand-alone case as well. The different behavior for front and back panels comes from the fact that different panel locations affect differently the wind flow. Panel inclination also contributes to this phenomenon and a different pressure field is created for different panel inclinations.

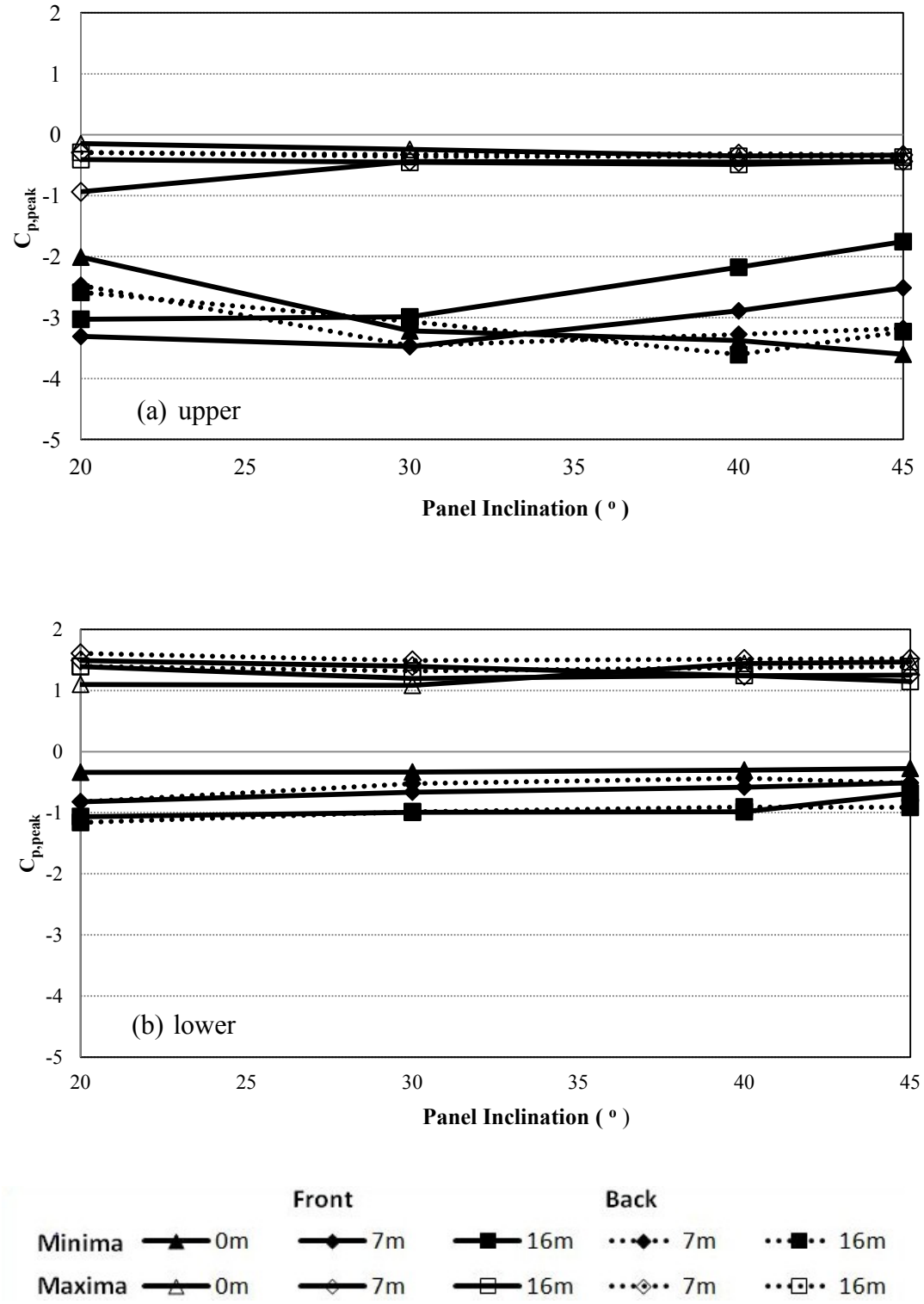

Figure 5.2.10 Peak pressure coefficients on (a) upper and (b) lower surface for 135^{o} wind direction

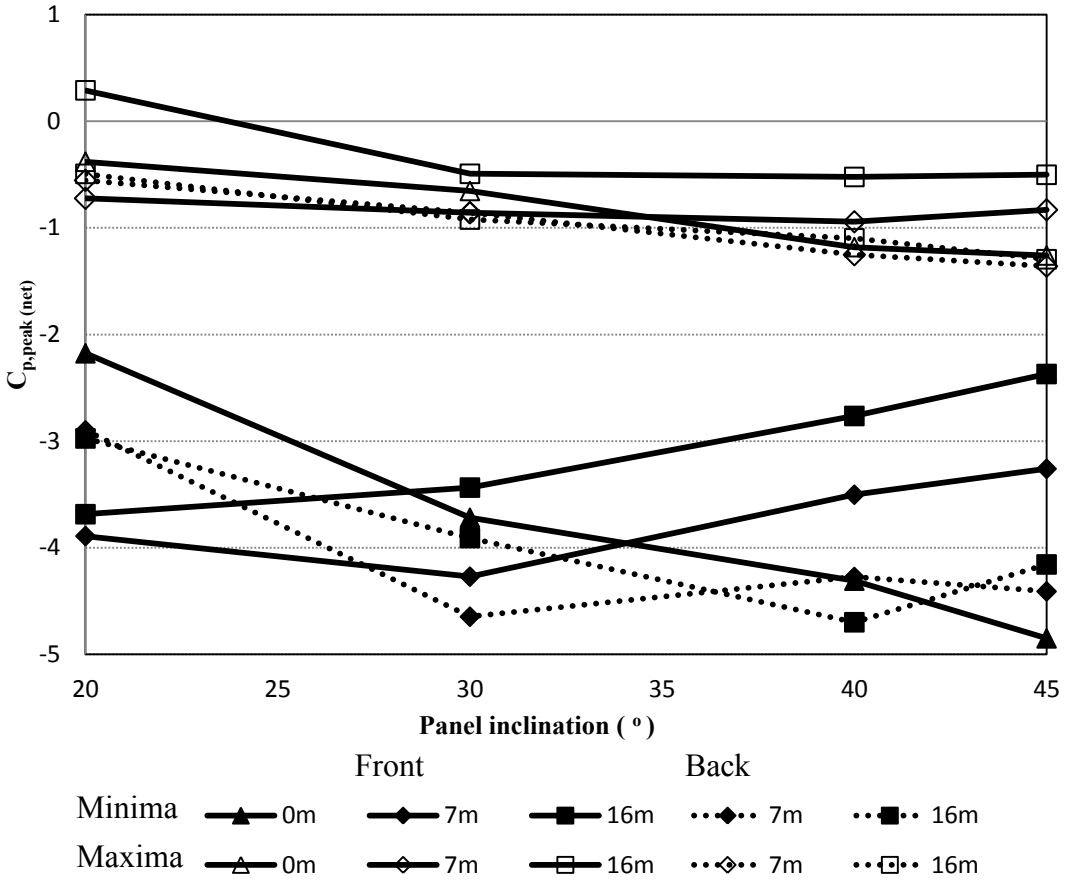

Figure 5.2.11 Net peak pressure coefficients for 135^{o} wind direction

5.3 EFFECT OF BUILDING HEIGHT ON MEASURED PRESSURE COEFFICIENTS

Different model configurations were tested in order to evaluate the effect of building height on the wind-induced load on solar panels. Figures 5.3.1 and 5.3.2 show how the local peak pressure coefficients from all pressure taps corresponding to different panel inclinations vary with building height for the most critical case of 135^{o} wind direction.

The peak pressure coefficients for front located panels are depicted in Figure 5.3.1 for the upper, lower panel surface and the net values. Figure 5.3.1(a) shows that increasing

building height results in lower suction for every panel inclination. On the contrary, the suction is smaller for the case of stand-alone panels and for 20^o panel inclination. As far as the lower surface of the panel is concerned, the minima and maxima of pressure coefficients trends for front location and 135^o wind direction follow the same pattern as shown in Figure 5.3.1(b)**.** Overall, slightly greater suctions do occur when the building height increases.

Figure 5.3.1(c) depicts the net values of peak pressure coefficients as a function of building height. Maximum values range from -1.2 to -0.2 as a function of the building height. As far as the minima are concerned, the 16 m high building results in lower suctions for every panel inclination compared to those appearing for 7 m high building. For panels at the ground level, suction takes its greatest value for 40^o and 45^o panel inclination, while the lowest suction appears for 20^o panel inclination. The trend of 30^o panel inclination ranges from -4.2 to -3.7 and thus no significant building height effect is observed

.

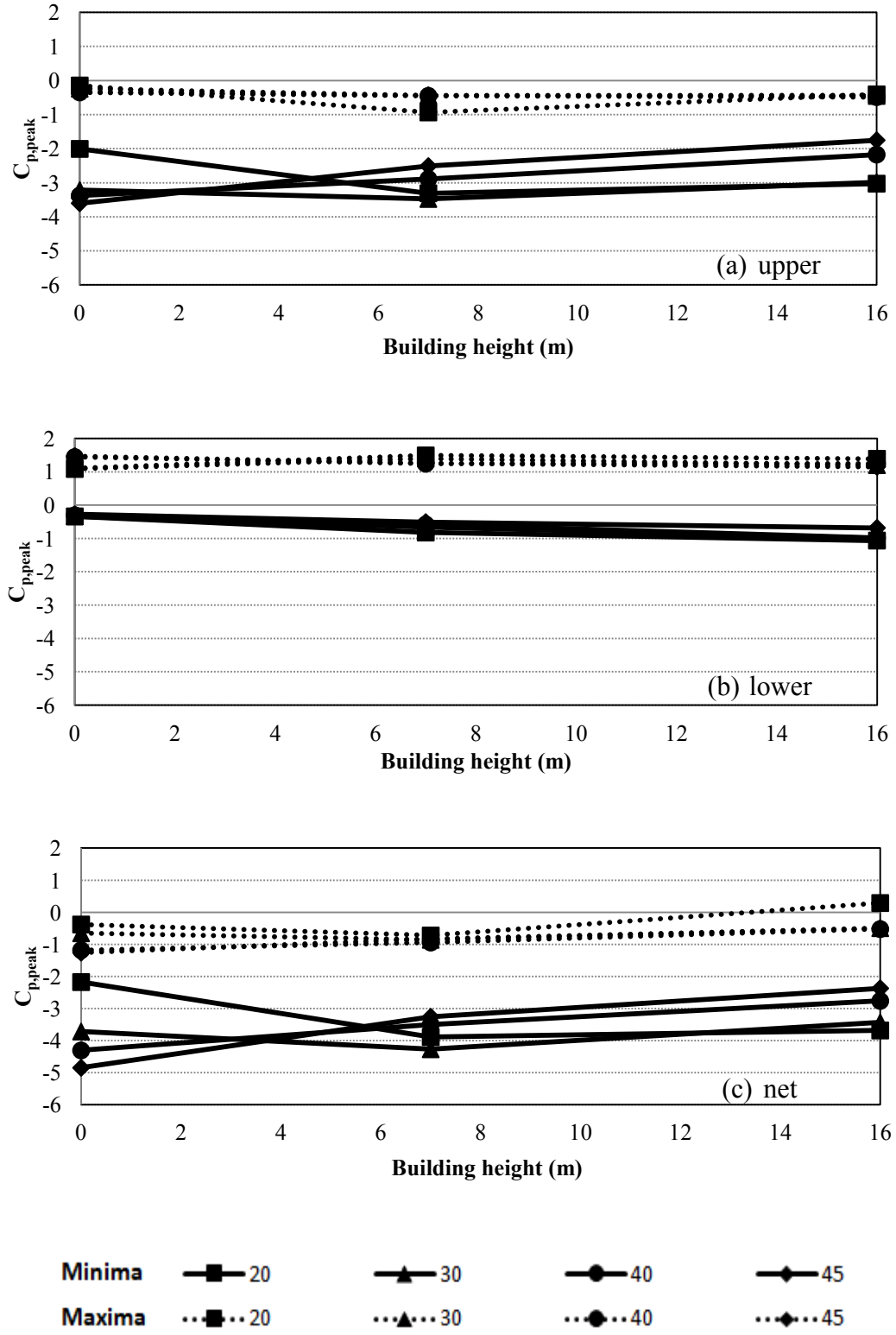

Figure 5.3.1 (a) upper, (b) lower surface peak pressure coefficients and (c) net peak pressure coefficients for front location and 135^{o} wind direction

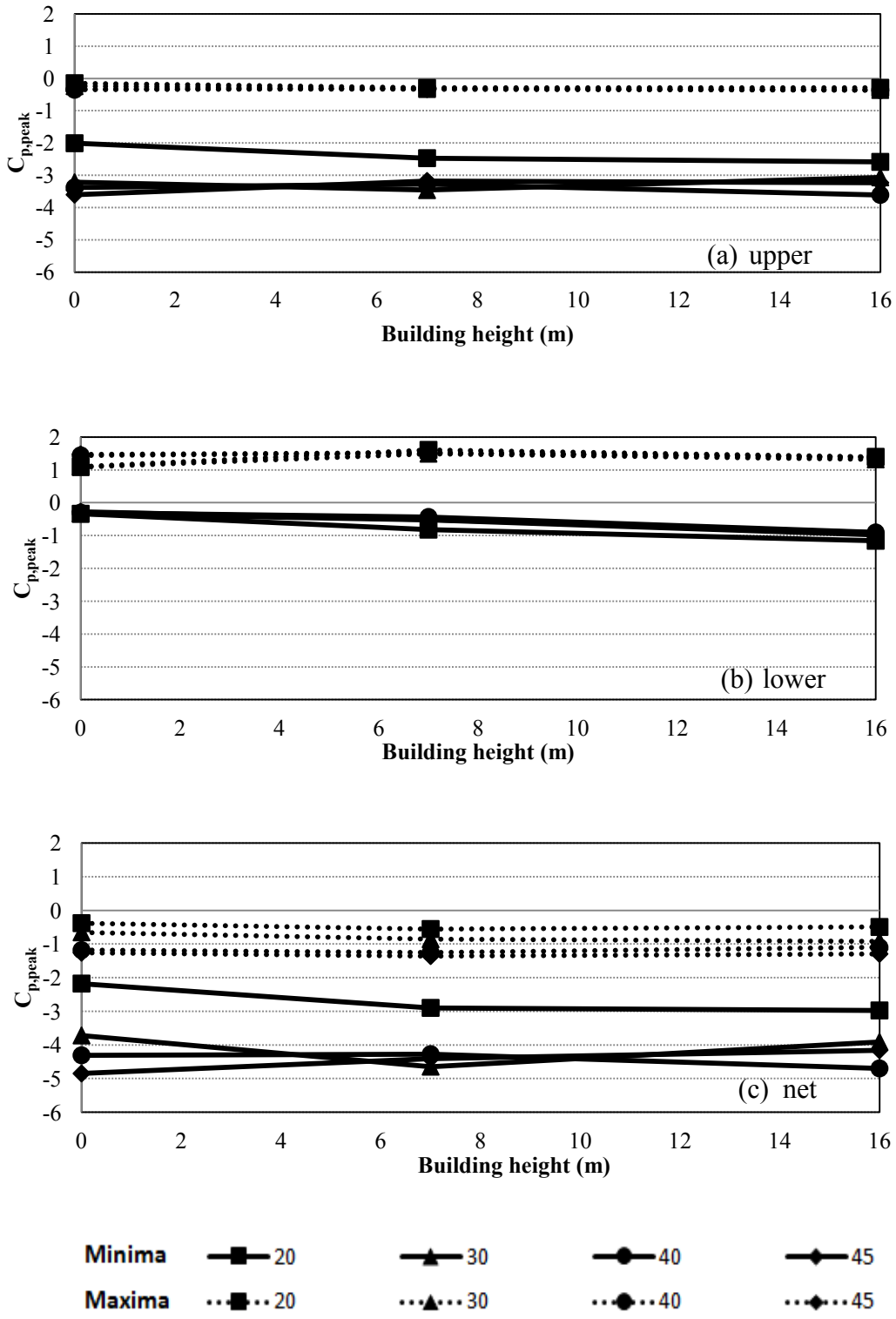

Figure 5.3.2 (a) upper, (b) lower surface peak pressure coefficients and (c) net peak pressure coefficients for back location and 135^{o} wind direction

For the back location, as depicted in Figure 5.3.2(a) and in which the peak pressure coefficients appear for the upper surface, the trends remain almost constant for both building heights and stand-alone panels.

Figure 5.3.2(b) demonstrates the peak pressure coefficients at the lower surface for back location and 135^{o} wind direction from which can be concluded that increasing building height results in higher suction in total. Maximum values are almost constant and remain within the same range.

Finally, the net values of pressure coefficients for the critical 135^{o} wind direction and back location are depicted in Figure 5.3.2(c). The results show that there are differences compared to Figure 5.3.1(c) indicating that panel location plays an important role especially as far as the minimum pressure coefficients are concerned. The trends for the minimum values of 30-, 40- and 45- degree panel inclination range from -4.6 to -3.7 while the one of 20-degree panel inclination takes values from -2.9 to -2.1. Further comparison between the two figures also makes evident the fact that absolute values of minimum pressure coefficients are greater for the back location and their range is within -5 and -4 for 30-, 40-, 45- degree panel inclination.

5.4 EFFECT OF PANEL LOCATION AND WIND DIRECTION ON NET PEAK PRESSURE COEFFICIENTS

This section presents the effect of wind direction and panel location on experimental results expressed as net peak pressure coefficients. Figures 5.4.1 to 5.4.2 demonstrate how the net peak pressure coefficients vary as a function of wind direction for stand-alone panels and panels attached to 7 m and 16 m high building when panels are inclined by 20-, 30-, 40-, 45- degrees. Moreover, Figures 5.4.2(a) and 5.4.2(b) illustrate the results for both front and back panel location. In general, the following comments can be made for these figures:

- As far as the minimum values are concerned, higher suction occurs for wind directions ranging from 120^o to 165^o. On the other hand, maximum value extremes appear within the range of 15^o to 60^o of wind direction.
- Building height increase results in greater suction.
- Back location is mainly responsible for greater suction while front location is responsible for slightly greater overpressure.
- Overall, overpressure is not as significant as suction in terms of absolute values.

More specifically, Figure 5.4.1 shows the peak pressure coefficients for the case of stand-alone panels for the panel inclinations examined. The peaks appear for 30^o and 135^o wind directions for the maximum and the minimum values respectively. It is also evident that suction is greater than overpressure in absolute value.

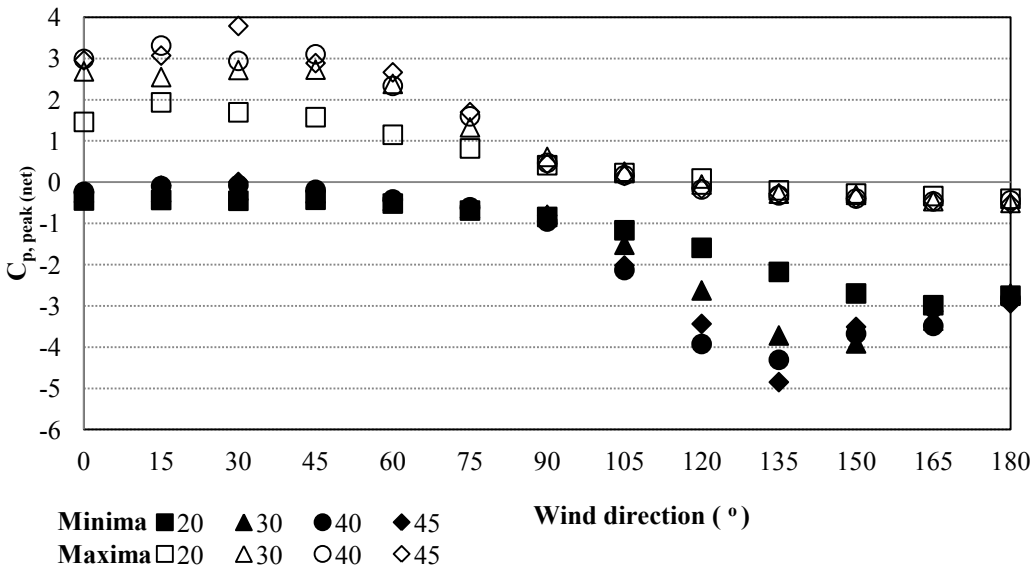

Figure 5.4.1 Net peak pressure coefficients for ground level panels with respect to wind direction

The case where the panels are attached to a 7 m high building, located at the front and back of the roof is shown in Figure 5.4.2(a). For wind directions 120^{o} and 135^{o} the extreme values do occur for 45- and 30- degree panel inclination respectively, when the panel is back located. The maximum positive pressure can be observed for 30^{o} wind direction when the panels are located at the front position and are inclined by 45^{o}.

Figure 5.4.2(b) presents the case where the panels are attached to a 16 m high building from which can be concluded that suction is overall greater than overpressure in terms of absolute values. In addition, greater suction appears for back located panels while overpressure is greater for front located panels. These phenomena can be attributed to the flow separation occurring due to the sharp building edges. The greatest suction occurs for 135^{o} wind direction when the panel location is back, and the panel inclination is 30

degrees, since airflow moves towards the building at an oblique wind angle of attack and therefore two delta wing vortices are developed across its edges. The extreme values for overpressure appear for 45^{o} wind direction, 40^{o} panel inclination and front location.

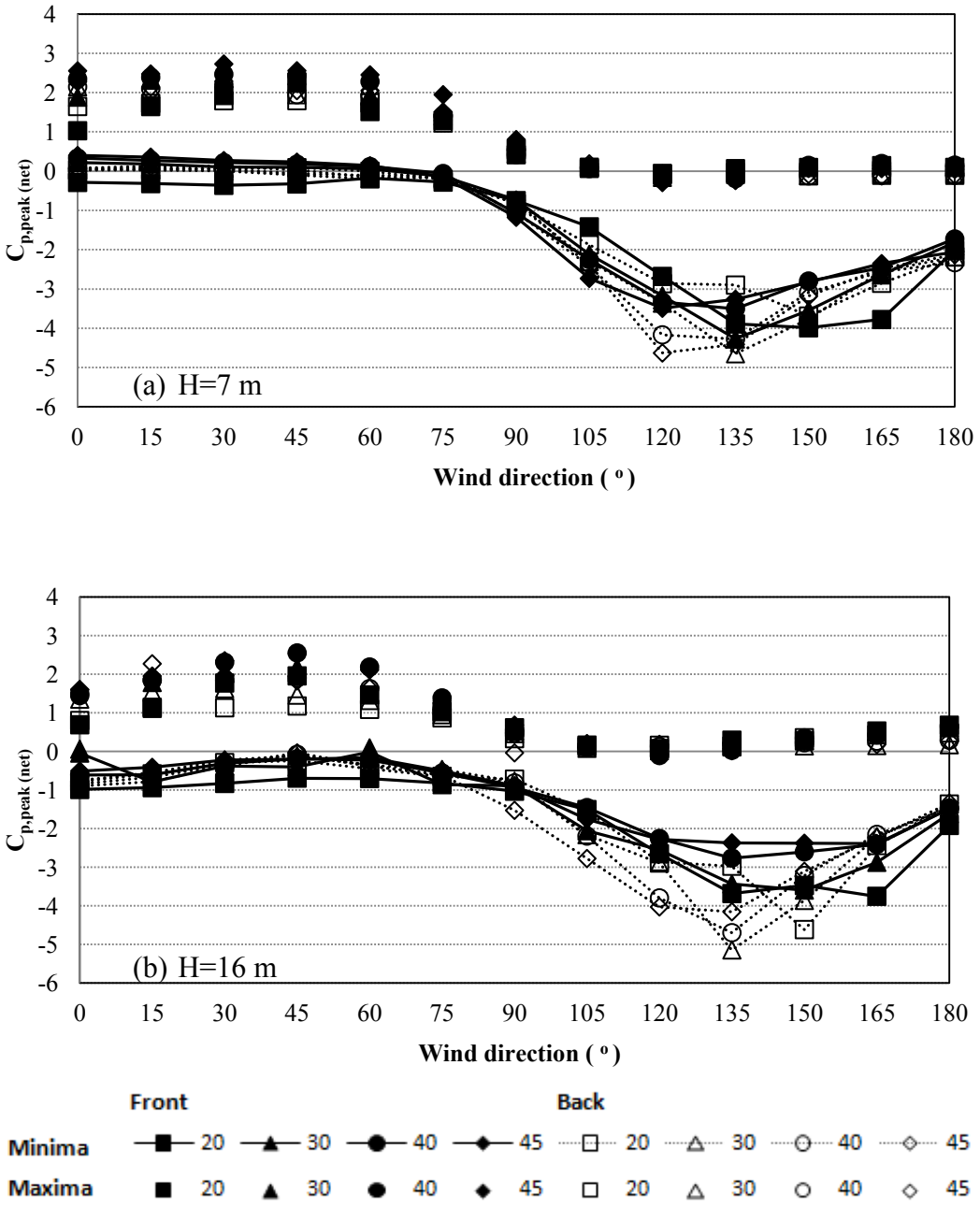

Figure 5.4.2 Net peak pressure coefficients for panels attached on (a) 7 m and (b) 16 m high building for front and back location

5.5 EFFECT OF WIND DIRECTION ON MEASURED PRESSURE COEFFICIENTS FOR SELECTED PRESSURE TAPS

The figures presented in this section demonstrate the wind direction effect on selected pressure taps as far as the mean and peak values are concerned. These pressure coefficients are measured on the upper and lower surface of the panels and their combined effect is presented in terms of net pressure coefficients. The pressure taps examined correspond to a 7 m high building with panels at the front location.

Figure 5.5.1 demonstrates the mean, minimum and maximum values of pressure coefficients corresponding to pressure tap number 1 (see Figures 5.1.1 and 5.1.2) for both front and back panel locations. As can be observed the extreme minima appear for wind directions in the range of 105^o to 165^o. The greatest suction occurs for 120^o wind direction, 45^o panel inclination and back location. The maximum peak value (see Figure 5.5.1(c)) occurs for 0^o wind direction and 40^o panel inclination for back location.

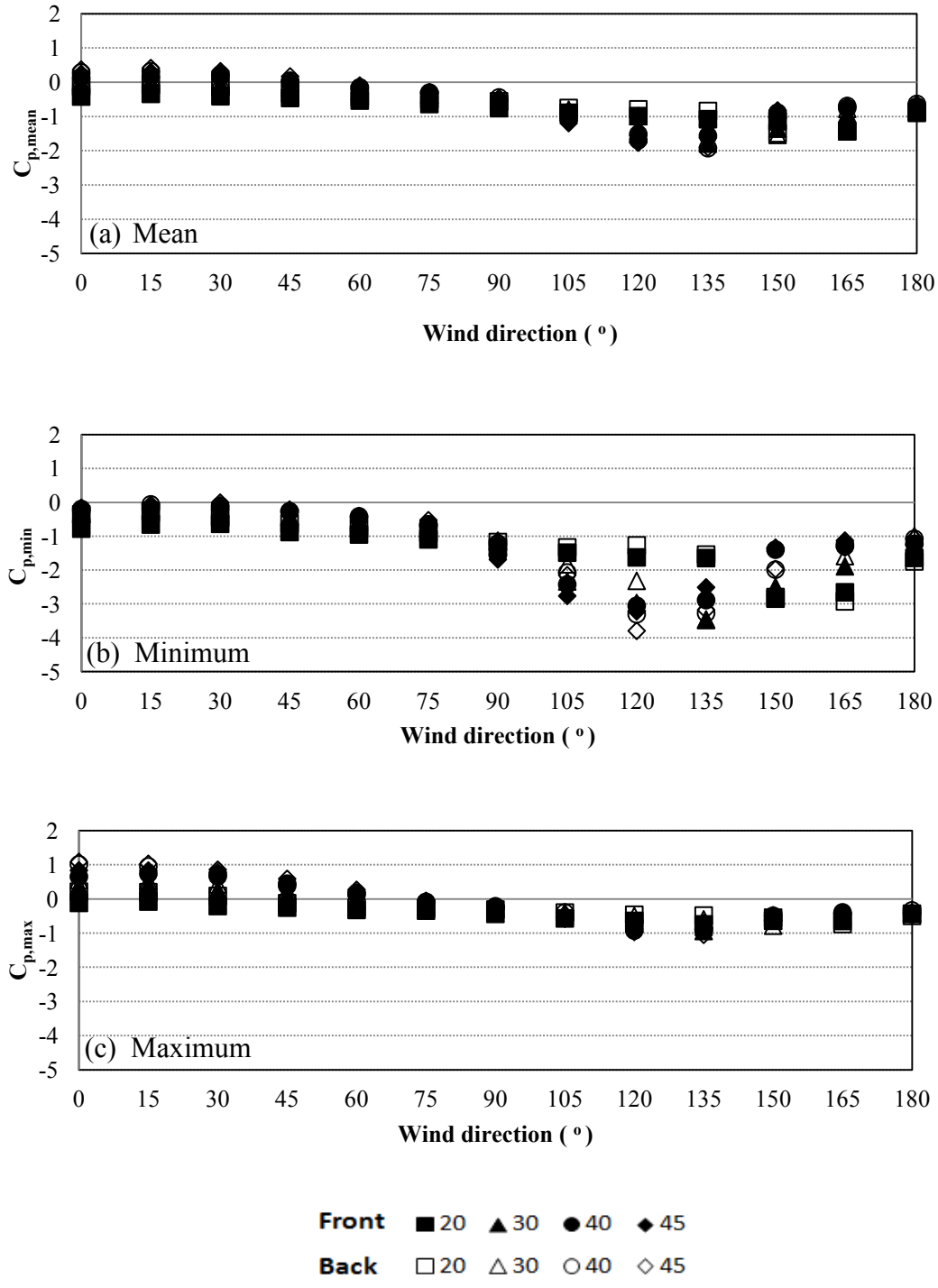

Figure 5.5.1 (a) Mean, (b) Minimum and (c) Maximum C_p values for pressure tap #1 on upper panel surface

The mean, minimum and maximum values of pressure coefficients for the lower surface of panels as a function of wind direction are depicted in Figure 5.5.2. As can be observed in Figure 5.5.2(b) in which minimum values of pressure coefficients are depicted for pressure tap number 2 (see Figures 5.1.1 and 5.1.2), higher suction occurs for 60^o wind direction, 45^o panel inclination and front location. In comparison with those at the upper surface, the suction becomes lower for wind directions within the range 120^o to 180^o. As far as the maximum values of pressure coefficients are concerned at the lower surface of solar panels, they become more significant for wind directions within the range of 135^o to 165^o. The extreme maximum value occurs for 150^o wind direction and 45^o panel inclination at the front location.

The net values of the local pressure coefficient is the difference between the pressure coefficients occurring at the lower surface (pressure tap number 2) deducted by those occurring at the upper surface (pressure tap number 1) simultaneously. Figure 5.5.3 depicts the net mean, minimum and maximum values of pressure coefficients. The minimum values can be seen in Figure 5.5.3(b) in which it is evident that greater suctions occur for wind directions in the range of 120^o to 165^o. The maximum peak value appears for 60^o wind direction, 45^o panel inclination and front location.

Concluding, net minimum pressure coefficients take much greater values compared to net maximum pressure coefficients in terms of absolute values. In general, wind direction can be considered as a crucial parameter for the wind flow, which is formed around the panel. Previous figures show clearly that extreme values of pressure coefficients do not occur for every single wind direction. On the contrary, there is a range of wind directions for which either greater suction or positive pressure appears.

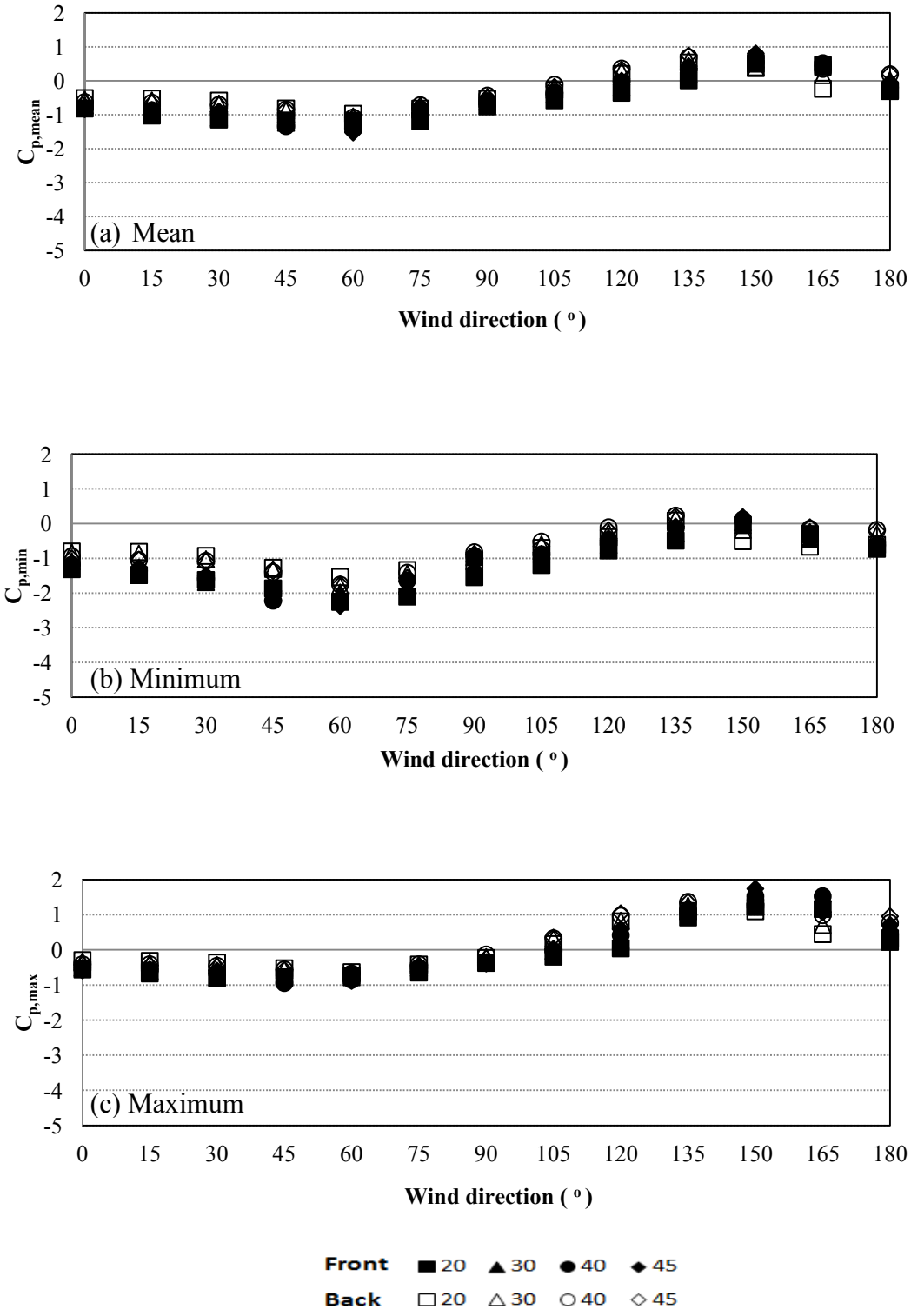

Figure 5.5.2 (a) Mean, (b) Minimum and (c) Maximum C_p values for pressure tap #2 at lower panel surface

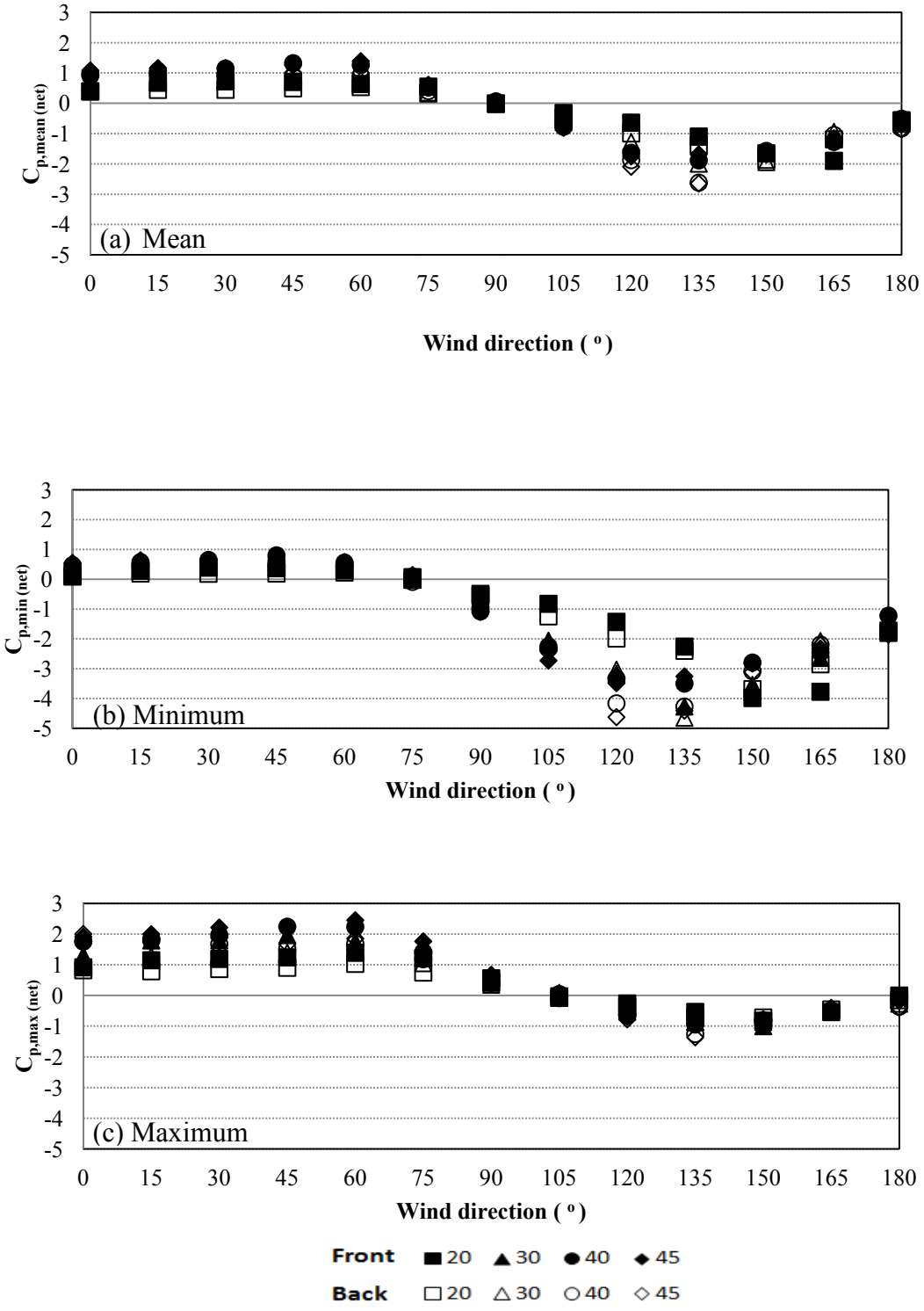

Figure 5.5.3 Net (a) Mean, (b) Minimum and (c) Maximum C_p values for pressure taps # (1-2)

5.6 CRITICAL VALUES OF NET PRESSURE COEFFICIENTS

This section presents the most critical values of net minimum pressure coefficients which are mainly used for design purposes. These values are the most critical detected for every single pressure tap considering all configurations for 30^o panel inclination, regardless of the wind direction. It is evident from the contour plots that greater suction occurs for panel 1, while this suction is smaller for panel 3.

The greatest suction occurs for panel 1 attached to 16 m high building for back location and 30^o panel inclination – see Figure 5.6.5. At the same time, the smallest suction is also observed for the same configuration.

Figure 5.6.1 presents the contour lines corresponding to panels at the ground level. Suction is significant for panel 1 and somewhat smaller for panel 3.

The contours for panels attached to 7 m and 16 m high buildings are presented in Figures 5.6.2 to 5.6.5. These figures show that for panels located at the front, lower suction appears with increase of building height. The opposite happens for panels located at the back since increase of building height results in greater suction when inclined by 30^o.

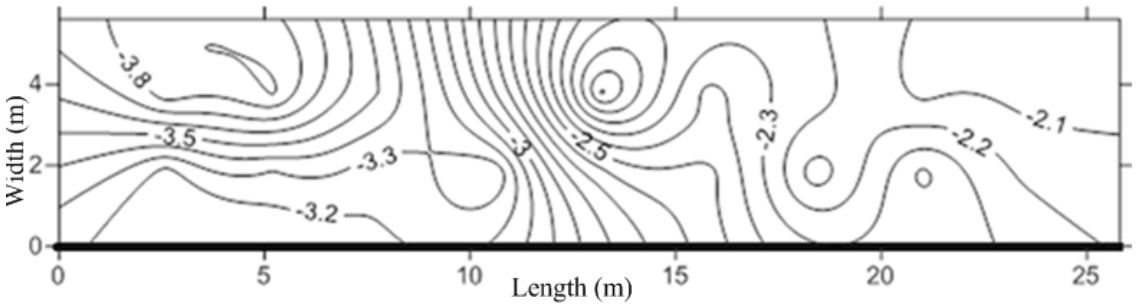

Figure 5.6.1 Critical net minimum C_p for stand-alone panels and 30^o panel inclination

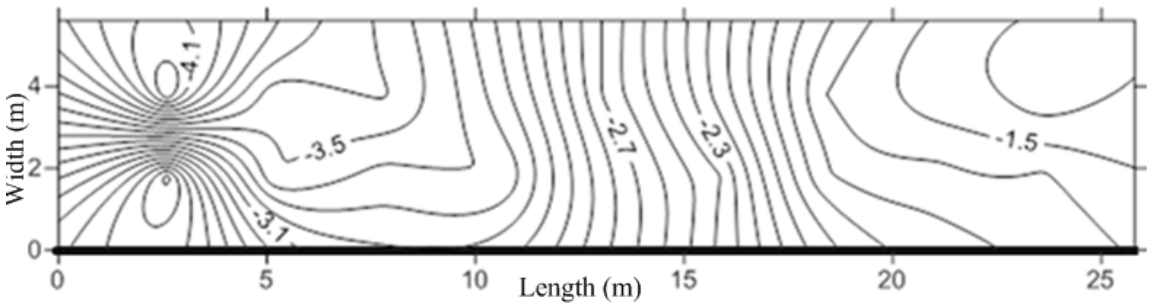

Figure 5.6.2 Critical net minimum C_p for panels attached to 7 m high building, 30^o panel inclination and front location

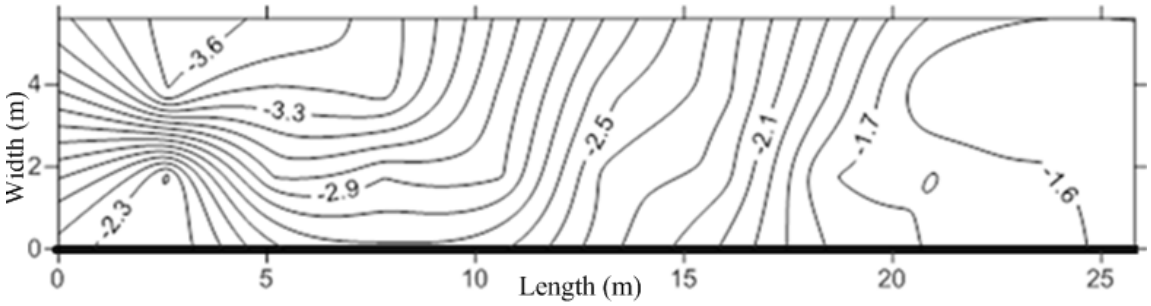

Figure 5.6.3 Critical net minimum C_p for panels attached to 16 m high building, 30^o panel inclination and front location

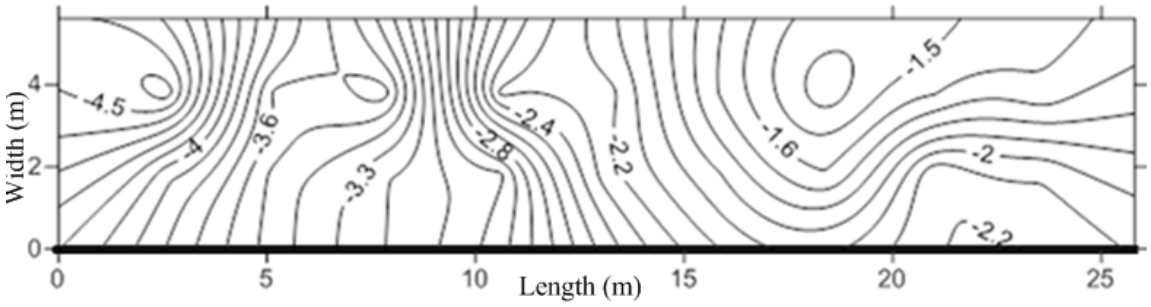

Figure 5.6.4 Critical net minimum C_p for panels attached to 7 m high building, 30^o panel inclination and back location

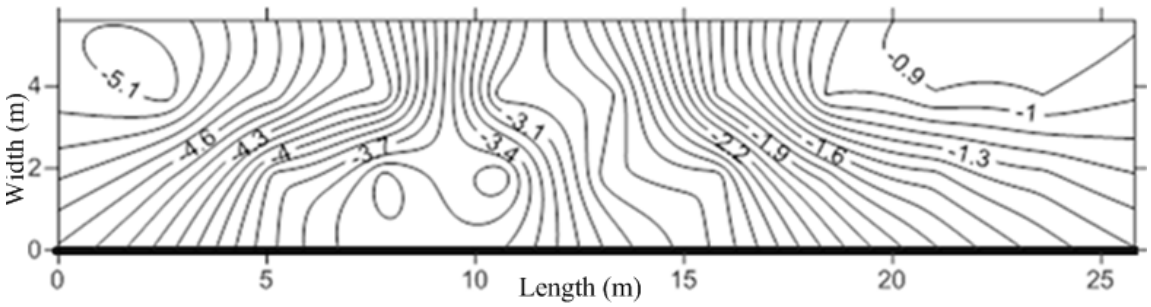

Figure 5.6.5 Critical net minimum C_p for panels attached to 16 m high building, 30^o panel inclination and back location

5.7 EFFECT OF PANEL INCLINATION ON FORCE COEFFICIENTS

This section refers to the effect of panel inclination on force coefficients for panels attached to buildings of different heights and stand-alone panels. The peak values of force coefficients are presented for each panel as a function of panel inclination.

Figure 5.7.1 demonstrates the peak values of force coefficients for the case of stand-alone panels and for 135^o wind direction. The trends of force coefficients for the three panels follow the same pattern for both minima and maxima. The suction observed becomes greater with increasing panel inclination, while greater overpressure occurs for smaller panel inclination. Panel 1 shows the greatest suction for 45^o panel inclination followed by panel 2 and 3.

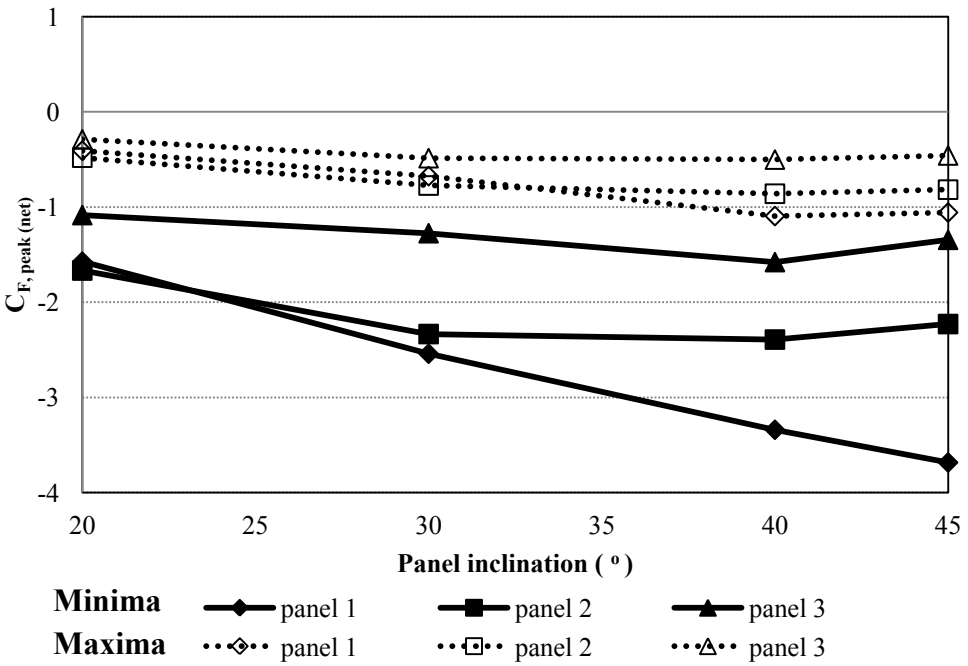

Figure 5.7.1 Net peak force coefficients for 135^{o} wind direction applied on stand-alone panels

Figure 5.7.2 shows the minimum values of force coefficients for panels mounted on 7 m and 16 m high buildings. The trends follow the same pattern for the front located panels, which does not differ significantly, from those corresponding to back located panels for both building heights. As can be observed, the greatest suction occurs for panel 1 attached to 7 m high building, located at the back, when inclined by 45 degrees, which is followed by panel 1 located at the front. For panel 1 attached to 16 m high building, the greatest suction occurs when it is back located and inclined by 30^{o}. For panels 2 and 3 front located, the suction is greater compared to that corresponding to back location for both building heights in terms of absolute values. Panel 2 suffers smaller suction than

panel 1, while panel 3 experiences the smallest suction that becomes even smaller for back location in terms of absolute values.

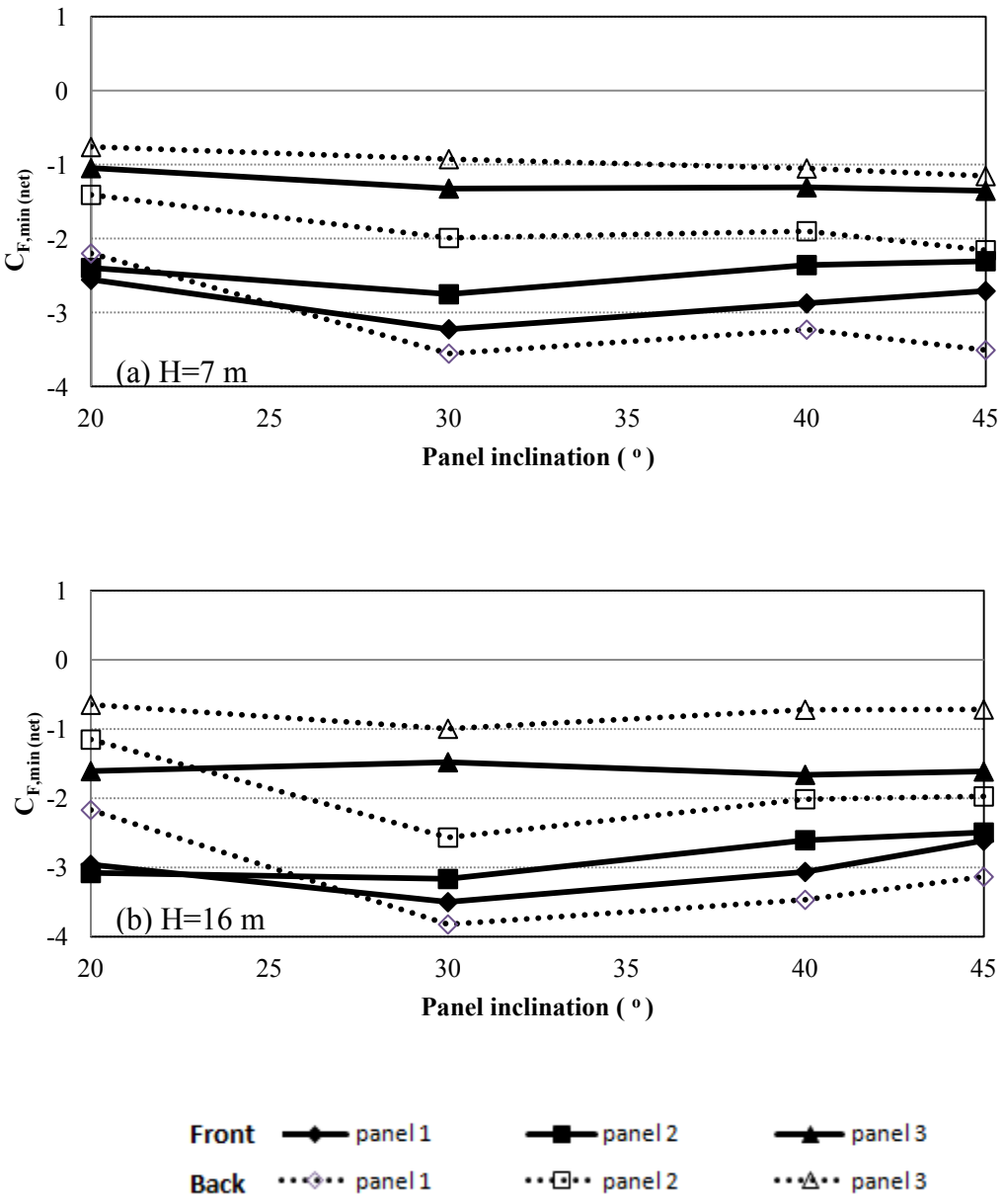

Figure 5.7.2 Net minimum force coefficients for 135^{o} wind direction applied on panels attached to (a) 7 m and (b) 16 m high building for front and back location

Figure 5.7.3 depicts the maximum values of force coefficients as a function of panel inclination for building heights of 7 m and 16 m. These values for all three panels range from 0 to approximately -1 for both front and back location. The greatest value of maximum force coefficients appears for panel 3 when attached to a 16 m high building, front located and inclined by 20 degrees. Slight overpressure is observed for panel 3,at 20^{o} panel inclination, front location and 16 m high building.

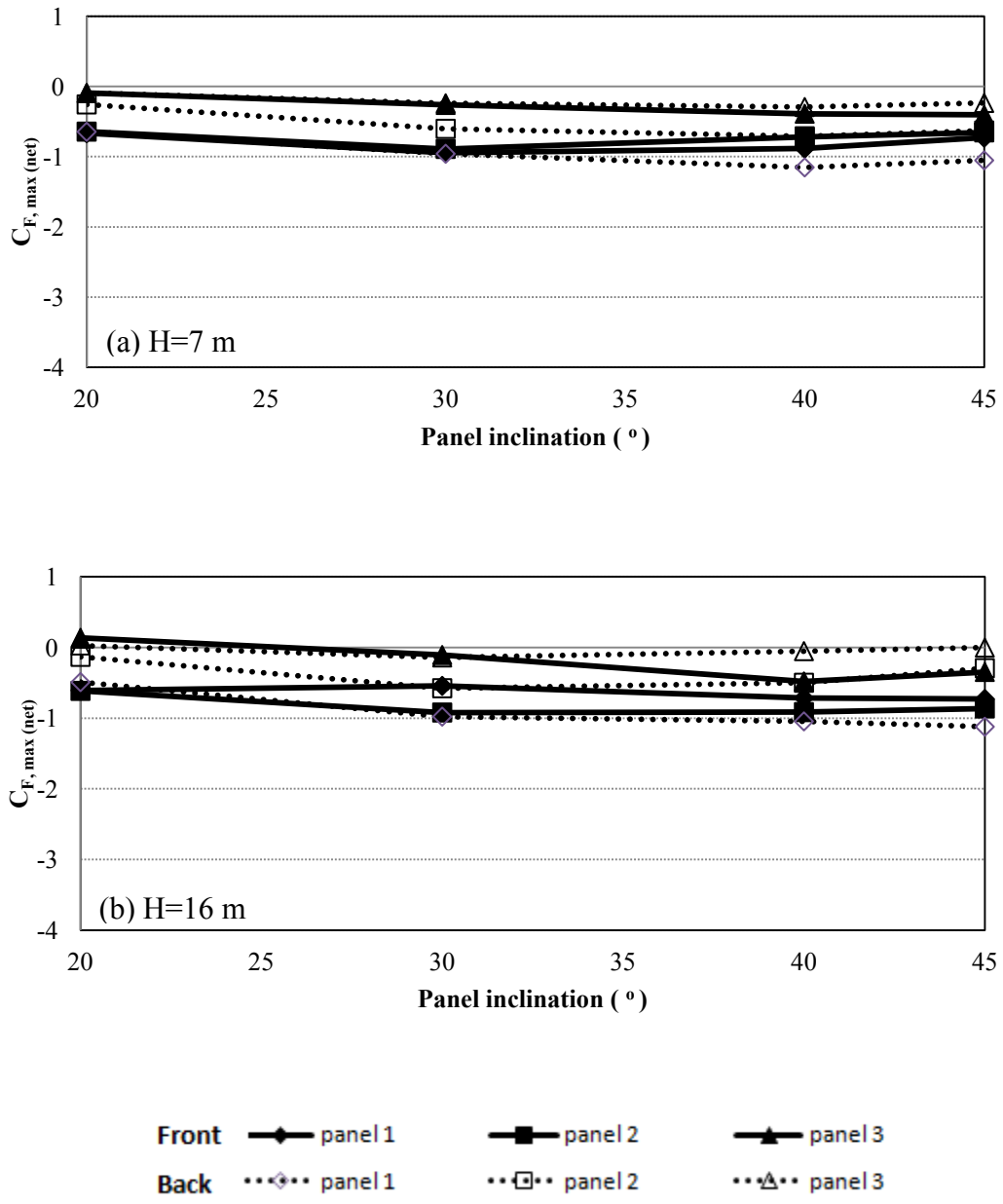

Figure 5.7.3 Net maximum force coefficients for 135^{o} wind direction applied on panels attached to (a) 7 m and (b) 16 m high building for front and back location

5.8 EFFECT OF BUILDING HEIGHT ON FORCE COEFFICIENTS

The effect of building height on force coefficients is examined in this section for the three panels considered. The net minimum and maximum force coefficient values as a function of building height are depicted in Figure 5.8.1 for panels located at the front position. As far as the minima are concerned -see Figure 5.8.1(a) - the 20^o and 30^o panel 1 inclination trend shows that increasing building height results in lower suction, while the opposite happens for 40^o and 45^o panel inclination. The trends of 40^o and 45^o panel 2 inclinations remain almost constant with building height. However, the trends of 20^o and 30^o panel 2 inclinations show greater suction with increasing building height. Panel 3 experiences significantly smaller suction for both building heights. Stand-alone panels inclined by 30^o show the smallest suction, which becomes greater with increasing building height.

Figure 5.8.1(b) depicts the net maximum values of force coefficients as a function of building height. It is clearly demonstrated that increasing building height results in increased values of force coefficients, which remain negative. Positive value of force coefficients appears only for panel 3, inclined by 20^o. For the interval 7 m to 16 m building height, the values of force coefficients range from -1 to 0 for all the cases, while suction is greater for stand-alone panels.

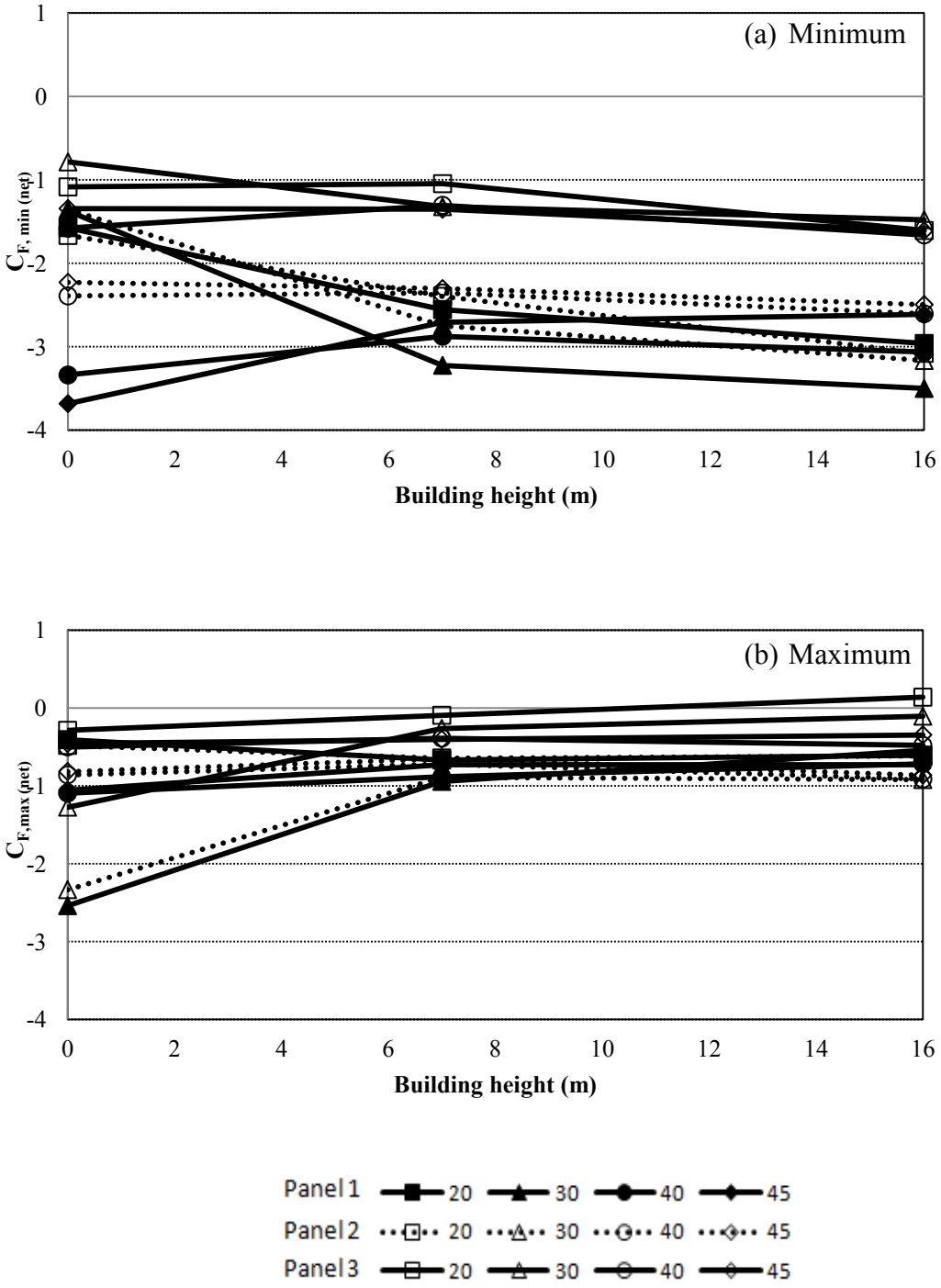

Figure 5.8.1 Net (a) minimum and (b) maximum force coefficients for 135^{o} wind direction, applied on 3 panels for front location

The net peak values of force coefficients are depicted in Figure 5.8.2 for the back location. The net minimum values in Figure 5.8.2(a) show that higher suction appears for 30^o, 40^o, 45^o panel 1 inclination. The greatest suction occurs for 30^o panel inclination. For 45^o panel inclination, increasing building height results in lower suction while for 20^o, 30^o, 40^o in higher suction. As far as panels 2 and 3 are concerned, increasing building height results in smaller suction for 20^o, 40^o, 45^o panel inclination, while the opposite happens for 30^o panel inclination.

The net maximum values of force coefficients are depicted in Figure 5.8.2(b) from which can be concluded that, excluding the cases of stand-alone panels 1, 2, 3 when they are inclined by 30^o, values of force coefficients remain constant. The greatest suction appears for stand-alone panels 1, 2 when inclined by 30^o. The net maximum values of force coefficients range from -1 to 0 and remain independent of building height.

Comparison between Figures 5.8.1(a) and 5.8.2(a) draws to the conclusion that panel location is a parameter affecting significantly the wind flow around the panels and as a result, the force applied on them also depends on this flow.

Concluding, the peak net force coefficients, as far as the pressure trends are concerned, are not affected considerably by the building height. Panel 1 is experiencing the greatest suction compared to panel 2 that follows and panel 3 that is subjected to the least suction for both building heights and panel locations.

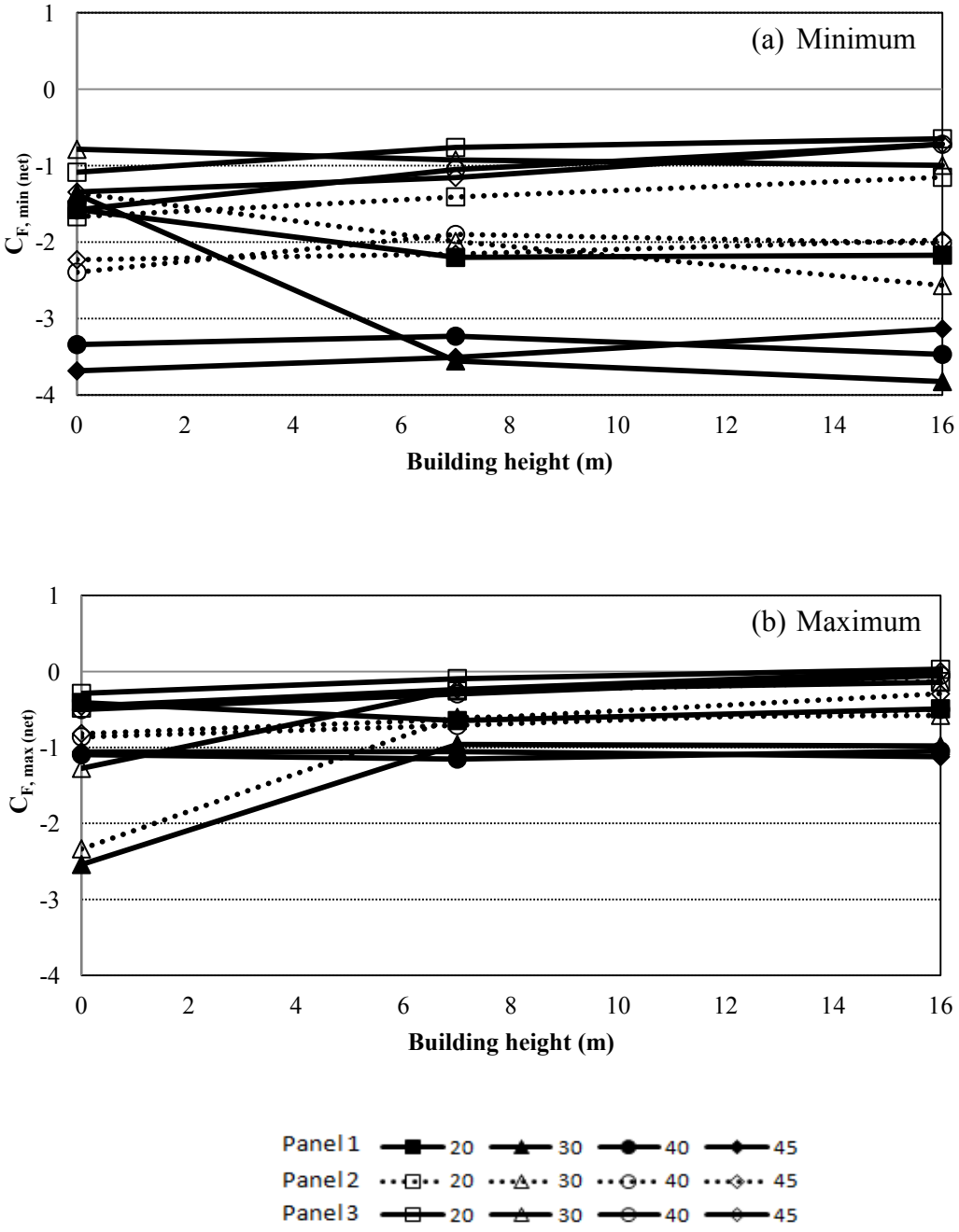

Figure 5.8.2 Net (a) minimum and (b) maximum force coefficients for 135^{o} wind direction, applied on 3 panels for back location

5.9 EFFECT OF WIND DIRECTION ON FORCE COEFFICIENTS

The wind direction effect on force coefficients was examined for the three panels and is presented in this section. The net peak force coefficients are given for panels inclined by 20, 30, 40 and 45 degrees, for the case of stand-alone panels and those mounted on the 7 m and 16 m high building.

Figure 5.9.1(a) shows the minimum and maximum values of force coefficients for panel 1 as a function of wind direction. It is evident that 135^o wind direction is critical since for 45^o panel inclination, the suction takes its greatest value. The maximum value is observed for 30^o wind direction and 45^o panel inclination.

Figures 5.9.1(b) and 5.9.1(c) refer to peak force coefficients on panels 2 and 3 respectively. In these two figures, the trends follow the same patterns with only difference being the fact that panel 3 experiences slightly smaller suction and overpressure. For both panels the minimum peak values are observed for 180^o wind direction and 45^o panel inclination. The maximum peak values for panel 3 occurs for 0^o wind direction and 40^o panel inclination, while for panel 2 appears for 30^o wind direction and 45^o panel inclination.

Figure 5.9.2 presents the net peak force coefficients for panels 1, 2, 3 when attached to 7 m high building for both front and back location. The trends follow similar patterns for the three panels. Differences can be detected regarding the magnitude of their extreme values and the wind direction for which these extremes occur. The minimum peak force coefficients, which are observed for panels 1 and 2, occur for 135^o wind direction, 30^o panel inclination, for panels located back and front respectively. Additionally, panel 3

peak force coefficients appear for 180^o wind direction, 40^o panel inclination and back location. The maximum peak force coefficient calculated for panel 1 occurs for 30^o wind direction, 45^o panel inclination, and front location. Panels 2 and 3 show their maximum peak force coefficients for 0^o wind direction, 45^o panel inclination and front location.

The net peak force coefficients for panels attached to the 16 m high building are depicted in Figure 5.9.3. Similar trends for panels attached to 7 m and 16 m high buildings can be observed for all three panels. Panel 1 experiences the greatest suction, followed by panel 2 for which suction is smaller and finally the smallest suction occurs for panel 3. Overpressure is almost the same for panels 1and 2 and becomes smaller for panel 3. More specifically, for panels 1 and 2 greatest suction occurs for 135^o wind direction, when panel 1 is back located and inclined by 30^o, and while panel 2 is front located and inclined by 20^o. Panel 3 gets its extreme minimum value for 120^o wind direction, when located at the front and inclined by 30^o. Concerning the maximum values of force coefficients for panels 1 and 2, the peaks occur for 45^o wind direction, 40^o panel inclination and front location. For panel 3 the greatest of the maximum values is observed for 30^o wind direction, 30^o panel inclination and front location.

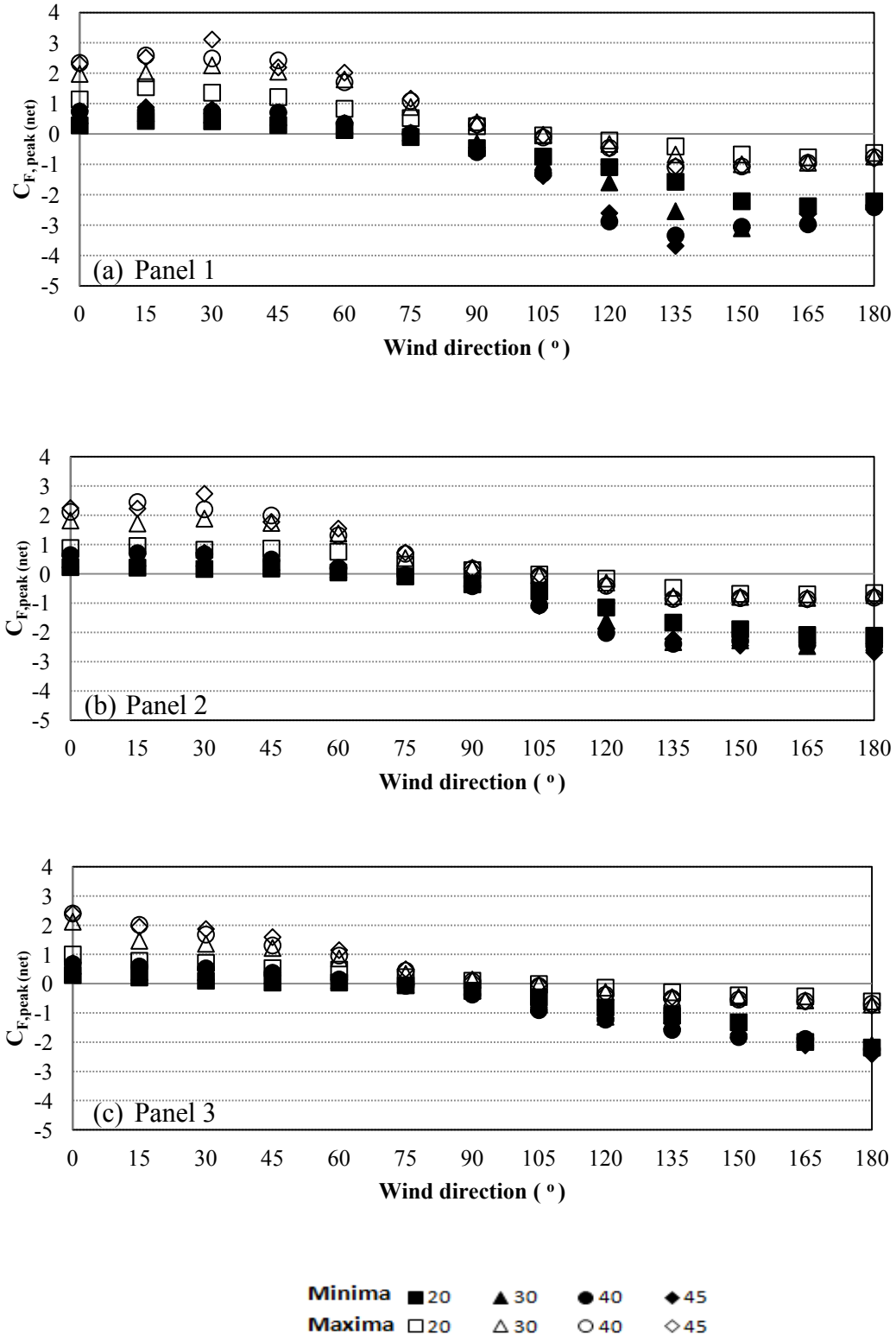

Figure 5.9.1 Net peak force coefficients for stand-alone (a) panel 1, (b) panel 2 and (c) panel 3

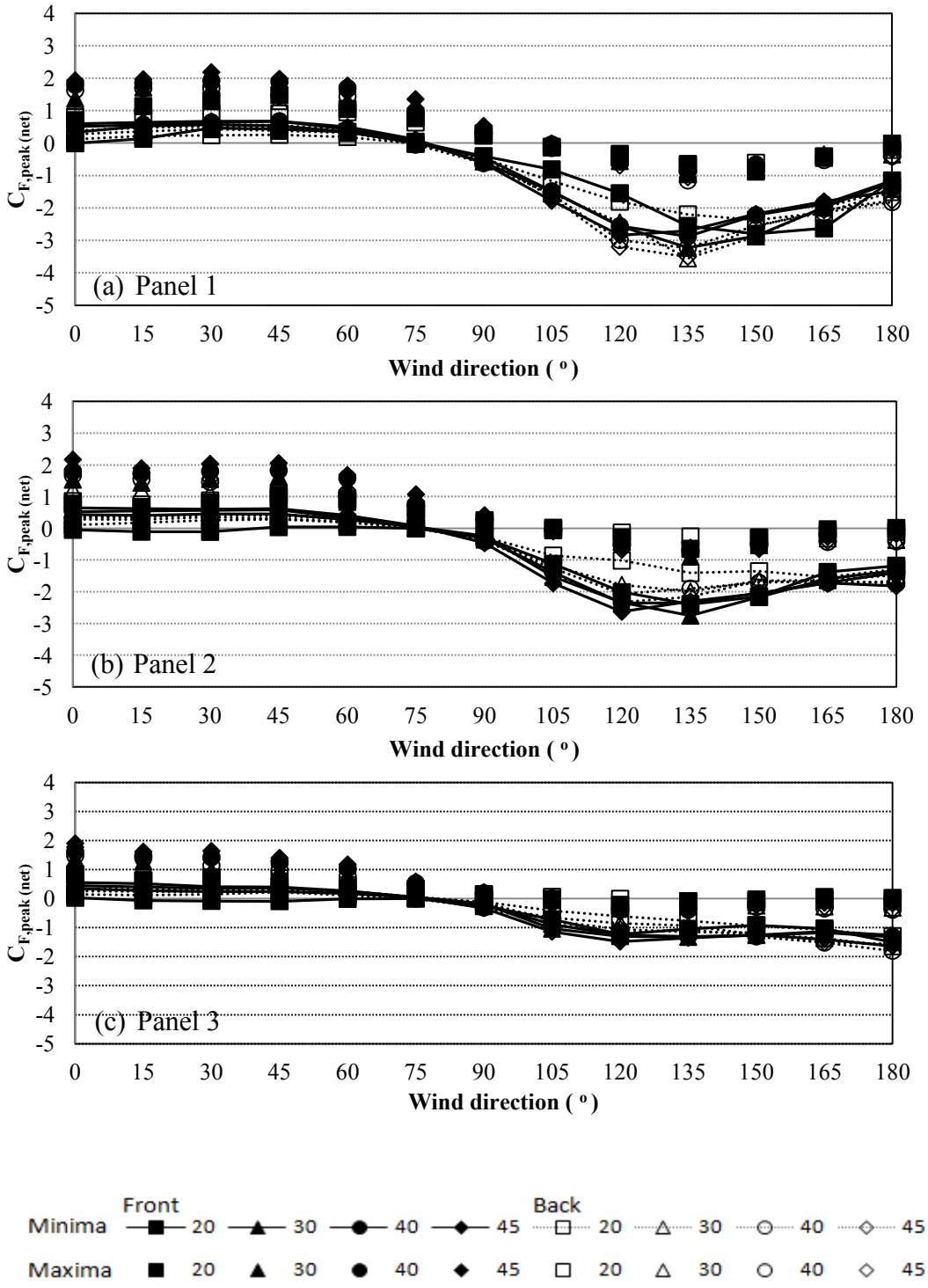

Figure 5.9.2 Net peak force coefficients for (a) panel 1, (b) panel 2 and (c) panel 3 when attached to 7 m high building, front and back location

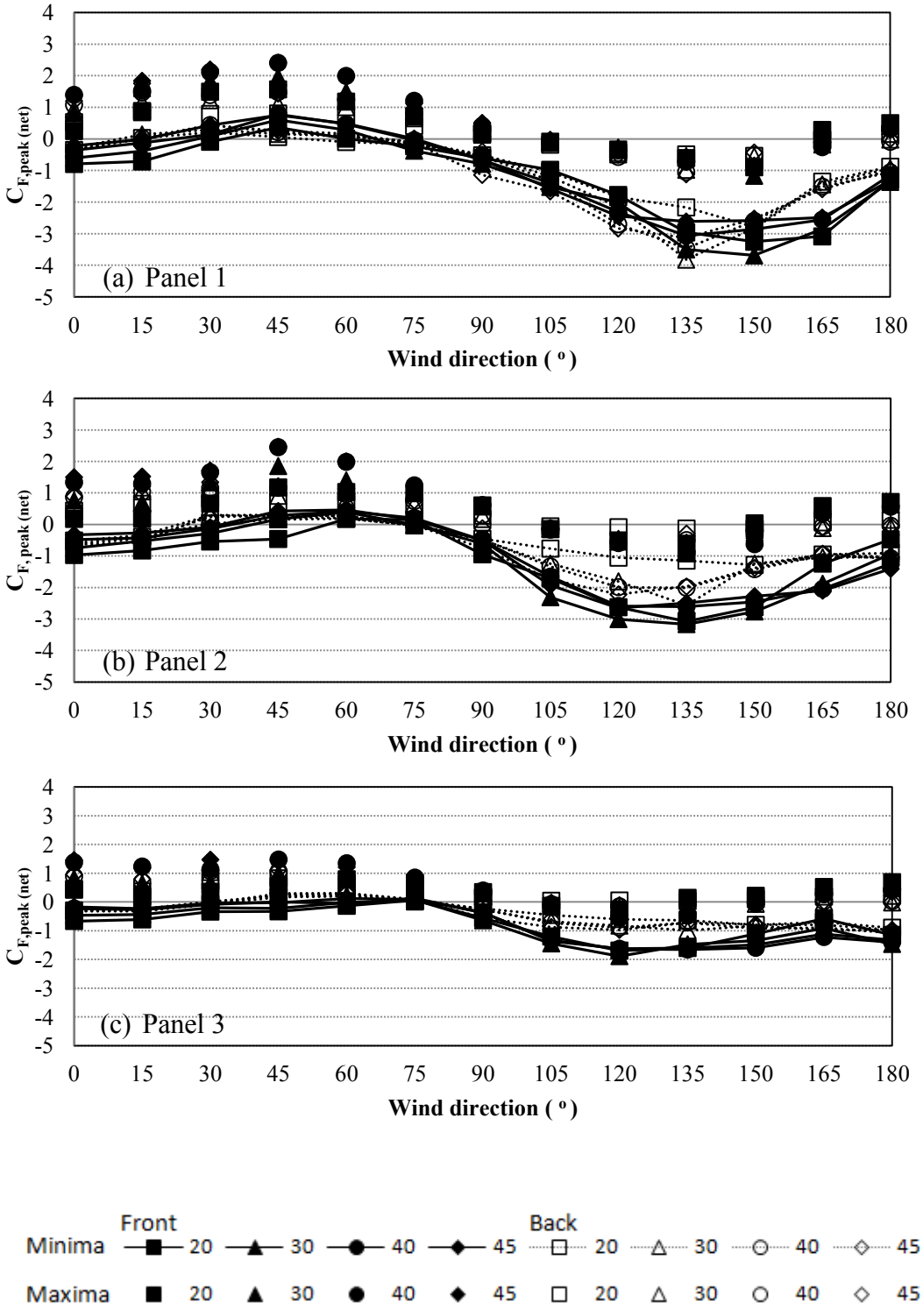

Figure 5.9.3 Net peak force coefficients for (a) panel 1, (b) panel 2 and (c) panel 3 when attached to 16 m high building, front and back location

5.10 COMPARISON BETWEEN LOCAL PRESSURE COEFFICIENTS AND FORCE COEFFICIENTS

This section demonstrates the net local pressure coefficients measured on every single pressure tap of panel 1 in comparison with the force coefficients, which are applied, on the whole surface when the panel is located at the front position of 7 m high building**.** Figure 5.10.1 shows the local pressure coefficients for pressure taps 1, 3, 5, 7, 9, 11, and the force coefficients for panel 1 at 20^o, 30^o, 40^o, 45^o panel inclination. The trends corresponding to the examined pressure taps and panel 1 follow the same pattern with respect to the wind direction. The force coefficient values result from the mean value of the local pressure coefficients, which are measured separately for every single pressure tap. The most critical values can be detected for wind directions ranging from 120^o to 180^o. Pressure tap number 1 is experiencing the greatest suction compared to the other taps and even greater than that experienced by the whole panel for all panel inclinations.

Figure 5.10.1(a) shows that for a panel inclined by 20^o, the minimum pressure coefficient value appears for 135^o wind direction at pressure tap number 5 while for panel 1 the minimum force coefficient takes its minimum at 150^o. Figures 5.10.1(b) and 5.10.1(c) indicate that pressure and force coefficients become most critical for 135^o wind direction at pressure tap number 1 and panel 1 for panels inclined by 30^o and 40^o respectively. For panel inclined by 45^o the results are shown in Figure 5.10.1(d) in which pressure and force coefficients become critical for 120^o wind direction at pressure tap number 1 and panel 1.

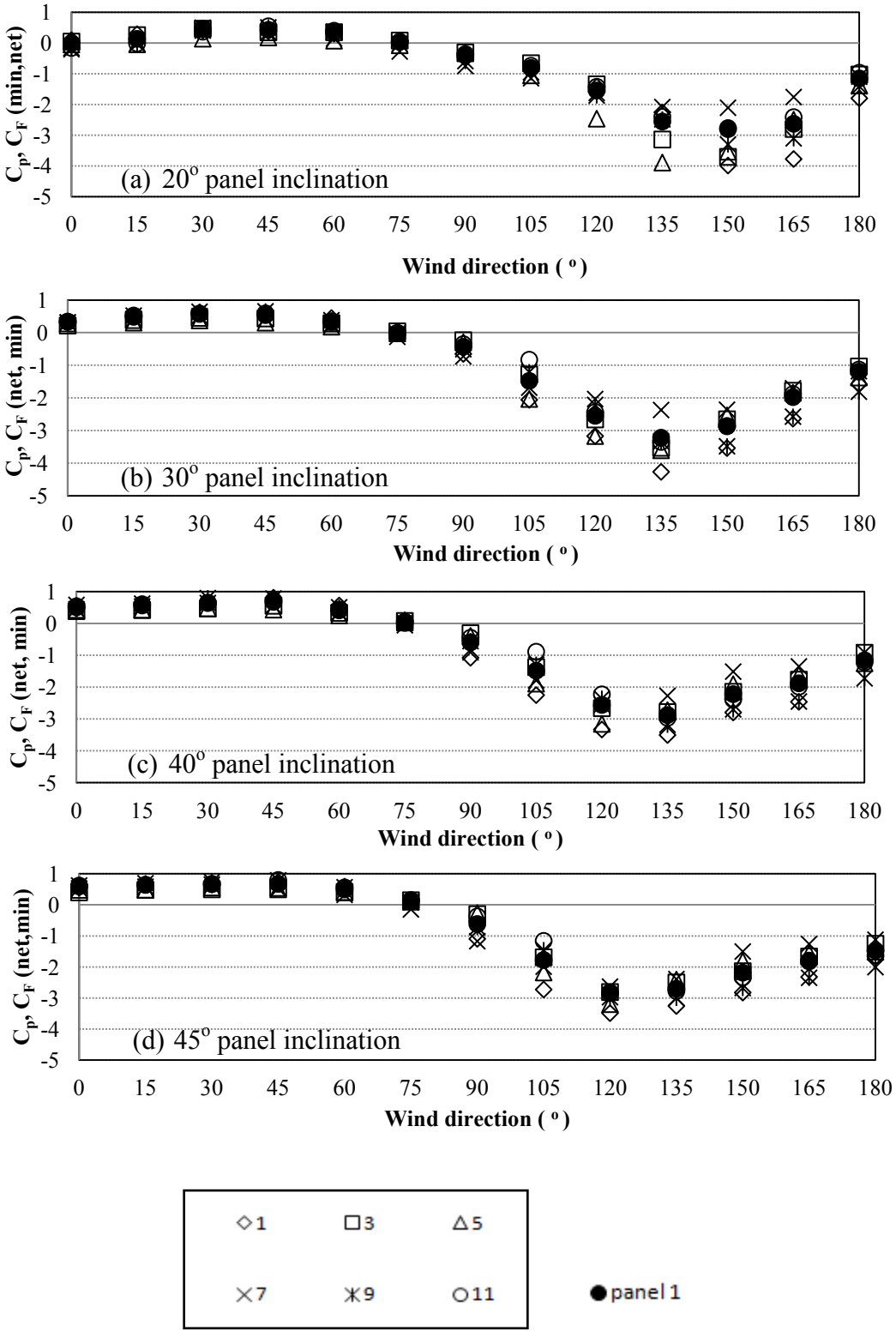

Figure 5.10.1 Comparison of local C_p and panel C_F for (a) 20°, (b) 30°, (c) 40° and (d) 45° panel inclination for 7 m high building and front location

5.11 AREA-AVERAGED PRESSURE COEFFICIENTS FOR 135^o WIND DIRECTION

The area-averaged pressure coefficients are depicted in this section as a function of the area when the wind direction is 135^o for panels inclined by 20^o, 30^o, 40^o, 45^o – see Figure 5.11.1. The values of peak area-averaged pressure coefficients are examined for three different cases, namely: for panels located at the ground level and for panels attached to roofs of two different building heights. The trends follow a similar pattern for the three cases for both minima and maxima. Increase of the considered area leads to reduction of the area-averaged pressure coefficient.

Figure 5.11.1(a) presents the net peak area-averaged pressure coefficients for the case of stand-alone panels. The minimum area-averaged pressure coefficients, take their extreme values for panel inclination of 45^o. These values show small differences to the cases of 40^o and 30^o whereas the 20^o case experiences significantly lower values. The maximum values range from -1 to 0 and the trend of 20^o panel inclination experiences the greatest suction, which slightly differs from that experienced by the panel for the rest of the panel inclinations. Figures 5.11.1(b) and 5.11.1(c) present the net peak area-averaged pressure coefficients for panels attached to 7 m and 16 m high buildings respectively. The extreme values occur for 30^o panel inclination at the back location. Greater suction is detected for back located panels for both building heights with only exception being the 20^o panel inclination case. For the case of front located panels when attached to 16 m high building, the suction experienced becomes smaller compared to that experienced by back located panels. The gradient of minimum values results in smaller suction overall, which can be reduced to almost half of the initial value. Maxima for both building heights range from

-1 to 0 with slight differences among the trends, which have a very small gradient with respect to the area.

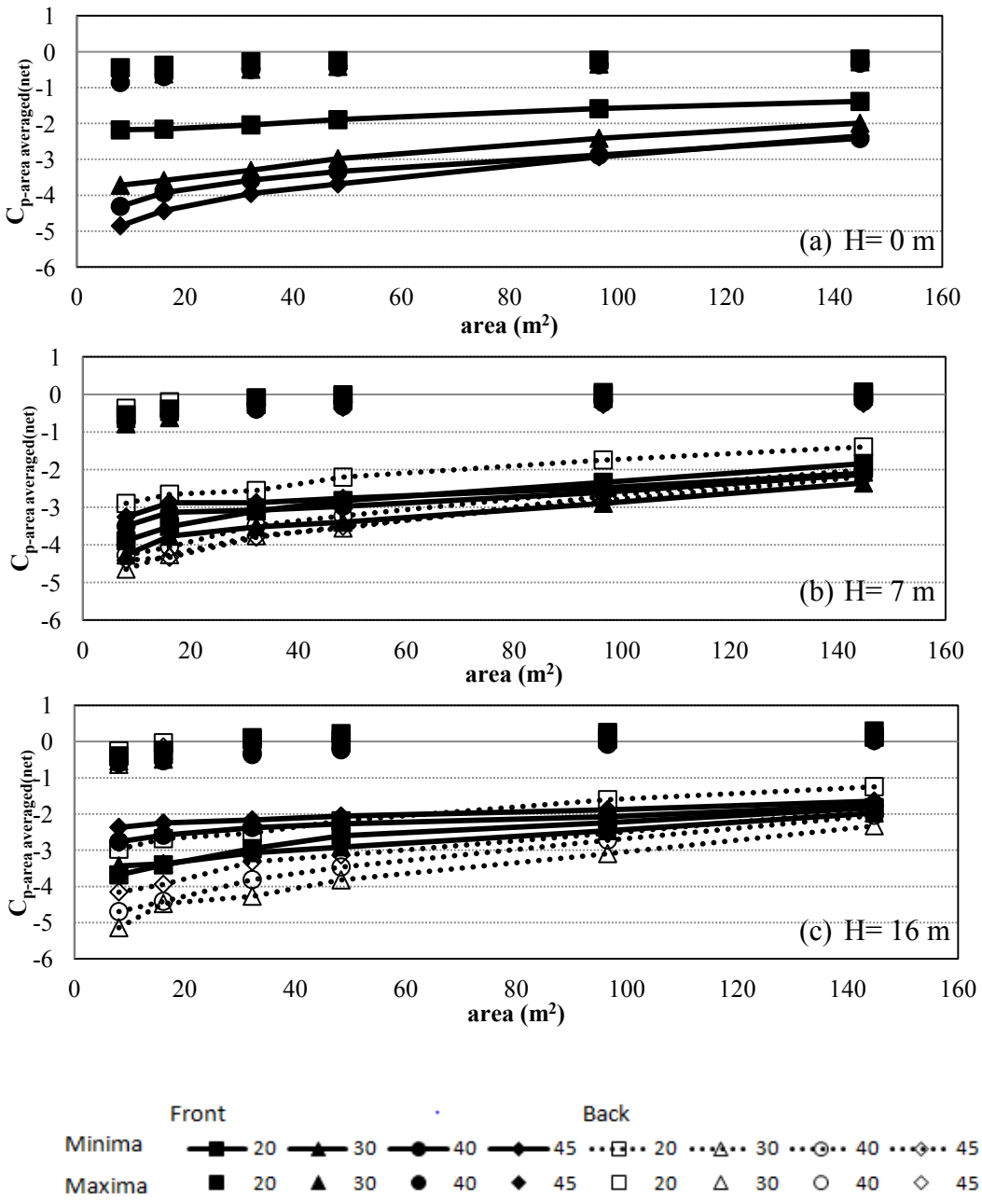

Figure 5.11.1 Net peak area-averaged pressure coefficients for panels (a) stand-alone, (b) attached to 7 m high building and (c) attached to 16 m building considering 135^{o} wind direction

5.12 COMPARISON WITH PREVIOUS STUDIES

In this section, a comparison between the experimental results of the current study and those of previous studies is made. The purpose of the comparison is to investigate how the results coming from different studies are related. The outcome data of these studies are referred to mean and peak values of pressure and force coefficients when the panels have the same or very close values of inclination and are located centrally at the roof, at the front corner or at central back position.

Figures 5.12.1 and 5.12.2 present the net mean and peak values of force coefficients respectively for panels located at the front corner of the building roof. The results of two previous studies, those of Erwin et al (2011) and Saha et al (2011) have been carried out for panels inclined by 15^o, while those of the current study refer to panels inclined by 20^o. The trends of mean and maximum values appear to have the same pattern for both the current and Erwin study for wind directions ranging from 0^o to 45^o, which changes radically for wind directions between 45^o and 180^o. As far as Saha et al study is concerned, the trend of maximum values remains almost constant when the wind direction changes. Regarding the minimum force coefficients for wind direction ranging from 0^o to 120^o, Saha et al reported a higher suction compared to the current study, which becomes smaller for Erwin's et al with increasing wind direction. For wind direction, ranging from 120^o to 165^o the current study demonstrates higher force coefficients applied on the panel. The discrepancies observed, can be attributed to different testing conditions under which the experiments from different studies were performed.

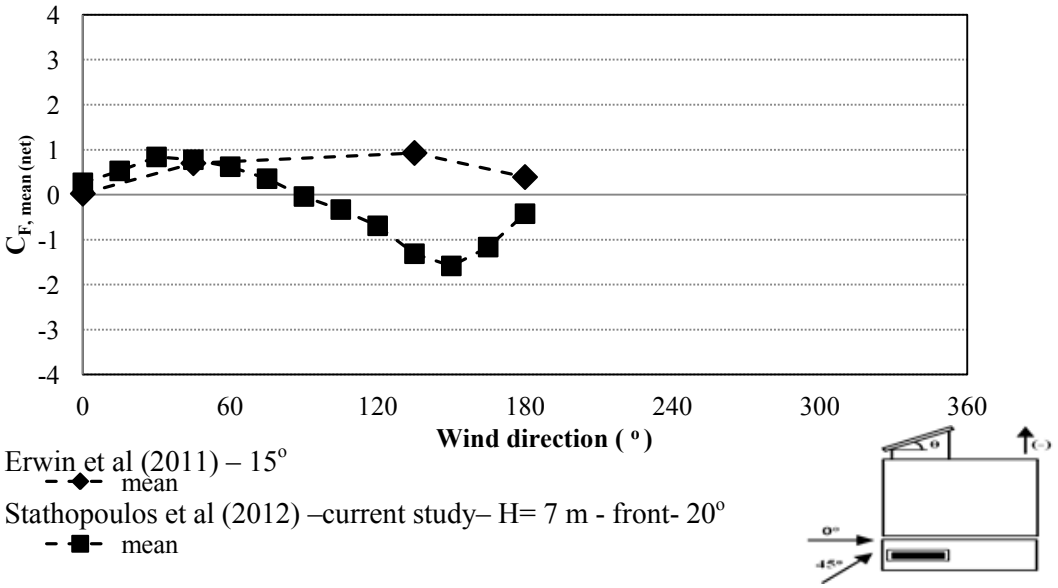

Figure 5.12.1 Net mean force coefficients for panels inclined by 15º and 20º, located at front corner

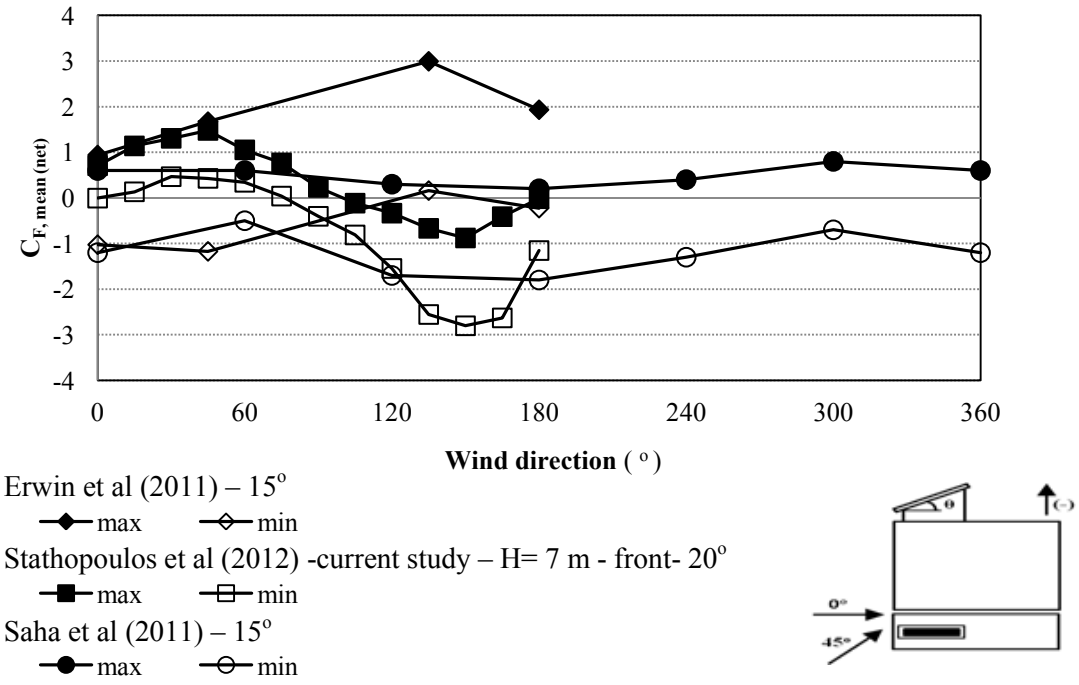

Figure 5.12.2 Net peak force coefficients for panels inclined by 15º and 20º, located at front corner

Experimental results coming from different studies such as Erwin et al (2011), Saha et al (2011) and the current study for panels located centrally at the building roof and inclined by 30^o are depicted in Figure 5.12.3. The mean values of the net pressure coefficients remain almost constant for the Saha et al (2011). On the contrary, in the current study experimental results show that for panels located at back position of 7 m high building roof, greater suction appears for wind directions ranging from 120^o to 180^o.

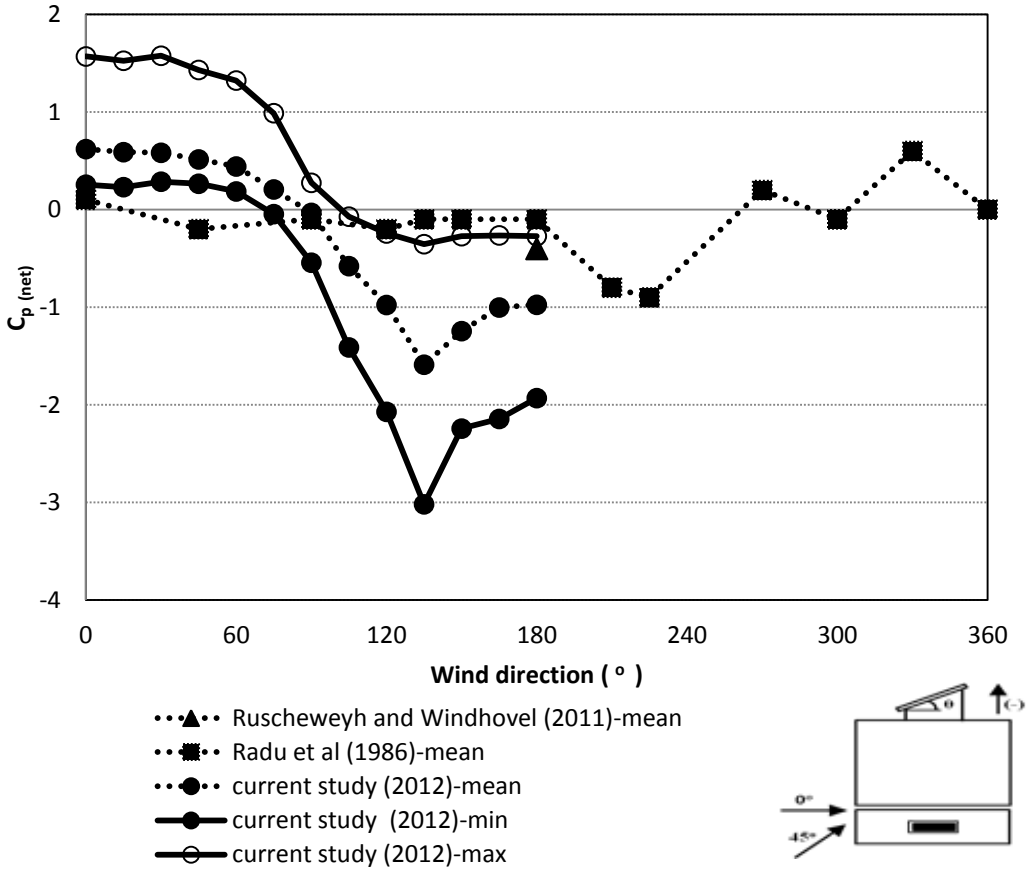

Figure 5.12.3 Net mean and peak pressure coefficients for panels centrally located and 30^o panel inclination

Figure 5.12.4 demonstrates the net mean force coefficients for panels attached to building roofs and inclined by 30^o and 45^o. These values follow similar patterns for both studies for wind direction ranging from 0^o to 135^o, and in general, there is a good agreement of their experimental results. However, the current study shows that when the wind direction ranges from 135^o to 180^o, the trends of mean force coefficients remain almost constant.

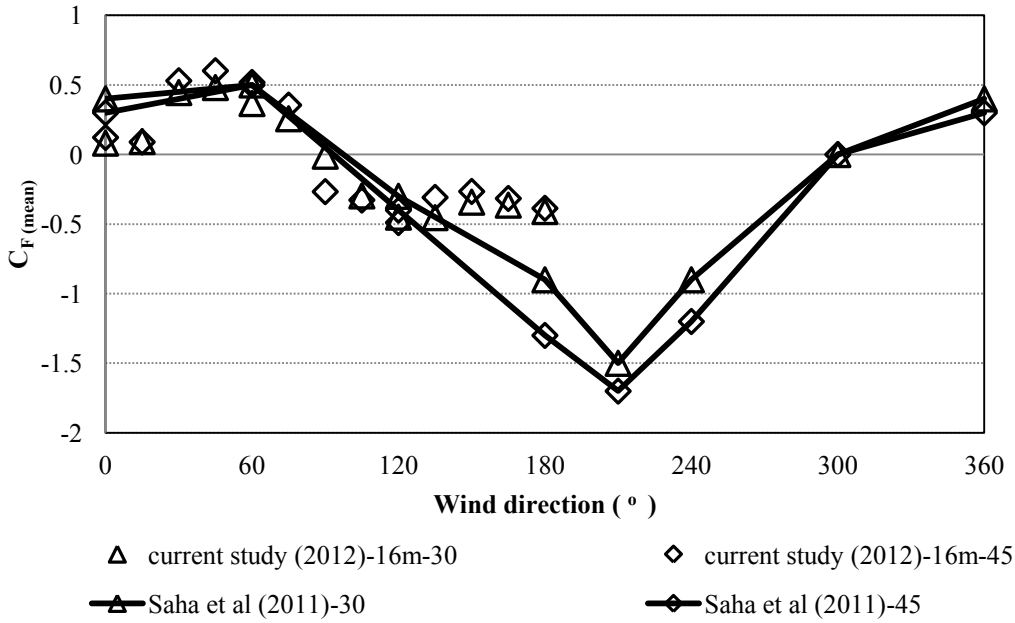

Figure 5.12.4 Net mean force coefficients for panels inclined by 30^o and 45^o, located at back corner

Finally, Figures 5.12.5 and 5.12.6 present the maximum and minimum values of net force coefficients respectively for panels located centrally near the back edge of the building roof. For the current study, the results corresponding to panel 2 and back location are demonstrated as well as those coming from Saha's et al (2011) study. In general, the

trends for both minimum and maximum values of the force coefficient follow the same pattern. The small discrepancies observed between the two studies can be attributed to different testing conditions; Saha et al (2011) conducted a wind test with suburban exposure, while an open terrain exposure was used for the current study.

As can be observed by Figure 5.12.5, the maximum values of force coefficients corresponding to Saha's et al study with panel inclined by 15^o are greater in total. Moreover, Figure 5.12.6 points out that Saha's et al (2011) experimental results show slightly greater force coefficients in terms of absolute values compared to the values of the current study.

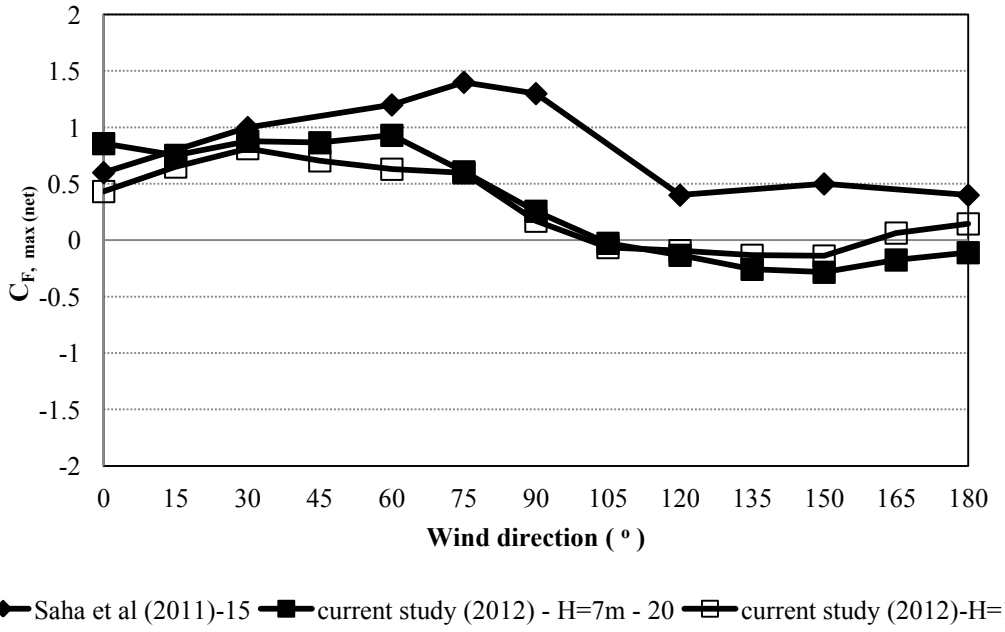

Figure 5.12.5 Maximum force coefficients for panels inclined by 15^o and 20^o, located at central back position

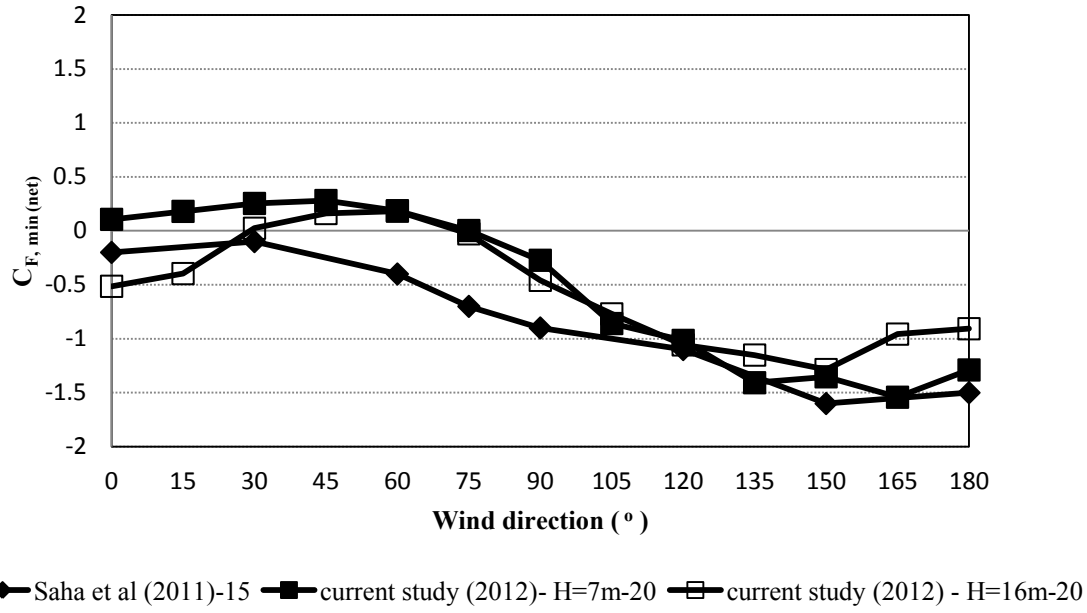

Figure 5.12.6 Minimum force coefficients for panels inclined by 15^{o} and 20^{o}, located at central back position

CHAPTER 6: SUMMARY AND CONCLUSIONS

6.1 SUMMARY

The scope of this study was to better understand the wind pressure distribution on stand-alone panel surfaces and panels attached to flat building roofs. For this purpose, sophisticated physical models of solar panels of different configurations were constructed and appropriate instrumentation was used during the experimental process in the boundary layer wind tunnel in order to evaluate relevant wind-induced loads.

A complex model was constructed using a 1:200 geometric scale. Three model panels were equipped with 36 pressure taps in total (both surfaces) for point and area-averaged pressure/force measurements. Pressure and force coefficients were computed for every pressure tap and for all the panels. Different configurations were tested under similar conditions in order to examine the effect of each parameter on the experimental results.

6.2 CONCLUSIONS

The conclusions of this study can be summarized as follows:

- The wind direction of 135^{o} can be considered critical since most critical pressure coefficients occur for this wind direction. More specifically, the greatest suction is experienced by the corner panel located at the roof corner facing the wind flow (panel 1) for 135^{o} wind direction. The most critical values of local net pressure coefficients occur at pressure tap denoted “1” which is found at the upper corner of panel 1.

- The net values of pressure coefficients corresponding to different configurations are affected by the panel inclination for the critical 135^o wind direction. For panels located at the ground level, increasing panel inclination results in greater suction, as well as for panels attached to 7 m and 16 m high buildings, located at the back position of the roof. On the contrary, for front located panels attached to 7 m and 16 m high buildings, suction becomes smaller with increasing panel inclination.
- The increase of building height for panels which are located at the front position of the building roof results in slightly smaller suction, while for panels located at the back, the suction remains almost constant for 135^o wind direction.
- As far as the panel location is concerned, clearly back located panels suffer higher suction than front located panels, at least for the critical 135^o wind direction.
- From all configurations examined, panel 1 shows the greatest net force coefficient values because it is located at the roof corner and exposed obliquely to the 135^o angle of attack. The suction becomes even greater for this panel when located at the back position of the roof.
- Considering the building height, it is clear that higher suction occurs for panel 1 (corner panel), at the front location and the 135^o wind direction. Middle-panel (panel 2) follows with slightly smaller suction and finally the corner panel (panel 3) sees the smallest suction.
- Comparison of the two panel locations (i.e. front and back) demonstrates that force coefficients are greater for the back located corner panel at the roof building when exposed obliquely to the wind. However, for the same exposure, the values

of force coefficients for the middle-panel (panel 2) and the other corner panel (panel 3 is at the opposite side of the one facing the wind flow) are greater when they are located in the front of the building.

- The net values of force coefficients with respect to the wind direction show clearly that the extreme values appear within the range of 105^o and 180^o wind directions. For all the configurations examined, the force coefficients are larger for the corner panel (panel 1).
- Comparison of the experimental results of the current study with those of previous studies show that the values of net mean force coefficients are in good agreement, while discrepancies are observed for the net peak force coefficient values.

6.3 RECOMMENDATIONS FOR FURTHER STUDY

The effect of a number of different parameters were examined in the current study, however, more experimental work in the wind tunnel could offer the opportunity to investigate the effect of additional important parameters.

One parameter related to a better performance of solar panels is the panel inclination, which in some cases exceeds the 45^o or is smaller than 20^o. Therefore, further investigation for more panel inclinations would be necessary. Furthermore, solar panels are often located on flat roofs in different rows of arrays and very little provision is available for this case. It should also be mentioned that, experiments should be carried out for different types of terrain so as to better examine the effect of landscape in the panel wind loading.

Moreover, it would be really interesting to examine cases of inclined panels attached to pitched roofs with different slopes than the roof because studies so far focus mainly on panels located parallel to roofs. Other parameters that should be further inspected because of their contribution in better panel functionality are the gaps between the panels and the roof, as well as, the distance among the panels. Careful examination of these parameters would provide information useful in determining the design wind loads in which structures are subjected and improving the building code.

REFERENCES

Bienkiewicz, B., & Endo, M. (2009). Wind Considerations for Loose-Laid and Photovoltaic Roofing Systems. *Structures Congress 2009* (pp. 1-10). Austin, Texas, United States: American Society of Civil Engineers.

Bitsuamlak, G. T., Dagnew, A., & Erwin, J. (2010). Evaluation of wind loads on solar panel modules using CFD simulation (CWE2010). *The fifth International Symposium on Computational Wind Engineering Conference.* Chapel Hill, NC.

Blackmore, P. A., & Geurts, C. P. (2008). Wind loads on roof mounted PV modules. *Paper presented at the WES Conference*. Guildford, UK.

Bronkhorst, A. J., Geurts, C. P., Bentum, C. V., & Grepinet, F. (2010). Wind tunnel and CFD modelling of wind pressures on solar energy systems on flat roofs. *5th International Symposium on Computational Wind Engineering (CWE2010)*, (p. 8). Chapel Hill, North Carolina, USA.

Chung, K., Chang, K., & Chou, C.-C. (2011). Wind loads on residential and large-scale solar collector models. *Journal of Wind Engineering and Industrial Aerodynamics, 99*(1), 59 - 64.

Chung, K., Chang, K., & Liu, Y. (2008). Reduction of wind uplift of a solar collector model. *Journal of Wind Engineering and Industrial Aerodynamics, 96*(8-9), 1294-1306.

Chung, K.-M., Chang, K.-C., & Chou, J.-C. (2009). Wind Loading of Solar Collector Models. *The Seventh Asia-Pacific Conference on Wind Engineering*, (pp. 631-634). Taipei, Taiwan.

Geurts, C., & Steenbergen, R. (2009). Full scale measurements of wind loads on stand-off photovoltaic systems. In C. Borri (Ed.), *5th European and African conference on wind engineering (EACWE)*, (pp. 1-12). Florence, Italy.

Hosoya, N., Cermak, J. E., & Steele, C. (2001). A Wind-Tunnel Study of a Cubic Rooftop AC Unit on a Low Building. *9th Americas Conference on Wind Engineering (ACWE)*, (pp. 1-10). Clemson, South Carolina, USA.

Houghton, E. L., & Carruthers, N. B. (June 1976). *Wind Forces on Buildings and Structures: An Introduction.* John Wiley & Sons Inc.

Kopp, G. A., Surry, D., & Chen, K. (2002). Wind loads on a solar array. *Wind and Structures, 5*(5), 393-406.

Liu, H. (1990). *Wind Engineering: A Handbook for Structural Engineers.* (B. M. Stewart, Ed.) USA: Prentice-Hall.

Meroney, R. N., & Neff, D. E. (2010). Wind effects on roof-mounted solar photovoltaic arrays: CFD and wind-tunnel evaluation. *5th International Symposium on Computational Wind Engineering (CWE2010)*, (pp. 1-8). Chapel Hill, North Carolina, USA.

Radu, A., & Axinte, E. (1989). Wind forces on structures supporting solar collectors. *Journal of Wind Engineering and Industrial Aerodynamics, 32*(1-2), 93-100.

Radu, A., Axinte, E., & Theohari, C. (1986). Steady wind pressures on solar collectors on flat-roofed buildings. *Journal of Wind Engineering and Industrial Aerodynamics, 23*(0), 249-258.

Ruscheweyh, H., & Windhövel, R. (2011). Wind loads at solar and photovoltaic modules for large plants. *13th International Conference on Wind Engineering (ICWE13)*, (pp. 1-8). Amsterdam, The Netherlands.

Saha, P. K., Yoshida, A., & Tamura, Y. (2011). Study on wind loading on solar panel on a flat-roof building: Effects of locations and inclination angles. *13th International Conference on Wind Engineering (ICWE13)*, (pp. 1-8). Amsterdam, The Netherlands.

Shademan, M., & Hangan, H. (2009). Wind Loading on Solar Panels at Different Inclination Angles. *11th Americas Conference on Wind Engineering*, (pp. 1-9). San Juan, Puerto Rico.

Shademan, M., & Hangan, H. (2010). Wind loading on solar panels at different azimuthal and inclination angles. *The Fifth International Symposium on Computational Wind Engineering (CWE2010)*, (pp. 1-8). Chapel Hill, North Carolina, USA.

Sparks, P. R., Akins, R. E., & Tieleman, H. W. (1981). Wind Force Coefficients for Solar Collectors Derived from Full-Scale Load and Pressure Measurements. *4th U.S. National Conference on Wind Engineering Research*, (pp. 321-331). Seattle, WA, USA.

Stathopoulos, T. (1984). Design and fabrication of a wind tunnel for building aerodynamics. *Journal of Wind Engineering and Industrial Aerodynamics, 16*(2-3), 361 - 376.

Stathopoulos, T., Zisis, I., & Xypnitou, E. (2012). Wind Loads on Solar Collectors: A Review. *ASCE/SEI Structures Congress*, (pp. 1169-1179). Chicago.

Stenabaugh, S. E., Karava, P., & Kopp, G. A. (2011). Design wind loads for photovoltaic systems on sloped roofs of residential buildings. *13th International Conference on Wind Engineering*, (pp. 1-8). Amsterdam, The Netherlands.

Wood, Graeme S; Denoon, Roy O; Kenny, C.S. Kwok;. (December 2001). Wind loads on industrial solar panel arrays and supporting roof structure. *Wind and Structures, 4*(6), 481-494.

Zisis, I. (2006). Structural monitoring and wind tunnel studies of a low wooden building. *Masters thesis, Concordia University*.

BIBLIOGRAPHY

Cook, N. J. (1985). *The Designer's Guide to Wind Loading of Building Structures.* Butterworths, London: Building Research Establishment, Department of the Environment.

Dyrbye, C., & Hansen, S. O. (1997). *Wind loads on structures.* John Wiley & Sons.

Lawson, T. V. (1990). Wind Effects on Buildings: Design applications. In T. V. Lawson, *Wind Effects on Buildings* (Vol. 1, p. 318). Applied Science Publishers.

Simiu, E., & Scanlan, R. H. (1996). *Wind Effects on Structures: Fundamentals and Applications to Design* (3rd ed.). John Wiley.

APPENDIX A

Appendix A includes the contour plots regarding the upper, lower surface and net values of pressure coefficients for all configurations examined and wind direction 135^{o}.

UPPER SURFACE, H = 7 m

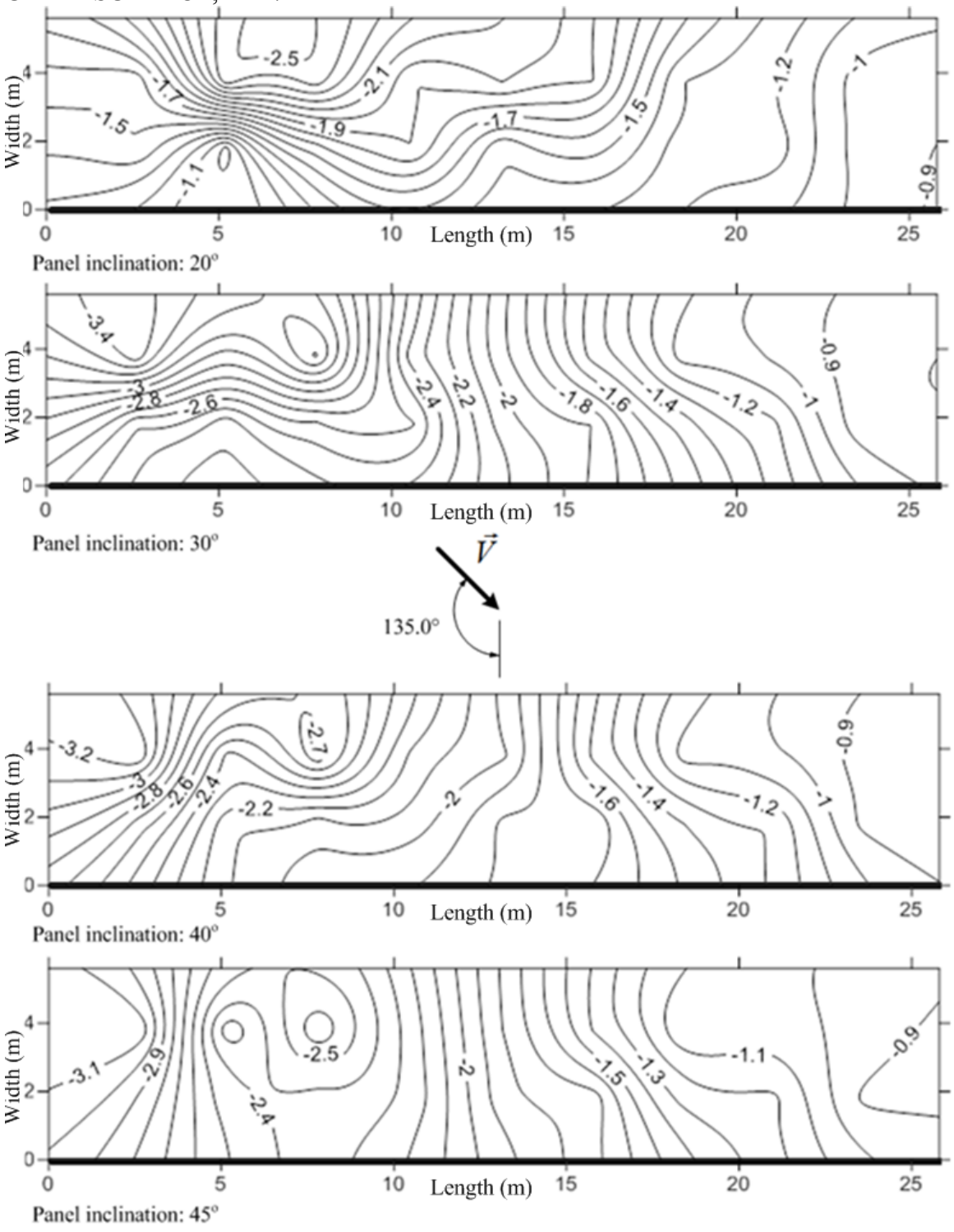

Figure A 1 Minimum C_p values for the upper panels surface, attached to 7 m high building and back located

LOWER SURFACE, H = 7 m

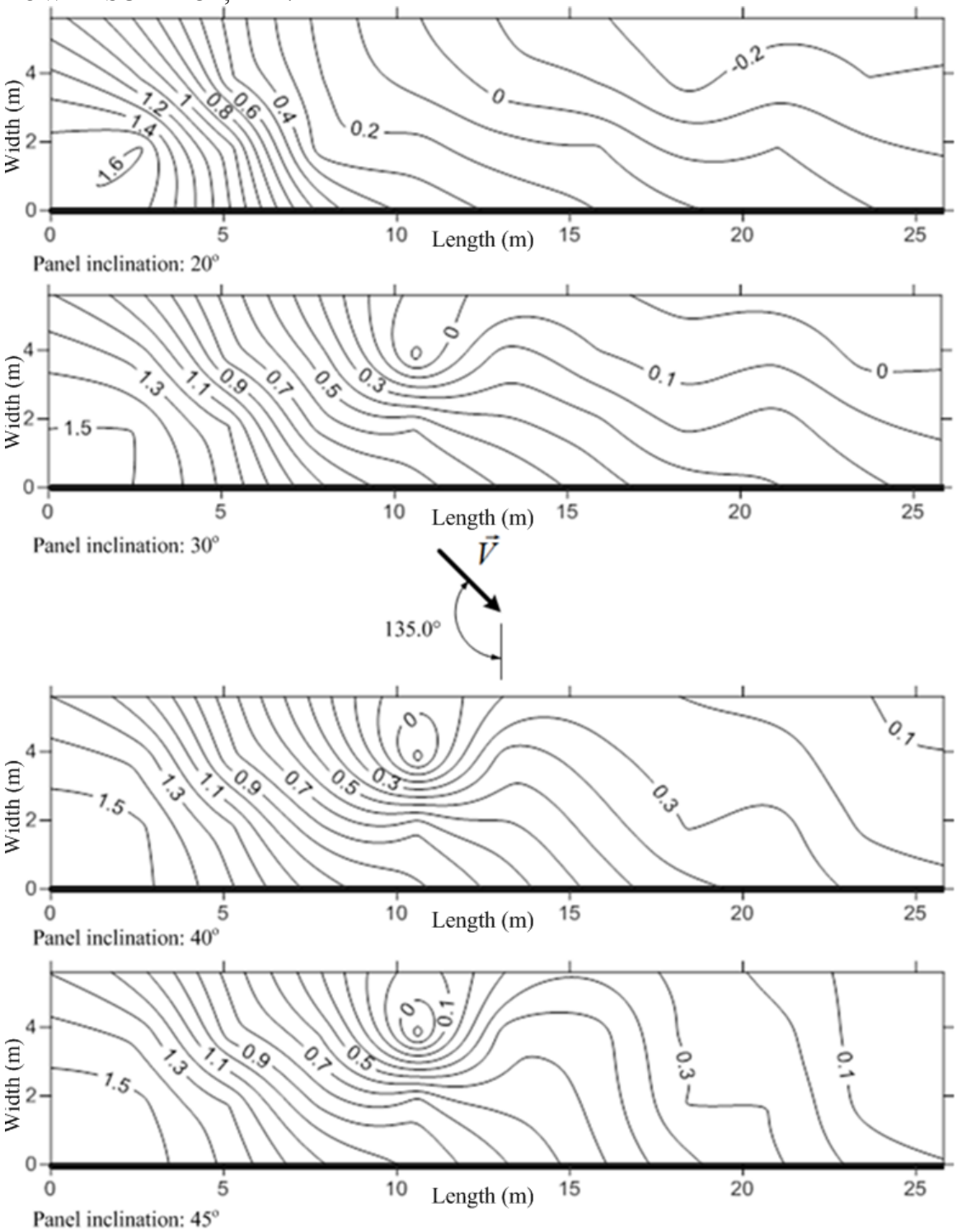

Figure A 2 Maximum C_p values for the lower panels surface, attached to 7 m high building and back located

NET, H = 7 m

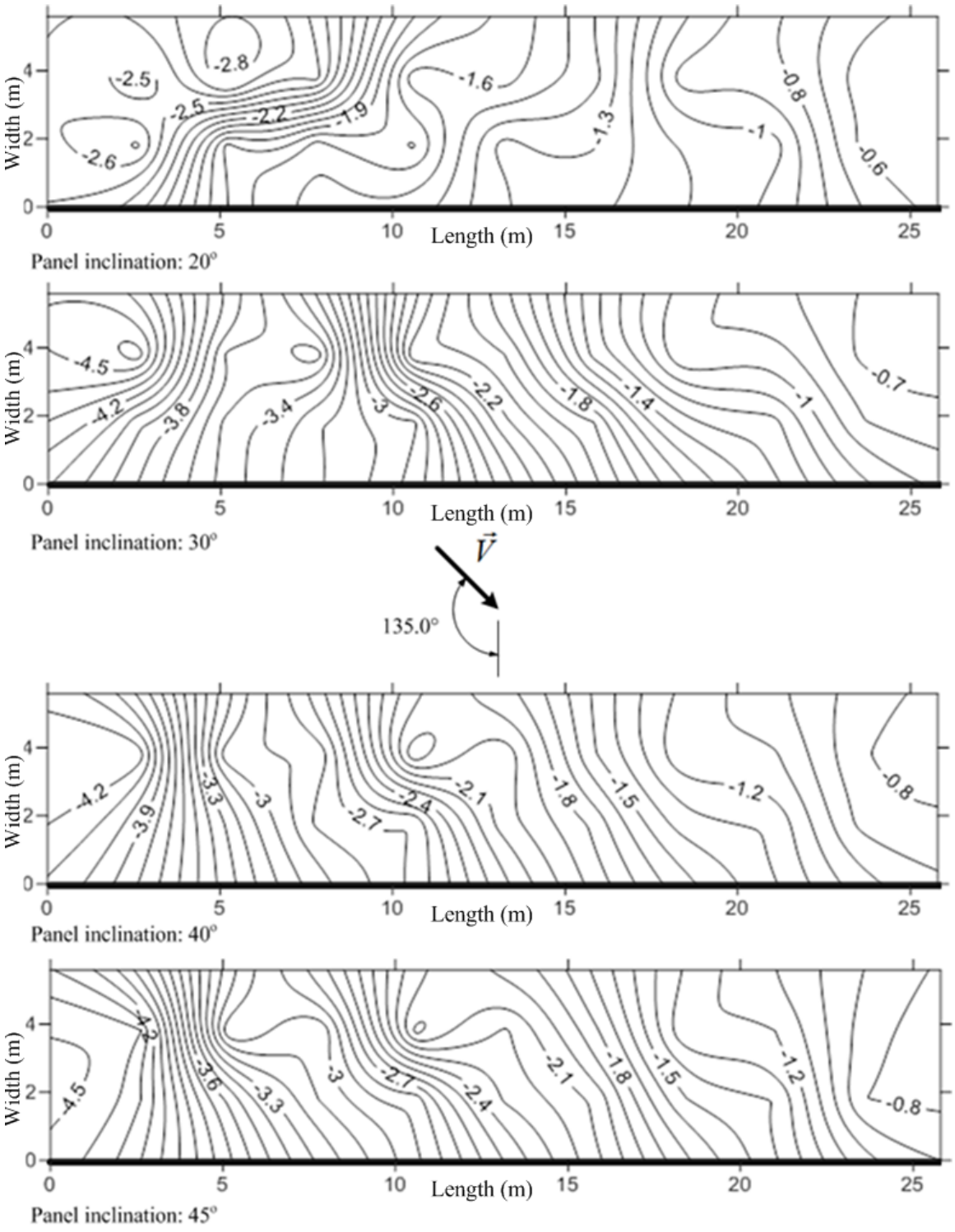

Figure A 3 Net minimum C_p values for panels attached to 7 m high building, back located

UPPER SURFACE, H = 16 m

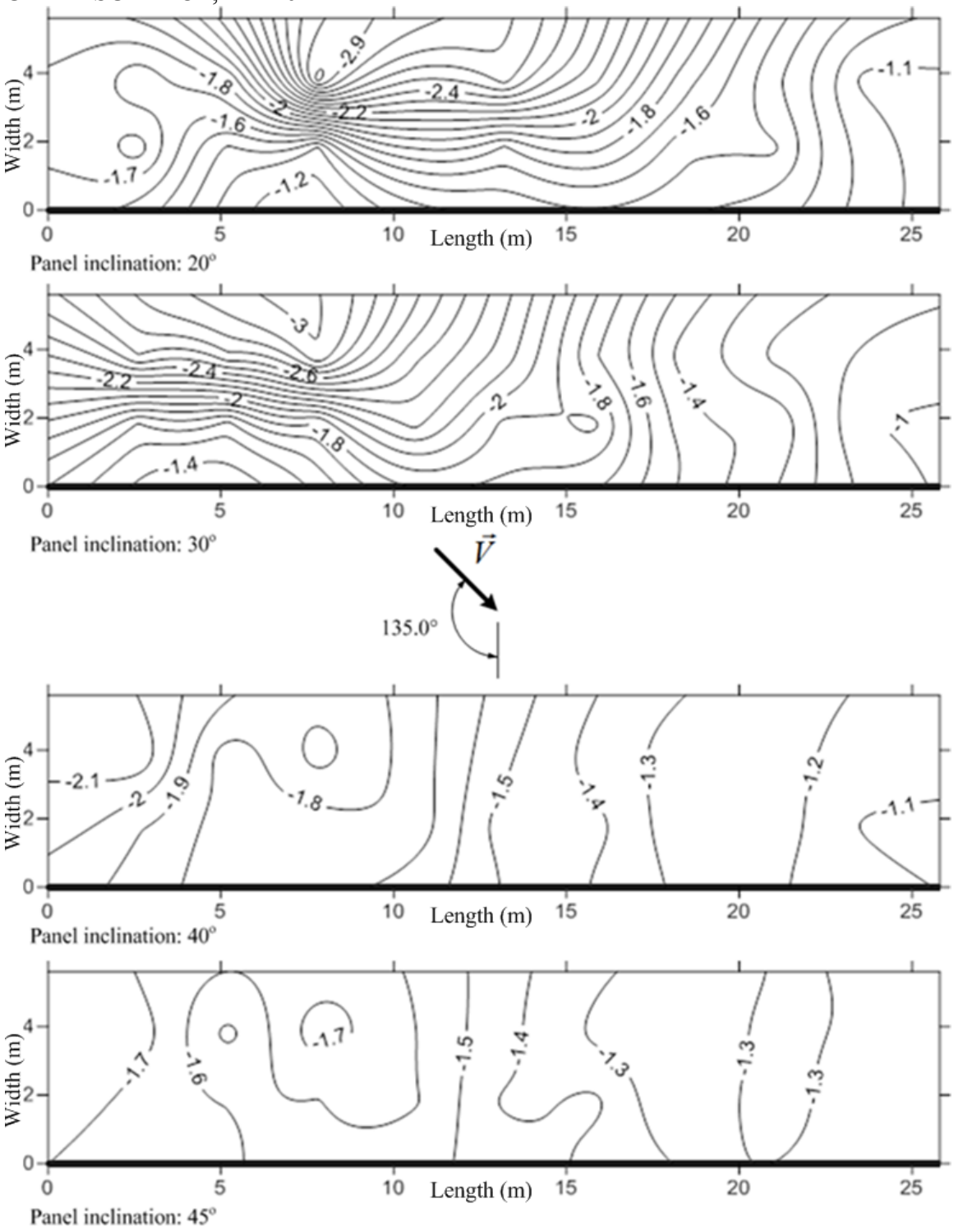

Figure A 4 Minimum C_p values for the upper panels surface, attached to 16 m high building and front located

LOWER SURFACE, H = 16 m

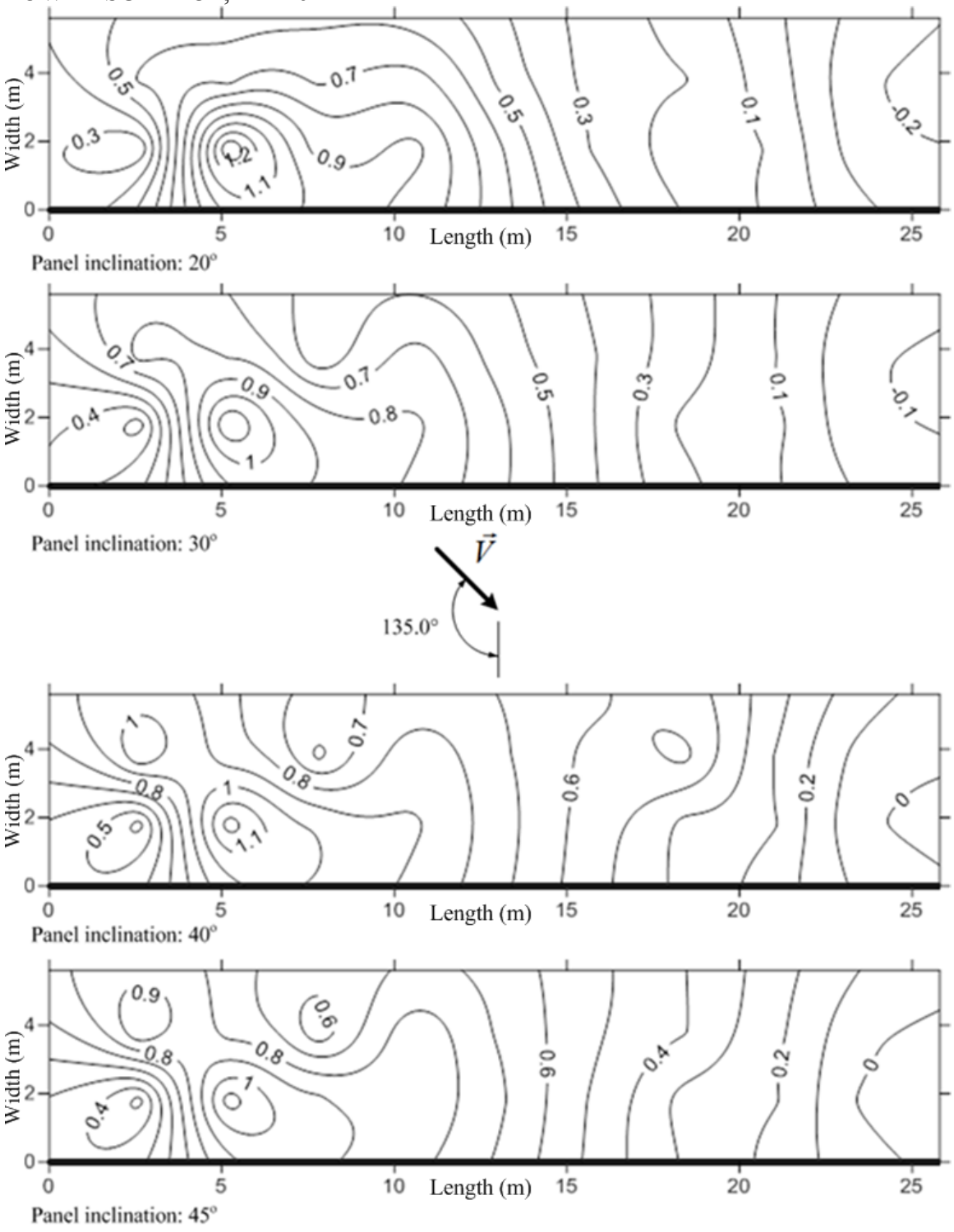

Figure A 5 Maximum C_p values for the lower panels surface, attached to 16 m high building and front located

NET, H= 16 m

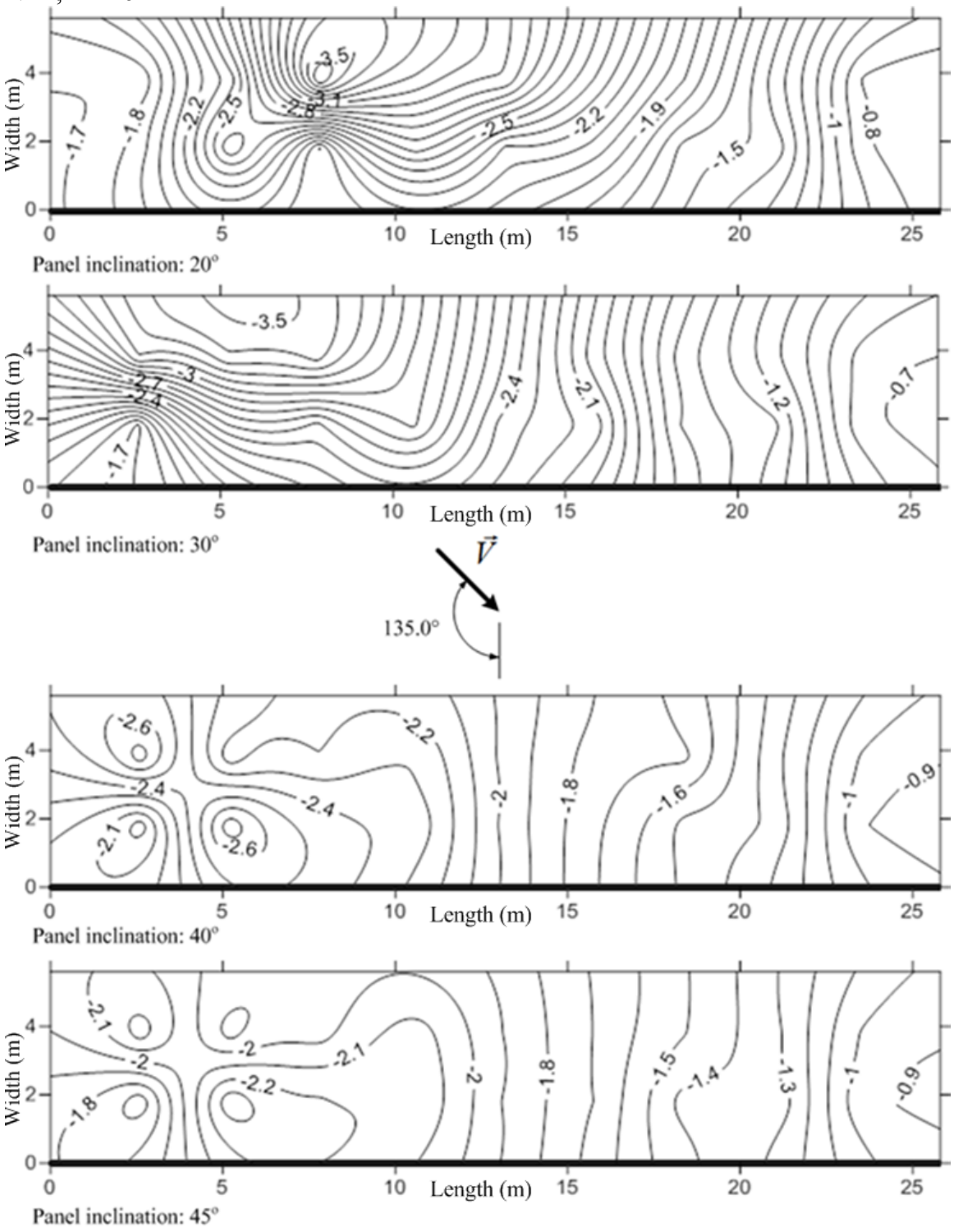

Figure A 6 Net minimum C_p values for panels attached to 16 m high buildings, front located

UPPER SURFACE, H = 16 m

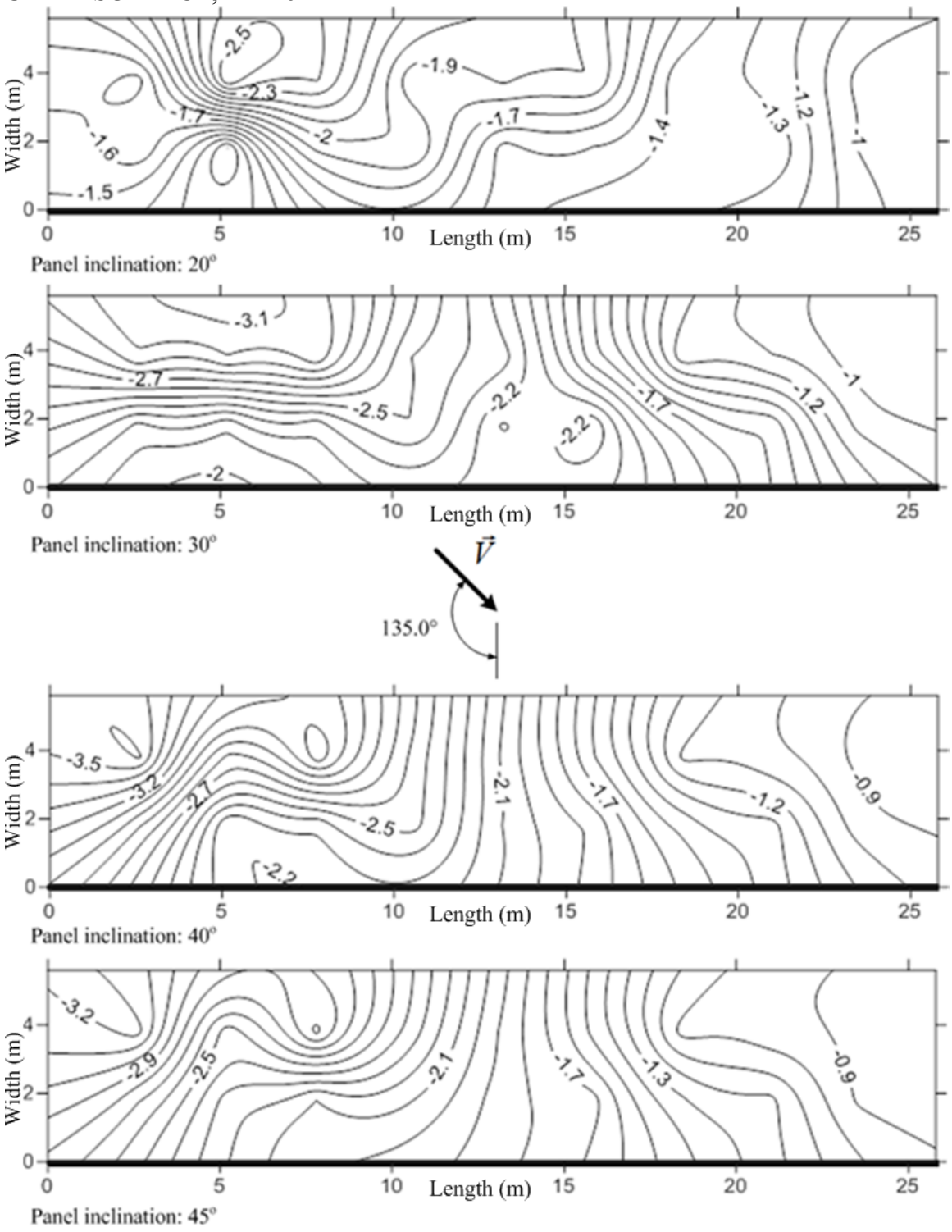

Figure A 7 Minimum C_p values for the upper panels surface, attached to 16 m high building and back located

LOWER SURFACE, H= 16 m

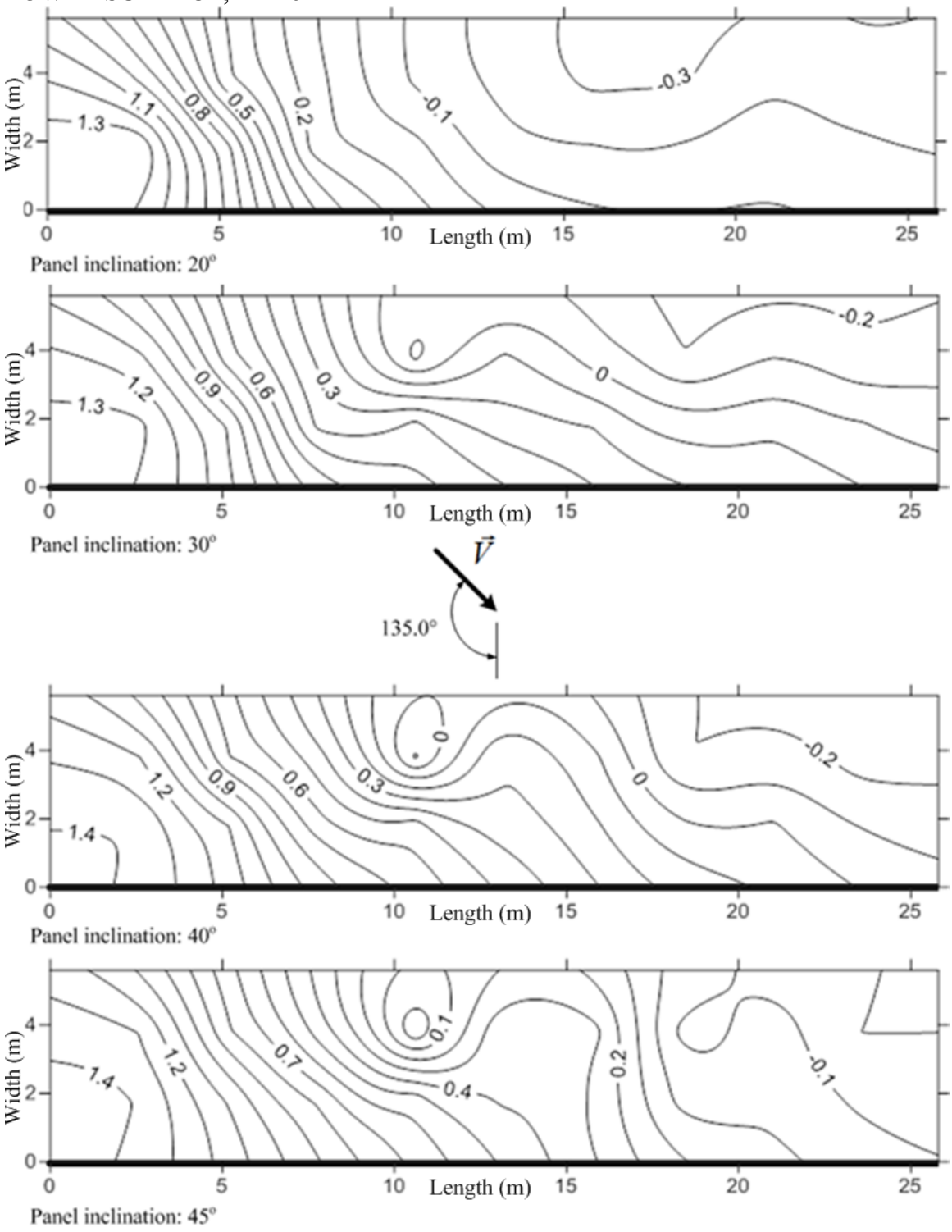

Figure A 8 Maximum C_p values for the lower panels surface, attached to 16 m high building and back located

NET, H = 16 m

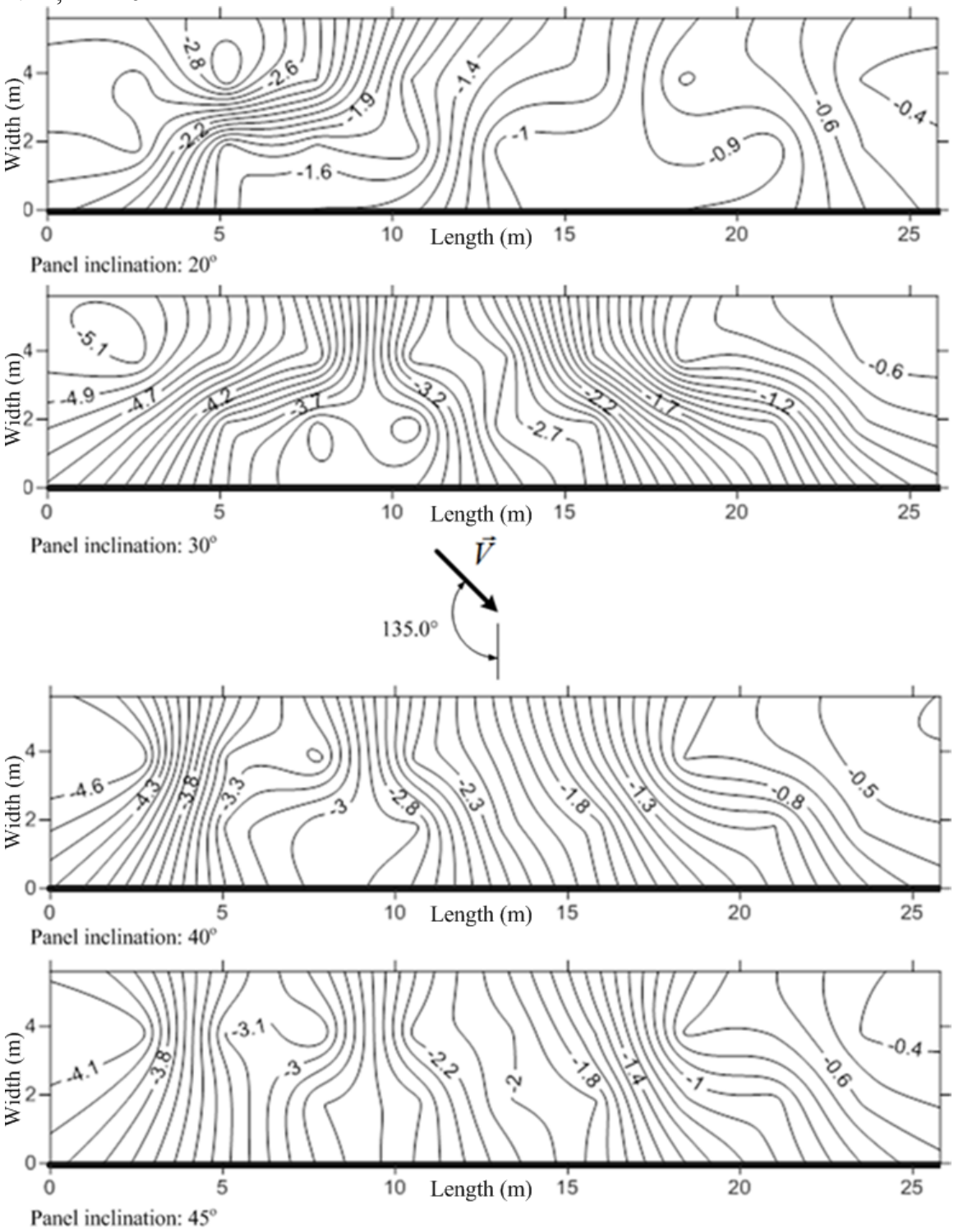

Figure A 9 Net minimum C_p values for panels attached to 16 m high building, back located

UPPER SURFACE, PANELS AT THE GROUND LEVEL

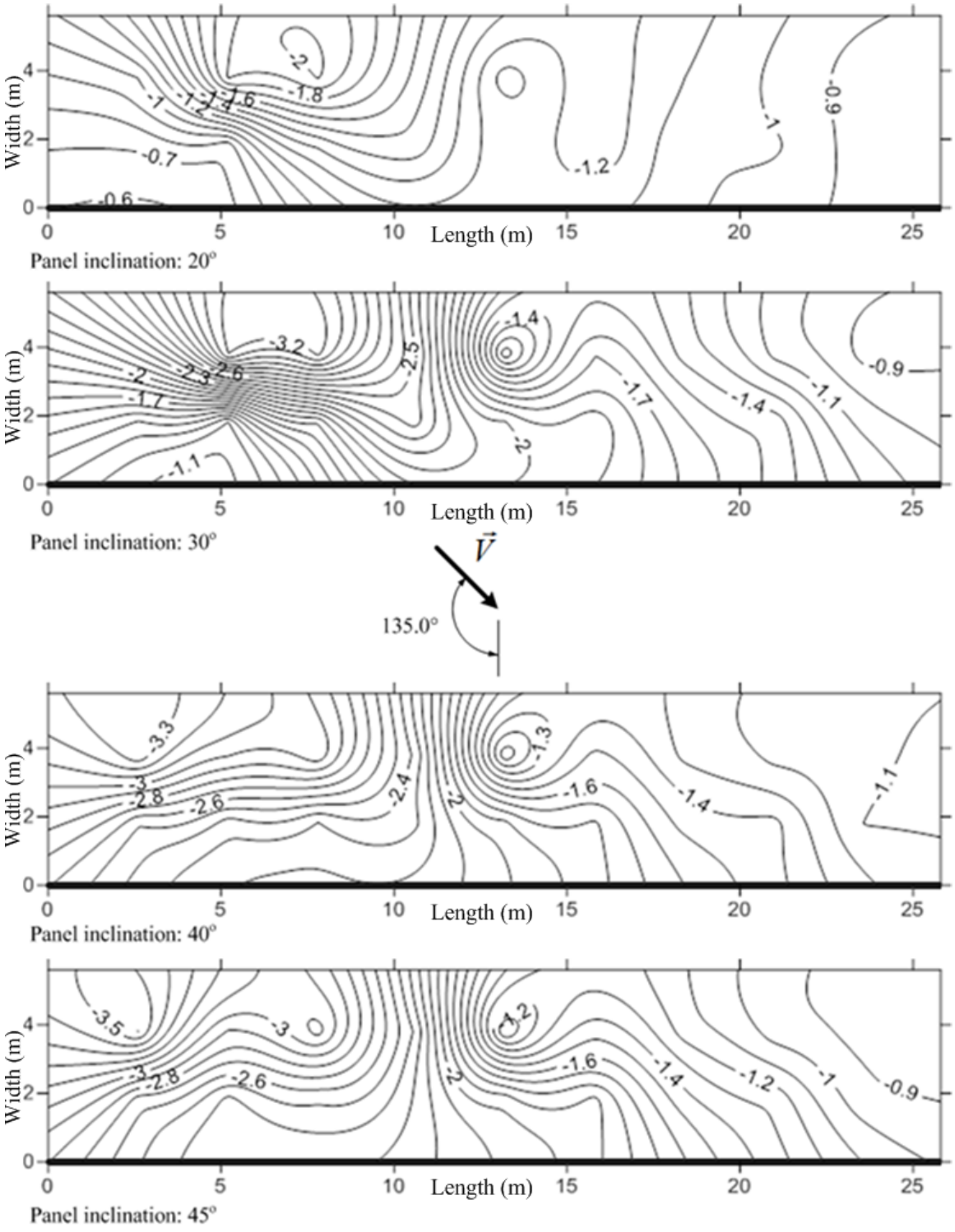

Figure A 10 Minimum C_p values for the upper panels surface at the ground level

LOWER SURFACE, PANELS AT THE GROUND LEVEL

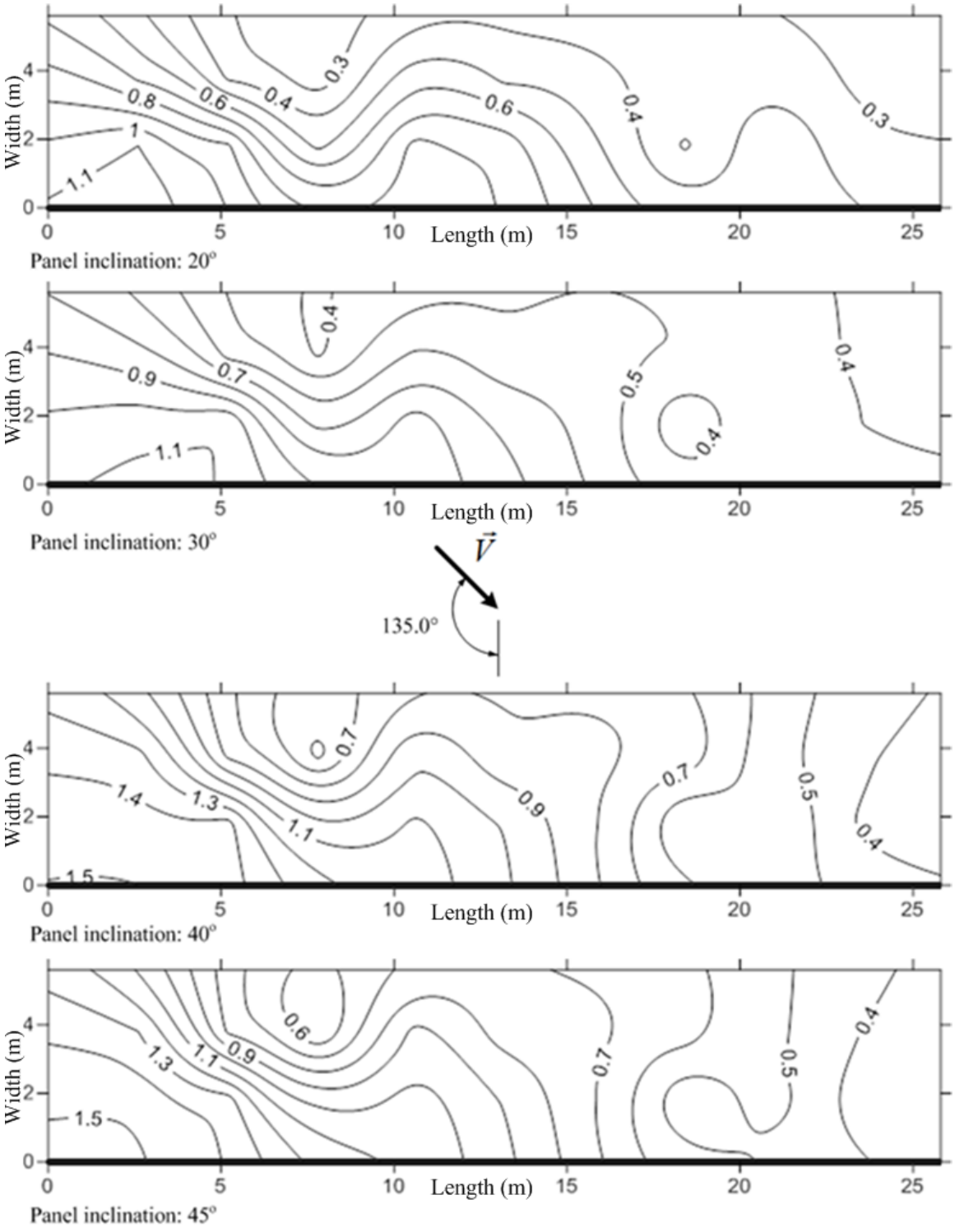

Figure A 11 Maximum C_p values for the lower panels surface at the ground level

NET, PANELS AT THE GROUND LEVEL

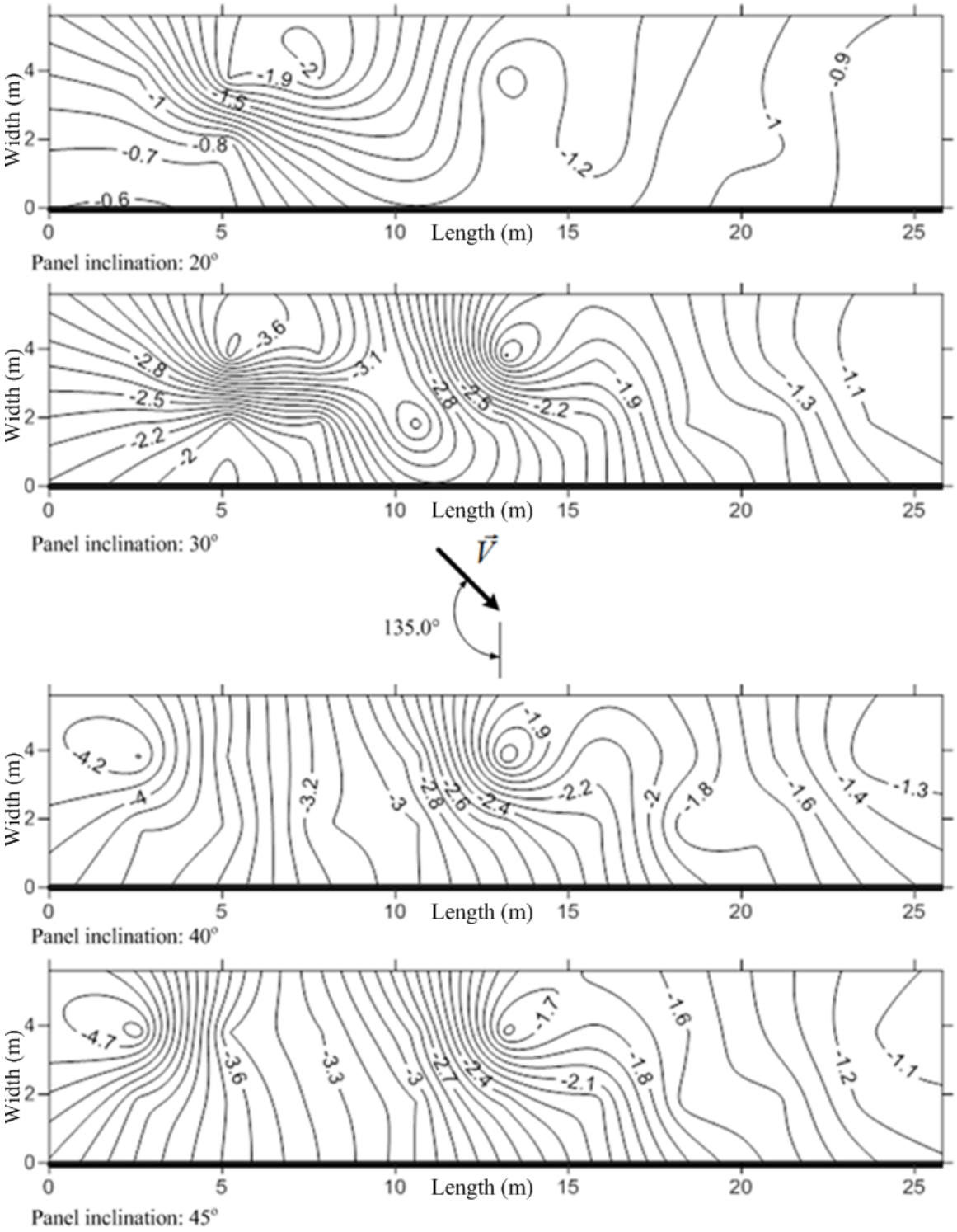

Figure A 12 Net minimum C_p values for panels at the ground level

APPENDIX B

Appendix B includes the contour plots regarding the most critical values of pressure coefficients regardless the wind direction for all configurations tested.

H = 7 m, FRONT LOCATION

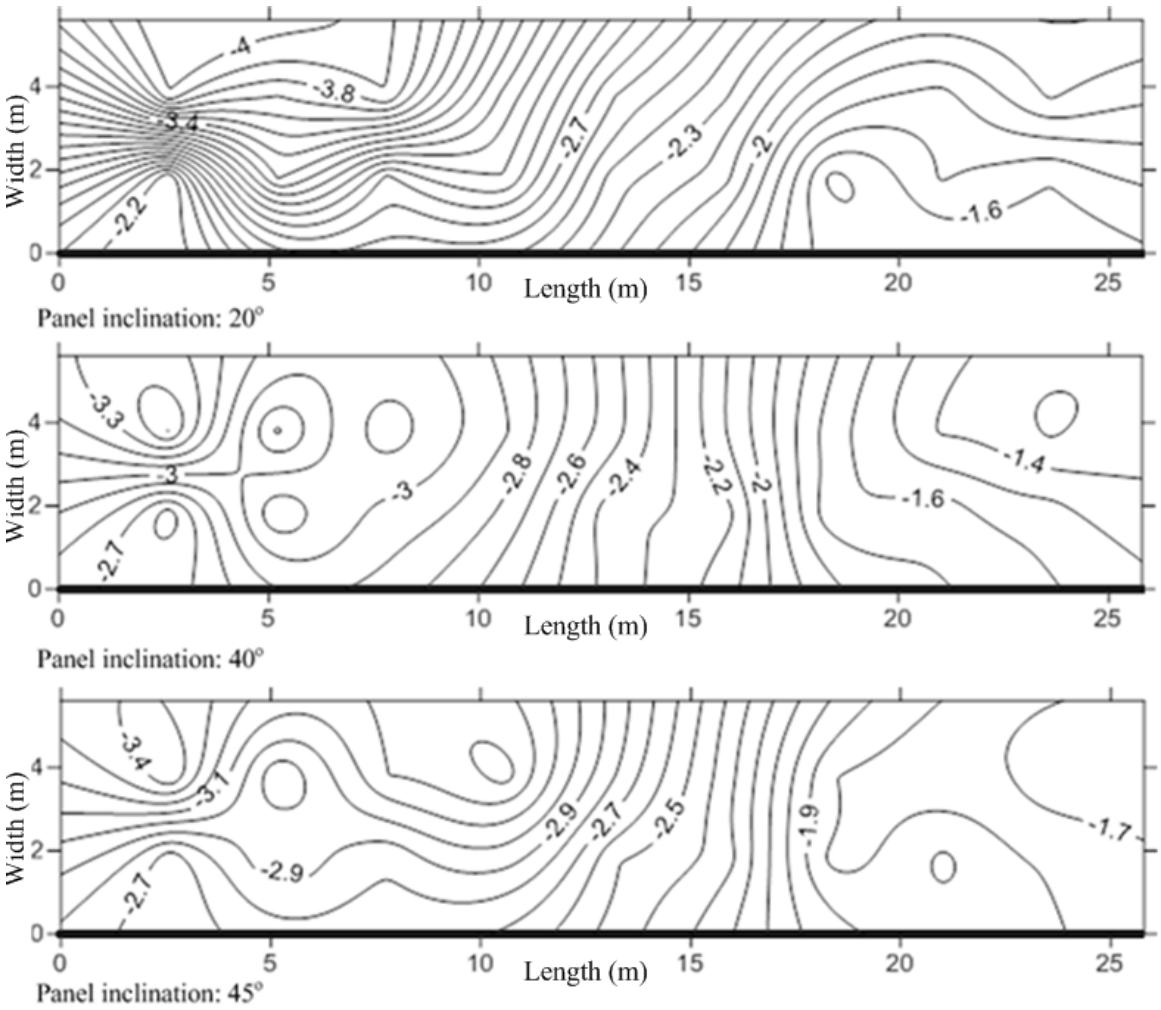

Figure B 1 Net minimum C_p values for panels attached to 7 m high building and front located

H = 16 m, FRONT LOCATION

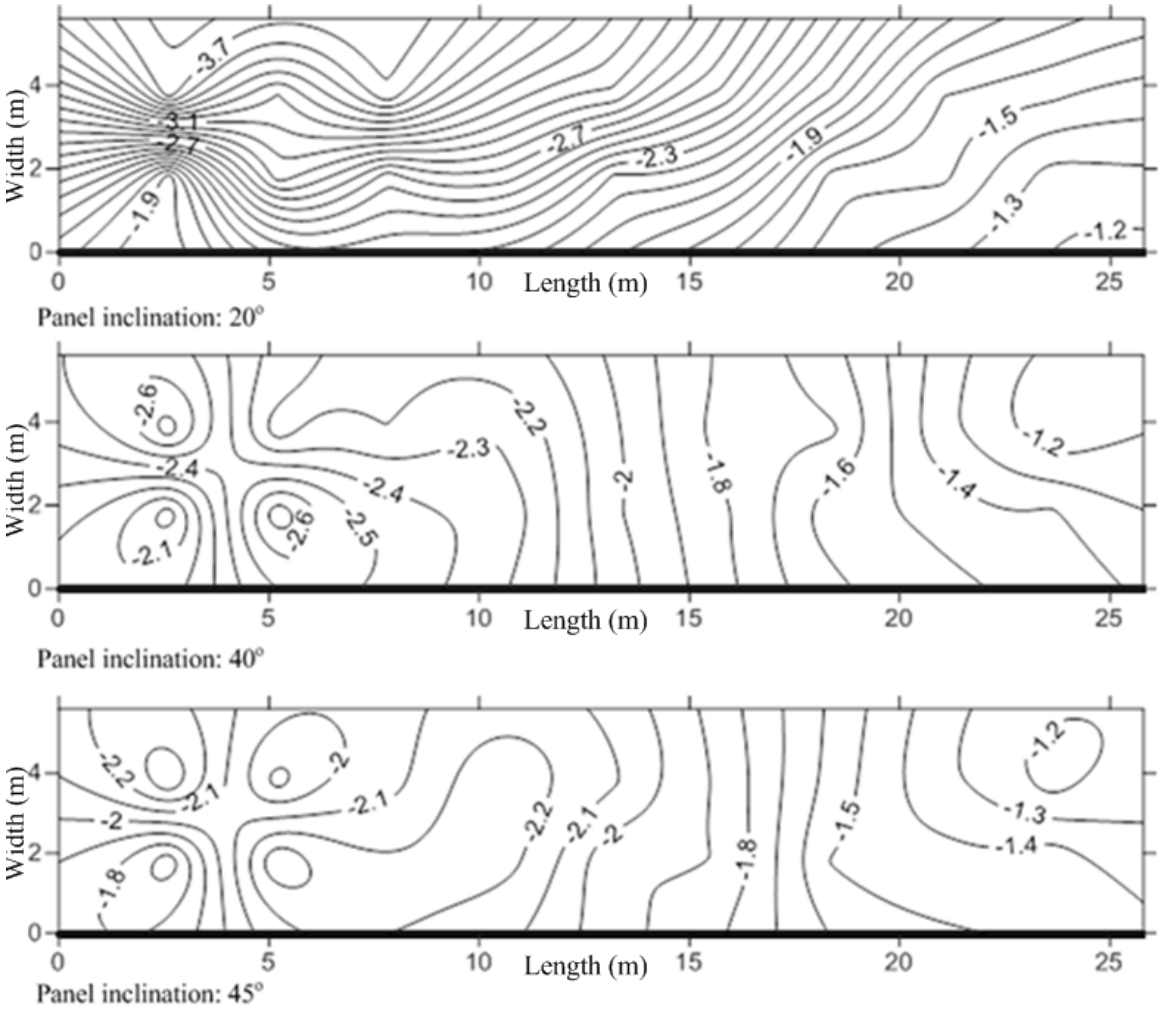

Figure B 2 Net minimum C_p values for panels attached to 16 m high building and front located

H = 7 m, BACK LOCATION

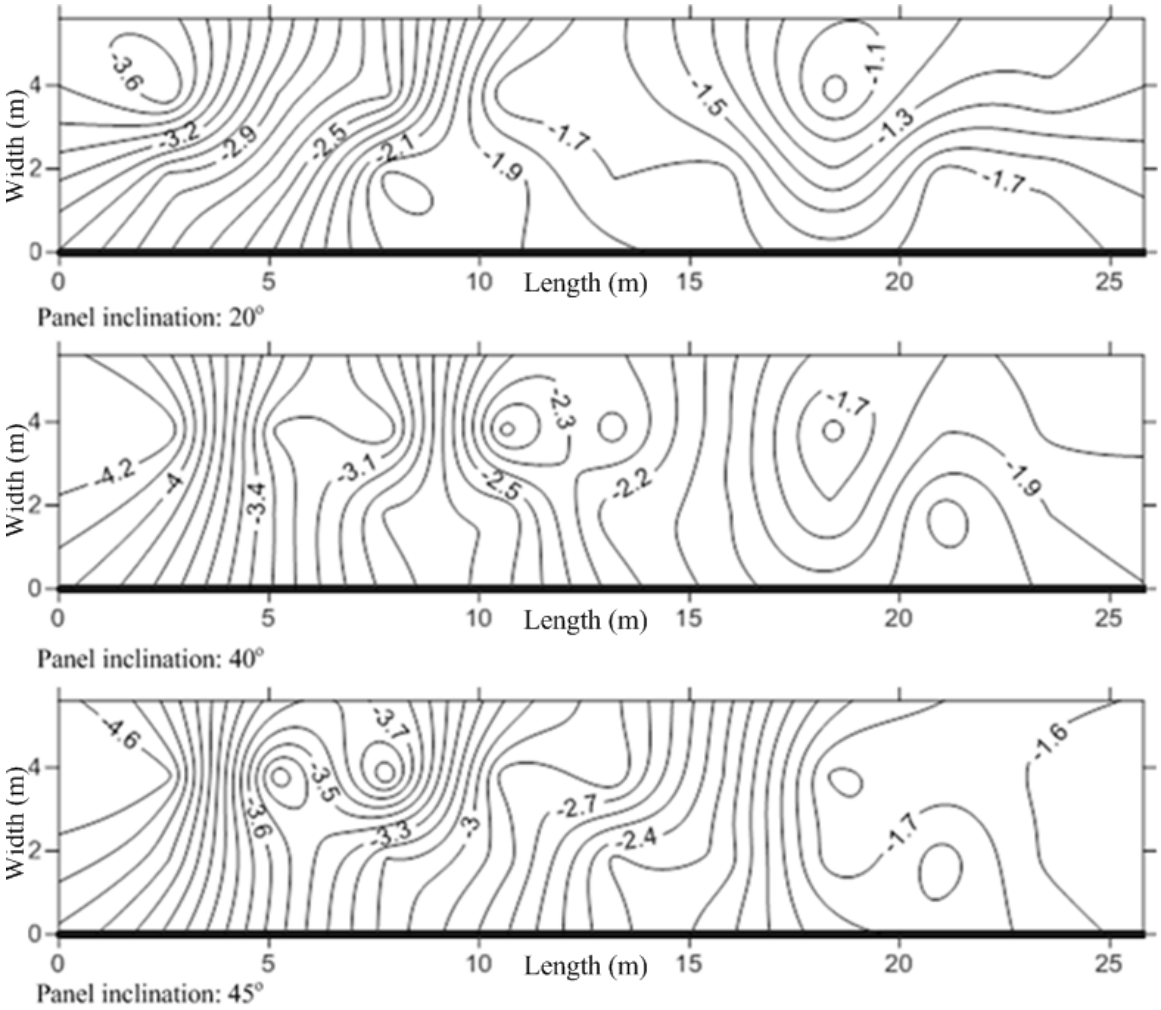

Figure B 3 Net minimum C_p values for panels attached to 7 m high building and back located

H = 16 m, BACK LOCATION

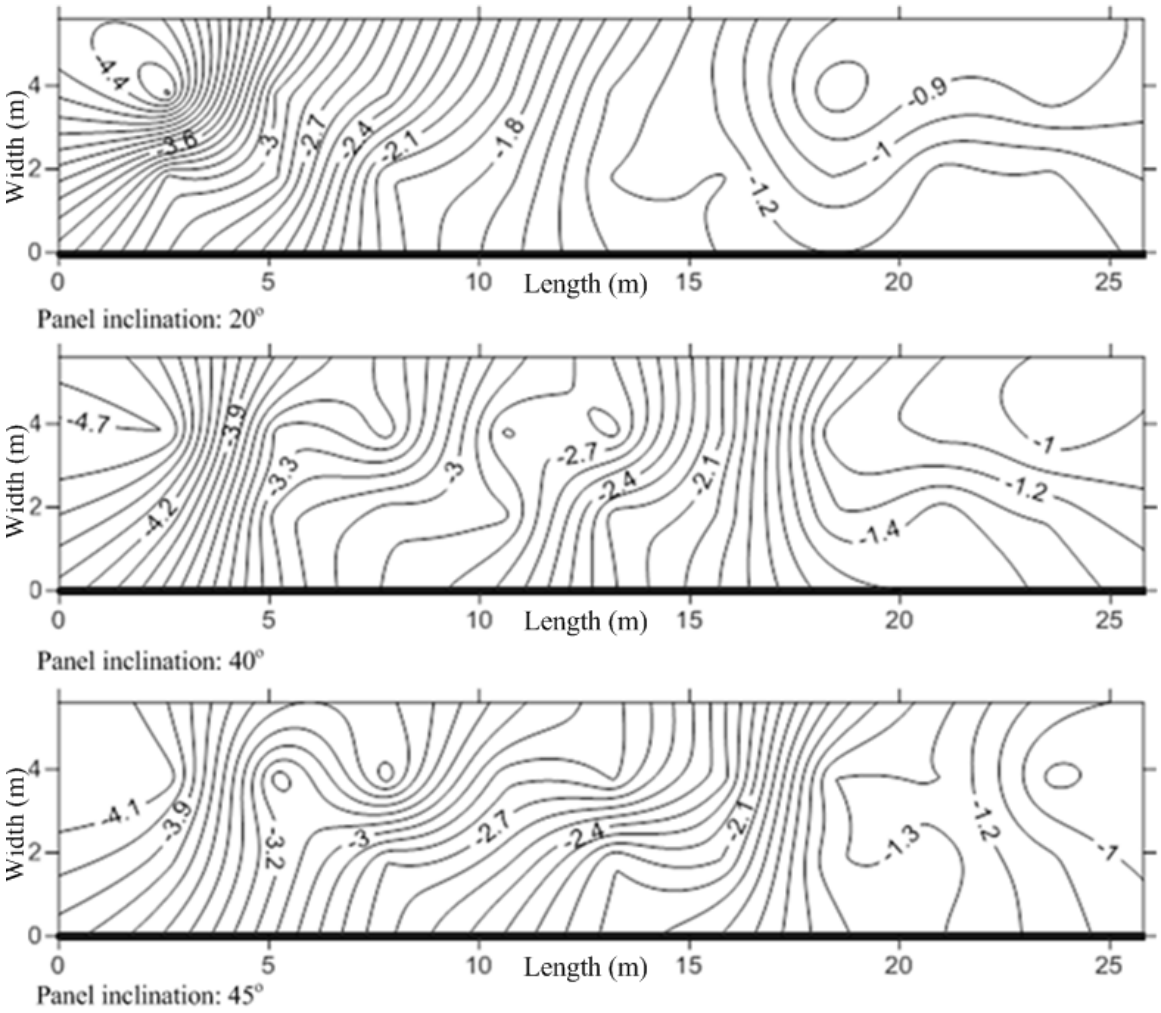

Figure B 4 Net minimum C_p values for panels attached to 16 m high building and back located

GROUND LEVEL

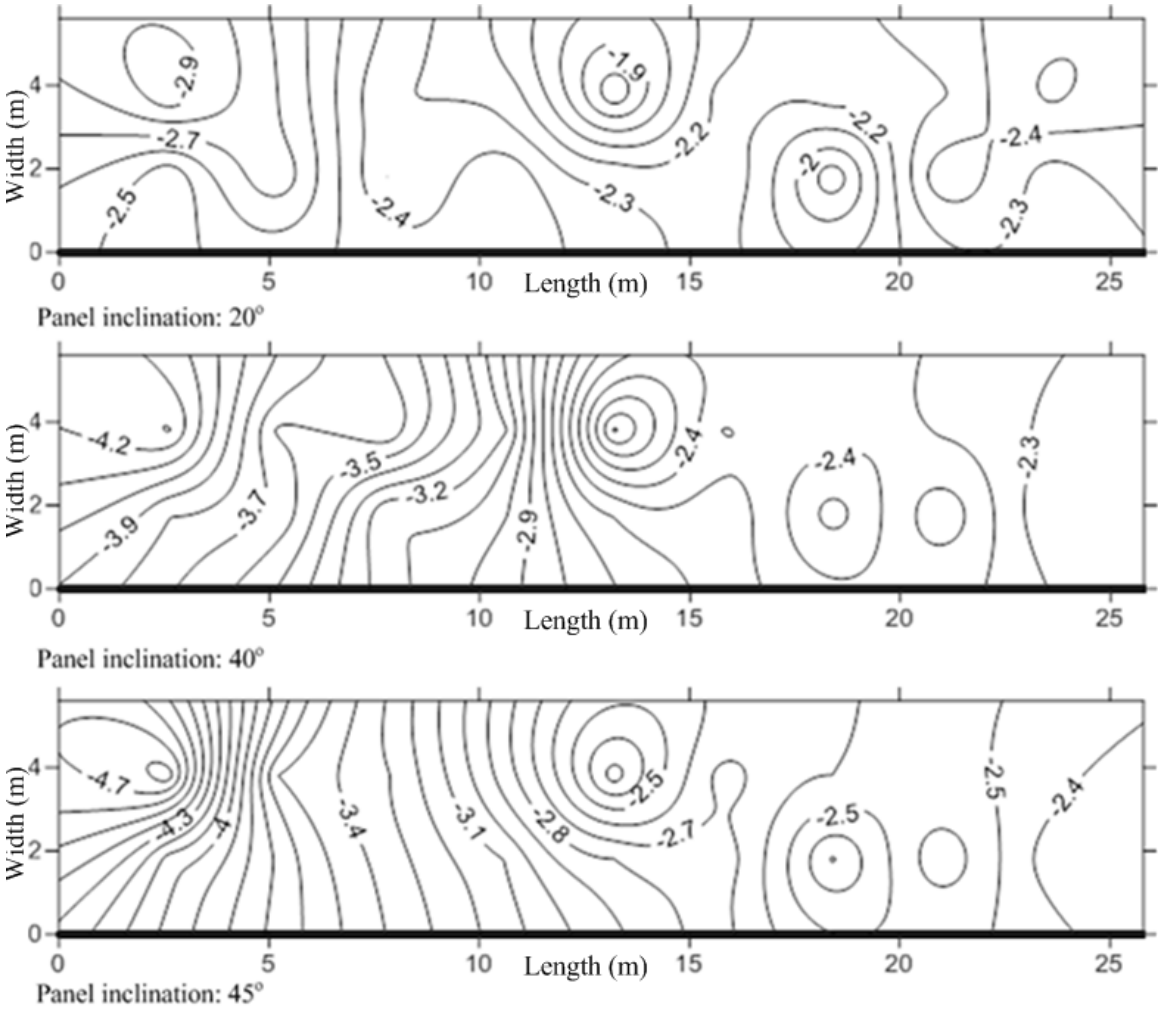

Figure B 5 Net minimum C_p values at ground level